INVESTIGATIONS ON THE MECHANISM OF ALLOSTERIC ACTIVATION OF RABBIT MUSCLE GLYCOGEN PHOSPHORYLASE *b* BY AMP

A Dissertation

by

ANDREW NATHAN BIGLEY

Submitted to the Office of Graduate Studies of
Texas A&M University
in partial fulfillment of the requirements for the degree of

DOCTOR OF PHILOSOPHY

May 2009

Major Subject: Biochemistry

INVESTIGATIONS ON THE MECHANISM OF ALLOSTERIC ACTIVATION OF RABBIT MUSCLE GLYCOGEN PHOSPHORYLASE *b* BY AMP

A Dissertation

by

ANDREW NATHAN BIGLEY

Submitted to the Office of Graduate Studies of
Texas A&M University
in partial fulfillment of the requirements for the degree of

DOCTOR OF PHILOSOPHY

Approved by:

Chair of Committee,	Gregory D. Reinhart
Committee Members,	Donald Pettigrew
	Frank Raushel
	Mary Bryk
Head of Department,	Gregory D. Reinhart

May 2009

Major Subject: Biochemistry

ABSTRACT

Investigations on the Mechanism of Allosteric Activation of Rabbit Muscle Glycogen Phosphorylase *b* by AMP. (May 2009)

Andrew Nathan Bigley, B.S., University of Houston Clear Lake

Chair of Advisory Committee: Dr. Gregory D. Reinhart

Much work has been carried out on glycogen phosphorylase over the last seventy years. Interest has persisted due not only to the usefulness of phosphorylase as a model system of allostery, but also due to the connection to the disease state in type II diabetes. The bulk of research consists of structural studies utilizing the wild-type enzyme from rabbit muscle. In this study we have employed linkage analysis in combination with structural perturbations via site-directed mutagenesis to test kinetic models of activation of phosphorylase *b* by AMP, and to examine the roles of the N-terminus, the acidic patch, α-helix 1 and the 280's loop in activation by AMP. Experiments have been carried out on purified glycogen phosphorylase *b* variants to determine the effects of perturbations *in vitro*.

The kinetic models of activation by AMP are found to be a relatively accurate description of kinetic behavior of wild-type phosphorylase *b*, but are found to be technically incorrect with respect to the absolute requirements of two equivalents of AMP to be bound prior to catalysis. Phosphorylase *b* demonstrates activity in the absence of AMP, though only at high concentrations of phosphate, and a hybrid

phosphorylase *b* with only a single functional AMP binding sight shows slight activation.

The truncate Δ2-17 shows weakened binding to AMP and phosphate in the apo enzyme, but maintains activation by AMP to an affinity similar to that of wild-type, indicating that the N-terminus is not required for activation by AMP, but has a role in establishing the affinity for both AMP and phosphate in the apo enzyme. Perturbations of the acidic patch indicate that interactions between the acidic patch and the N-terminus enhance the affinities in the apo enzyme, suggesting that the structures of the N-terminus at the acidic patch may represent an active form of the enzyme. α-helix 1 is found to have a role in homotropic cooperativity in phosphorylase *b*, but not in heterotropic activation by AMP, while the 280's loop is confirmed to have a role in the heterotropic coupling between AMP and phosphate. Based on the findings in this study an alternate structural model of activation by AMP involving α-helix 8 is proposed.

DEDICATION

To my dear wife Elizabeth and my children Tristen and Sam who have provided me constant motivation, support and encouragement through the years.

And, to my overly affectionate dog Blaze.

Ok, Trinity too.

ACKNOWLEDGMENTS

I would like to thank my committee for their guidance and encouragement through the years and their patience with me in my pursuit of this degree. I would especially like to thank Dr. Aron Fenton for his valued discussion of this and other projects and all his encouragement through the years. Much thanks also goes to current and former members of the Reinhart Lab especially Dr. Monique Parchartankul, Dr. Maurico Lasagna, and Dr. Michelle Lovingshimer, and to the members of the department who have shown such support in friendship through the years.

I would especially like to thank Dr. Michael Kladde for his assistance in designing the cloning portions of this project and Robert J. Fletterick for the generous gift of the plasmid pTACTAC containing the gene for wild-type rabbit muscle glycogen phosphorylase.

Finally, I would like to thank my family. You all have kept me grounded and given me the motivation to keep going. To Sharon, you have been the best sister one could ask for. You have always been there for me when I needed a hand or shoulder even when things were dark. To Roger, who faces the dangers in our stead that we might walk free, you deserve more credit than words could ever express, even if Sharon always gives you hell. To Karen and Royce, I could not live your life but I respect all that you do and appreciate all the effort you have made to keep me in your life. To Mom, all I can say is I love you, thanks for being there even if I have not made it easy for you. To Mark and Rhonda, you have welcomed me into your life and encouraged me, and for that I am eternally grateful. Finally, to my wife, Elizabeth, and son, Tristen, you bring me more

happiness than I could have ever imagined. You fill every day with joy and pride. It is for you this has all been worthwhile. I could not have done this without you.

NOMENCLATURE

Phosphorylase *b*	Unphosphorylated glycogen phosphorylase
Phosphorylase *a*	Glycogen phosphorylase phosphorylated at serine 14
Phosphorylase *b'*	Glycogen phosphorylase with residues 1-16 removed via limited proteolysis
Δ2-17	Glycogen phosphorylase from truncated phosphorylase gene with start codon at position 17
N-terminus	Residues 1-22 of glycogen phosphorylase
NADP(H)	Nicotinamide adenine dinucleotide phosphate
AMP	Adenosine-5-monophosphate
PMSF	Phenylmethylsulfonyl fluoride
PAGE	Polyacrylamide gel electrophoresis
SDS	Sodium dodecylsulfate
EDTA	Ethylenediaminetetraacetic acid

TABLE OF CONTENTS

LIST OF FIGURES

FIGURE Page

FIGURE Page

LIST OF TABLES

CHAPTER I

INTRODUCTION: A BRIEF HISTORY OF GLYCOGEN PHOSPHORYLASE AND ITS CURRENT RELEVANCE

Glycogen phosphorylase catalyzes the breakdown of glycogen stores via phosphorolysis to liberate glucose-1-phosphate (1). Phosphorylase has been conserved across the spectrum of life with homologues identified in mammals, yeast, slime mold, plants and bacteria (2). Generally, the properties of the catalytic core of the enzyme are maintained, but the regulation varies dramatically among species (2). In the mammalian system there are three isozymes; muscle, liver, and brain named for the tissue where they predominate (3). The biological roles of each differ along with their regulation (4). In the muscle and brain the glucose-1-phosphate is shuttled into glycolysis to provide energy for cellular function while in the liver glucose-1-phosphate is converted to glucose to maintain blood sugar (2,4).

The most extensively studied isozyme is phosphorylase from rabbit muscle (2). In the muscle, phosphorylase requires activation for significant activity to be observed (1,5). Activation can come in the form of allosteric activation by AMP or by covalent activation by phosphorylation of serine 14 (1,2). The unphosphorylated form is identified as phosphorylase *b* while the phosphorylated form is phosphorylase *a*. Phosphorylase *a* is further activated to a small degree by the addition of AMP (4). Physiologically, both forms of phosphorylase are inhibited competitively by glucose and allosterically by ATP

This dissertation follows the style of *Biochemistry*.

(1, 6,). Phosphorylase *b* is also allosterically inhibited by the downstream product glucose-6-phosphate (1,7). Inhibition has also been shown *in vitro* with various purine analogs including FMN, caffeine and at high concentrations AMP. In addition, phosphorylase *b* can be activated *in vitro* with high concentrations of sulfate (1,8,9,10).

Structurally, glycogen phosphorylase is a dimeric enzyme with a subunit molecular weight of 97.5 kDa, though an inactive tetramer is known to form *in vitro* (2,11) (Figure 1.1). Each subunit can be roughly divided into an N-terminal regulatory domain (residues 1-348) and a C-terminal catalytic domain (residues 349-832) (2). Phosphorylase has five sites thought to interact with each other. The active site sits in a cleft between the domains of the subunit and contains the cofactor required for catalysis, pyridoxal-5-phosphate (1,2,12). Access to the active site is thought to be controlled by the 280's loop (residues 280-286), which appears bound at the active site cleft in inactive structures (2,13,14). The purine inhibition site that binds aromatic inhibitors lies between tyrosine 613 of the C-terminal domain and phenylalanine 285 of the 280's loop resulting in the closing off of the active site when an inhibitor is bound (9). The glycogen storage site is thought to hold the enzyme to the glycogen particle *in vivo*, and there is some structural evidence that binding is an activating event (15). The remaining two sites, the allosteric site, where the activator AMP and the inhibitors ATP and glucose-6-phosphate bind, and the phosphoserine recognition site, are located along the interface between the subunits (13). The subunit interface is made up of two sets of interactions, the α-helix 1 and 2 bundle and the tower helices. Both the allosteric site and

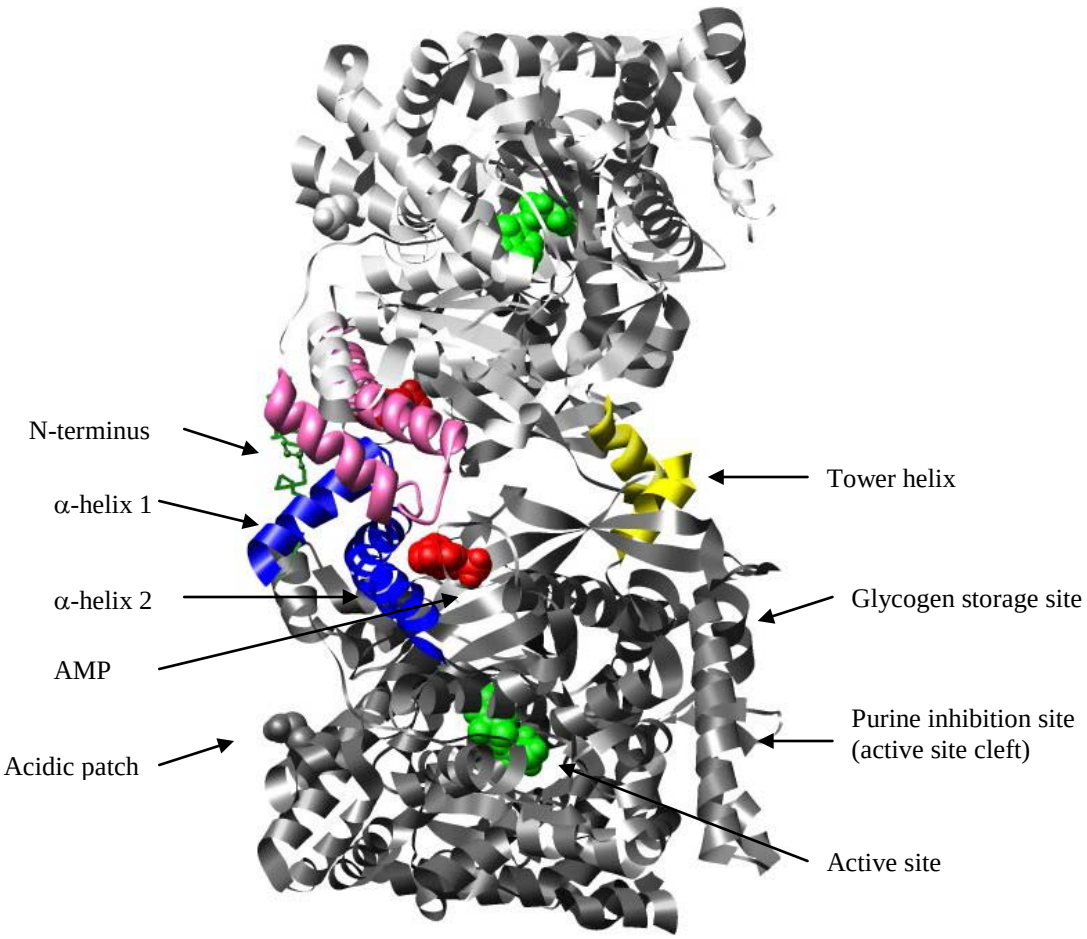

Figure 1.1: Dimeric structure of glycogen phosphorylase *b* activated by AMP. Subunit 1 is colored light grey. Subunit 2 is colored dark grey. Only subunit 2 is labeled for clarity. α-helices 1 and 2 are shown in blue for subunit 2 and pink for subunit 1. Tower helices are shown in yellow. Active site cofactor is shown in green. AMP bound to allosteric site shown in red. N-terminus is shown in forest green. Structure from Protein Data Bank entry 1pyg. Figure prepared with UCSF Chimera software from the Resource for Biocomputing, Visualization, and Informatics at the University of California, San Francisco (supported by NIH P41 RR-01081).

the phosphoserine recognition site are located on one side of the interface made up of interactions between α-helix 1 (residues 23-35) and α-helix 2 (residues 48-78) and the loop that connects them (the cap loop, residues 35-47) (13) (Figure 1.1). Though the sites are separated by approximately 15Å, both the allosteric site and the phosphoserine recognition site involve residues from α-helix 2 and residues from the cap loop of the opposing subunit. The opposite side of the subunit interface is made up of the interactions of α-helix 7 with its counterpart from the other subunit.

Glycogen phosphorylase was the first case of allostery discovered and the first case of regulation by phosphorylation (8,13). The study of glycogen phosphorylase has extended beyond seventy years now, and an appreciation of the historical context under which the knowledge of phosphorylase has been developed through the years is helpful in understanding the questions yet to be resolved.

A BRIEF HISTORY OF PHOSPHORYLASE

The study of glycogen phosphorylase has spanned the development of biochemistry as a discipline and served as a basis for the development of many of the theories currently in use. Glycogen phosphorylase activity was discovered in extracts of rabbit muscle in 1936 (16). Shortly thereafter, the same activity was found in extracts of various tissues, and the effect of AMP on this activity was noted (16,17). This unexplained observation was the first report of allostery. Throughout the remainder of the 1930's studies of this activity in extracts continued with the effects of metals, pH, and product inhibition being examined (18). Before the end of the decade the same

activity was also reported in peas and potato extracts, and the reversibility of the reaction was discovered (5).

The 1940's brought about the recognition of DNA as the material of genes, and glycogen phosphorylase was first purified in 1943 (5,19). During this study, two forms of phosphorylase in the muscle extracts were found, only one of which was being purified. The two forms of phosphorylase were found to differ significantly in their response to AMP (5). To distinguish the two forms of the enzyme they were identified as the *a* and *b* forms of the enzyme with the *b* form being more dependent on AMP for its activity. Researchers identified the apparent conversion from the *a* form to the *b* form if care was not taken during the purification (5). This interconversion was identified as being dependent on an enzyme in 1945 (20).

The 1950's ushered in major advances in protein science with the identification of the α-helix and β-sheet as secondary structural elements (19). In phosphorylase research, experiments using limited proteolysis of phosphorylase *a* gave rise to a phosphorylase (phosphorylase *b'*) that was distinct from both phosphorylase *a* and *b* (21). Fischer and Krebs reported in 1956 that they had partially purified phosphorylase *b* as well as an enzyme capable of converting it to phosphorylase *a* (22). That same study also found that the conversion from *b* to *a* was due to phosphorylation of the *b* form in the first case of protein phosphorylation to be reported. That same year, conditions were found to dissociate phosphorylase, allowing the identification of phosphorylase *a* as a tetramer and phosphorylase *b* as a dimer (23). The following year the cofactor of glycogen phosphorylase was identified as pyridoxal-5-phosphate (12). Shortly thereafter

the role of the cofactor in phosphorylase was shown to be different from the role observed in other enzymes by demonstration that the Schiff's base formed was unimportant to catalysis (24). 1958 brought about the first complete purification of phosphorylase *b* along with its crystallization (25). The 1950's drew to a close with the first structure of a protein being solved, myoglobin, by Kendrew in 1959 (19), and the sequence of the phosphorylated peptide from phosphorylase *a* was identified by the new technique of protein sequencing (26).

The 1960's saw major advances and the studies of allostery. In particular, the recognition that globular proteins have regular, definable structures led to proposals on how structure might lead to allostery. First, was the proposal by Monod, Wyman and Changex of the concerted model of allostery (MWC model) that requires molecular symmetry in multimeric enzymes (27). Shortly thereafter, Koshland, Nemethy, and Filmer proposed the alternate sequential model (KNF model) (28,29). Both of these models held that the allosteric properties were derived from the existence of two unique structures, the inactive T-state and the active R-state, and that the equilibrium between them defines the allostery. Phosphorylase, which shows both homotropic cooperativity (the binding of one ligand effecting the binding of subsequent identical ligands) and heterotropic coupling (the binding of one ligand effecting the binding of a different ligand), was one of the cases considered in the development of the MWC model, and the MWC model was soon applied to explain the observations being made in phosphorylase research (6). Later in the 1960's the inhibition by ATP and glucose-6-phosphate was discovered along with the activating effects of polyamines (7,30). The dimer of glycogen

phosphorylase was found to be the active species rather than the tetramer as had been presumed due to the isolation of phosphorylase *a* in a tetrameric form (11). In 1968 one of the most influential studies of phosphorylase to date was published (31). In this study, the enzyme species generated by limited proteolysis (phosphorylase *b'*) was studied in detail, and it was shown that phosphorylase *b'*, while requiring AMP, did not show the activation normally observed with phosphorylase *b*, and there was a loss of all homotropic cooperativity in binding the substrate phosphate and effector AMP. In light of the new models of allostery, it was proposed that the peptide removed by limited proteolysis was responsible for the transmission of the allosteric signal across the interface. The findings of the study of phosphorylase *b'* would later form the bases of the structural understanding of phosphorylase activation.

Studies on the catalytic mechanism, the dimer/tetramer equilibrium, and the nature and role of the glycogen particle continued into the 1970's (15,32,33). Experiments revealed that phosphorylase remained bound to the glycogen particle as did phosphorylase kinase and phosphatase (34). By 1970, it was recognized that glycogen phosphorylase in the liver has a role in the regulation of blood sugar (35), and later that there were different isozymes that were prevalent in different tissues (3).

In the field of phosphorylase allostery, numerous major advances were made in the 70's. In 1970, the sites for AMP and glucose-6-phosphate were shown to be at least partially overlapping (36). Studies were conducted to test the AMP site using synthetically derived inhibitors to determine what made the site specific for AMP (37). One of the first problems with using two-state models to describe allostery in

phosphorylase was reported in 1970. It was found that phosphorylase modified with glutaraldehyde to stabilize the structure was still responsive to AMP activation, but that there was no homotropic cooperativity in the binding of AMP as was called for by the MWC model (38).

1976 ushered in the first high resolution structures of phosphorylase *a* though the model built initially only gave the backbone positions (39). Later that year, it was shown that phosphorylase was active in the crystalline state, though at much reduced levels of activity (40). This finding was taken as evidence that the structure observed in the solved crystal structures was relevant to the physiologically active enzyme. The following year, the complete sequence of the muscle phosphorylase protein was published allowing the generation of true high resolution crystal structures (3Å) and the unambiguous identification of the N-terminus as the site of phosphorylation (41,42,43). The two-state models of allostery continued to be applied to phosphorylase, and as structures of both phosphorylase *a* and *b* appeared, the unique structures seemed to confirm the theory (39,44,45). The structure solved with maltopentose identified the site of attachment to the glycogen particle, as well as the fact that binding of the polysaccharide altered the structure of phosphorylase from that seen in the unbound structures (15). The study of polysaccharide binding also presented the first complex kinetic scheme of how phosphorylase might be allosterically activated. Caffeine was first recognized as an inhibitor of phosphorylase in 1978, and newly generated structural data allowed the identification of its binding site, later referred to as the purine inhibition site (9,10).

Structural work continued in earnest in the 1980's with more and more structures being generated with activators or inhibitors bound (46,47,48,49). The comparison of the differences in these structures allowed early attempts to explain the structural mechanism of allosteric activation in phosphorylase (14,47,49,50). The 80's also saw the first reported T-state structures of phosphorylase *b* and *a*, and the more difficult to generate R-state of phosphorylase *b* (14,46,48,51).

The 80's also brought great advancements in the sequence data available. More protein sequences were solved, and the advent of PCR allowed the DNA sequences to provide information from more organisms (19,52,53,54,55). This new information fueled a great deal of effort to understand the evolutionary relationships among species in the hope that understanding the relationships would provide insight on the regulation of the enzyme (52,56). The most important finding was that the catalytic core of phosphorylase was conserved, while the N-terminal 150 residues were highly variable and appeared to give rise to the unique regulation seen in each homolog.

The early 1990's held major advances for phosphorylase research. The chemical mechanism of phosphorylase was elucidated, though it would be in the late 90's before transition state analogs would finally remove any doubts that catalysis proceeds through a carbocation mechanism (57,58,59). Sulfate activation of phosphorylase *b* was studied in detail in 1990 (60,61). It would later be shown that sulfate activation was due to an interaction with the N-terminus (62). The two-state models were used to try to provide a uniform description of allostery in diverse systems through structural comparisons of other allosteric enzymes (63). This was in part due to the identification of a proposed

switch of residues R569 and D284 in the active site between the R- and T-states of phosphorylase, respectively (57,64).

Probably the most influential paper on phosphorylase structure was published by Barford and Johnson in 1991 (13). They reported the proposed R- and T-state structures of phosphorylase *a* and *b* and reviewed all known structural data. This combination of information allowed the discussion of the observed structural changes and the proposal of how those changes resulted in the propagation of the allosteric signal. The N-terminus (residues 1-22) was found bound at the subunit interface in the R-state and at the acidic patch in the T-state, which was interpreted to be the conduit for the allosteric signal across the interface as had been postulated from the work done with phosphorylase *b'* (31). Likewise, the movements of the helices at the subunit interface shown in the activated structures, and the disordering of the 280's loop (residues 280-286) that blocked access to the active site in the T-state structures were hypothesized to be important for allosteric activation (13). This paper acknowledged numerous problems with the limitations imposed by the two-state models of allostery, namely the numerous structures showed combinations of both R- and T-states, the ability to uncouple the homotropic and heterotropic effects, and the uncertain nature of the position N-terminus in phosphorylase *b*.

The early 90's also held two other major events in phosphorylase research. First, the successful expression of rabbit muscle glycogen phosphorylase in a bacterial system allowed the ready manipulation of the enzyme (65). Second, inappropriate activity of liver phosphorylase was linked to the high blood sugar seen in patients with type II

diabetes, which refreshed interest in the regulation of phosphorylase (66,67). The bacterial expression system allowed for testing of hypotheses based on structural perturbation for the first time, and the new link to a disease state brought about a search for inhibitors of phosphorylase (66).

Sequence comparisons between the known mammalian and later all known phosphorylase enzymes allowed predictions of what residues were important for allostery (2,4). Unfortunately, when put to the test those early predictions failed to deliver the predicted response (68,67,69). Specifically, residue P48 in muscle was predicted to be a switch between the R- and T-states, but when mutated there was a loss of homotropic cooperativity but not activation by AMP. Similarly, placing a negative charge at position 14 failed to create an enzyme that was active in the absence of AMP as predicted (70), and numerous reviewers were led to speculate that the special ionic character of the phosphoryl group was the key to its use in signaling (71).

Later, a report declared that the molecular activation switch in phosphorylase had been identified by engineering a metal binding site at the subunit interface, however in reality very little activation was observed, and the enzyme was retained little activity (72). Attempts to verify the 280's loop including aspartate 284 as important for allostery met with similar challenges as it was found that phosphorylase did not tolerate changes to the 280's loop (73). Ultimately in 1997, the continued difficulty in using the two-state models of allostery for phosphorylase led to the publishing of a continuous model of allostery in phosphorylase *b* to account for observed kinetics (74). The 90's drew to a

close with full scale efforts under way to generate inhibitors for the treatment of diabetes and to understand the complex regulation of glycogen metabolism in the liver (75).

Much the same efforts continued into the new century with a second continuous kinetic model of allostery being published for phosphorylase (76,77), and many more structures being published with inhibitors being bound to various sites (78,79,80,81,82,83). Reports on the effects of complex mixtures of physiological inhibitors and activators were published in an attempt to understand the regulation in the liver (84,85). Interest in glycogen phosphorylase has been maintained as of late by the continued efforts to develop therapeutic inhibitors, a search that has been complicated by the finding that the liver enzyme must be specifically targeted (86), and the discovery that there is a shunt from glycogen to the formation of numerous sugar moieties of glycoproteins (87). A recent study of phosphorylase has further highlighted the deficiencies in the current understanding of phosphorylase. This modeling study predicted that phosphorylase must have a minimum of three structural states to explain the existing kinetic data, and the authors postulate that the true active form is yet to be solved (88).

THE GENERALLY ACCEPTED STRUCTURAL MODEL OF ALLOSTERY IN GLYCOGEN PHOSPHORYLASE

Despite the aforementioned difficulties, the various structures with activated and inhibited phosphorylase that have been solved over the years have led to a proposed model of activation (1,13,63). It is generally accepted that the mechanism of activation is

the same for activation by both AMP and phosphorylation. The major differences between the active and inactive states that are thought to be important for activation involve the conformation of the interface, the movement of the N-terminus from the acidic patch (residues 96, 105, 109, 110, 120, 493, 501, 505, 509) to the interface, and the displacement of the 280's loop (1,13) . It is proposed that the binding of AMP to the allosteric site causes a shift in α-helix 2 and brings the cap loop of the other subunit into proximity of the AMP binding site (13) (Figure 1.2). The N-terminus is released from the acidic patch on its own subunit upon activation and moves to the subunit interface. The rearrangement of the interface is thought to result in a rotation of the subunits with respect to each other causing the tower helix to slide past its counterpart on the opposite subunit (8, 13) (Figure 1.3). The movement of the tower helices is proposed to cause the displacement of the 280's loop (residues 280-286) allowing substrate access to the active site (1,13) (Figure 1.3). Additionally, the activation of phosphorylase is thought to be brought about by the displacement of aspartate 284 from the active site where it is proposed to prevent phosphate binding (1,57). The negative charge of the aspartate is replaced by the positive charge from arginine 569 which is proposed to create the high affinity binding site for phosphate in the active enzyme (57). This model is predicted to be correct for both the activation by AMP and phosphorylation though minor local differences are acknowledged (13).

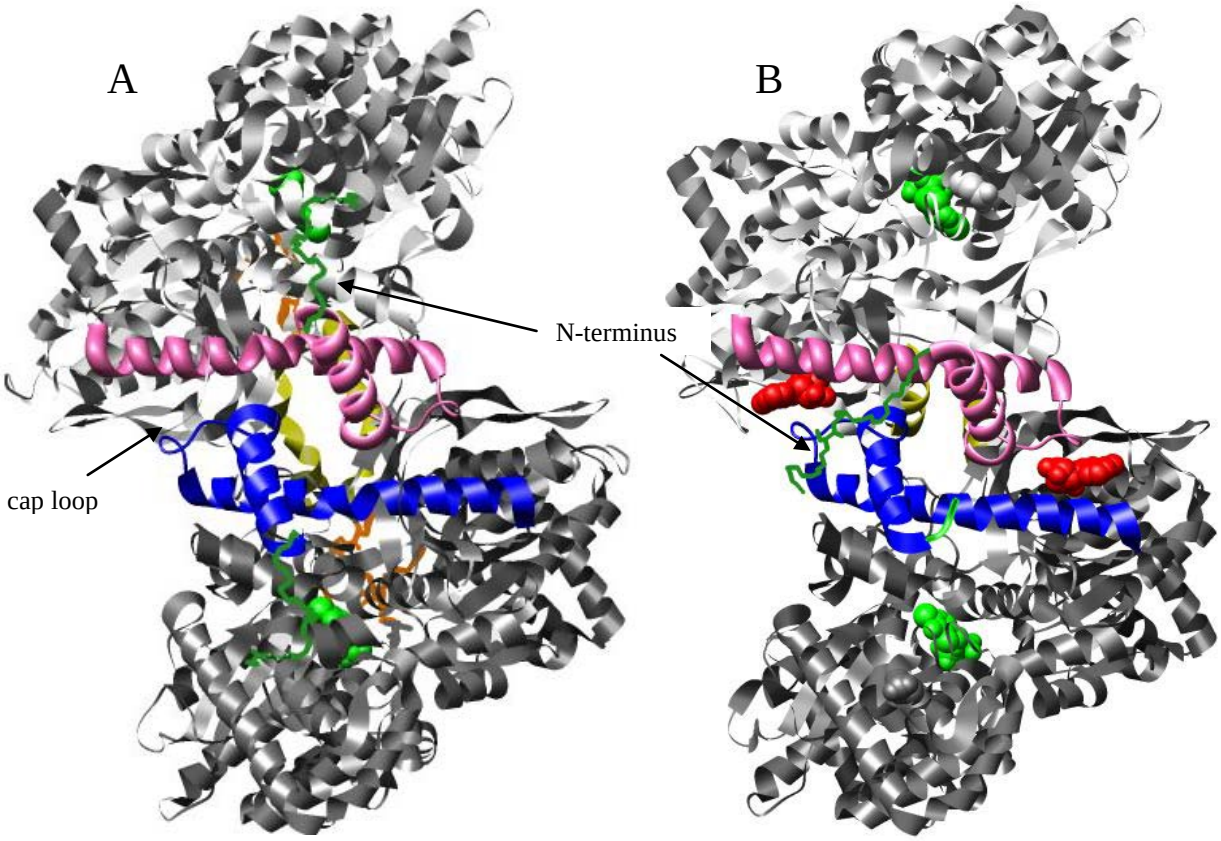

Figure 1.2: Dimeric structure of activated and inhibited phosphorylase *b* highlighting α-helices 1 and 2, cap loop, and N-terminus. Subunit 1 is colored light grey. Subunit 2 is shown in dark grey. α-helix 1 and 2 for subunit 1 are shown in pink. α-helix 1 and 2 from subunit 2 are colored in blue. The cap loop connects α-helices 1 to α-helix 2. Active site cofactor is shown in green. The N-terminus colored forest green. The tower helices (on the opposite face of protein) are shown in yellow. AMP bound to allosteric site is shown in red. A) Inhibitor bound structure (PDB 2gpb) with the N-terminus bound to the acidic patch. B) Activator bound structure (PDB 1pyg). Acidic patch marked by space-filled side chain of residue 501 in B. Figure prepared with UCSF Chimera software from the Resource for Biocomputing, Visualization, and Informatics at the University of California, San Francisco (supported by NIH P41 RR-01081).

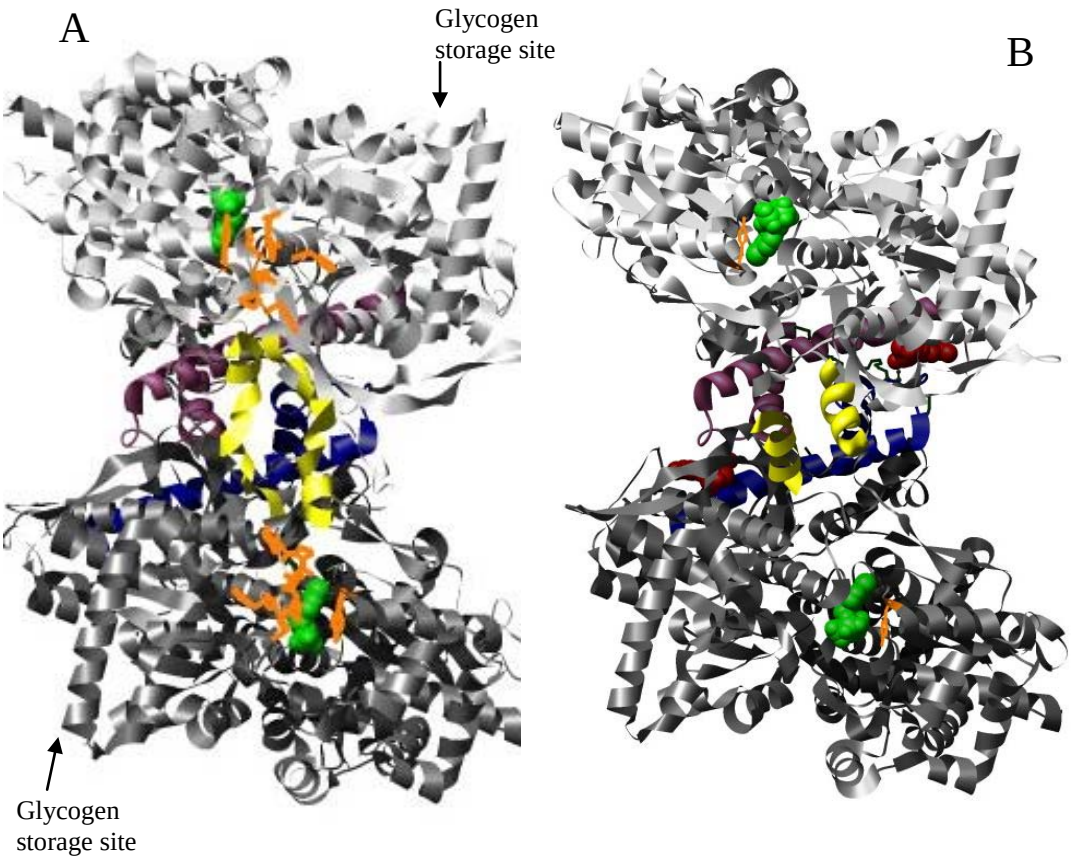

Figure 1.3: Dimeric structure of activated and inhibited phosphorylase *b* highlighting the tower helices and 280's loop. Subunit 1 is shown in light grey. Subunit 2 is colored dark grey. Tower helices are shown in yellow. The helix on right is from subunit 1. The helix on left belongs to subunit 2. Tyrosine 613 (purine inhibition site) and 280's loop are shown in orange (not visible in B). The active site cofactor is colored green. A) Inhibitor bound structure (PDB 2gpb). B) Activator bound structure (PDB 1pyg). α-helices 1 and 2 on opposite face of enzyme are shown in pink (subunit 1) and blue (subunit 2). Figure prepared with UCSF Chimera software from the Resource for Biocomputing, Visualization, and Informatics at the University of California, San Francisco (supported by NIH P41 RR-01081).

QUESTIONS REMAINING TO BE ANSWERED

After more than seven decades of research, major questions still remain about the regulation of mammalian glycogen phosphorylase. The two-state models of allostery have been shown to be inadequate to explain the kinetics of glycogen phosphorylase *b* (1,13,57,68). The extensive use of these models throughout the study of phosphorylase have influenced the type of data collected. Typically, kinetic data have been collected over narrow concentration ranges, and the analysis limited to whether the R- or T-state had been stabilized (31,73,89). The continuous models of phosphorylase *b* allostery were derived exclusively using wild-type data, and both contain the surprising requirement that two equivalents of AMP bind before catalysis takes place (74,75,76). To date these models have not been experimentally tested.

The structural changes brought about by phosphorylation are well understood along with the kinetics of phosphorylase *a* (13,47,90). The phosphoserine recognition site has been structurally defined and confirmed by mutagenesis (13,89). The regulation of phosphorylase *b* has remained more elusive. The accepted active state of the enzyme is based on phosphorylase *a*, which was solved as the inactive tetramer, and there is no dimeric structure of activated phosphorylase (13,47). Further complicating the structural evaluation of phosphorylase is the evidence that interaction with the glycogen induces changes to the structure which are thought to help activate the enzyme (1, 15). The kinetic data on the allosteric activation of phosphorylase are by necessity generated in the presence of polysaccharide, but the affects of allosteric effectors on the polysaccharide bound structure are unknown (1).

Even with the rabbit muscle enzyme the effects of AMP binding are unclear. The limited attempts that have been made to identify the roles of various structural units by modification of protein sequence have met with limited success (68,69,70,72,73,89). An attempt to verify the proposed role of α-helix 2 in activation by AMP by site directed mutagenesis was not successful and pointed to a role only in the homotropic cooperativity in AMP binding (68). The packing of α-helix 1 is known to change between the reported R- and T-states but its role in the activation by AMP has not been investigated (13). The 280's loop is proposed to be critical in activation (13, 14), but difficulties in working with the 280's loop have failed to verify a role in activation by AMP (73). The role proposed for the N-terminus in AMP activation is based on enzyme exposed to proteolysis, and ambiguity remains with respect to its localization in active phosphorylase *b* (13,31).

THE MODERN STUDY OF ALLOSTERY

Glycogen phosphorylase started the study of allostery, but it was nearly thirty years later that the first theories of allostery were developed (16,27,28,29). Those first theories were derived from the concept that proteins have constant structures, and that those structures dictate the function of the protein in question (19). The concept proposed by Monod, Wyman, and Changeux was that an enzyme might have two related but different structures each with its own properties giving rise to the phenomenon of allostery (27). The MWC model proposed that molecular symmetry must be maintained allowing the binding of a single ligand to alter the structure of all subunits giving rise to

the observed allostery. Among the arguments for this were the findings that allosteric enzymes tended to be multimeric and that homotropic and heterotropic properties appeared to be linked in these enzymes; that is, an effector that activated tended to alleviate the homotropic cooperativity in substrate binding (27). Given the limited data that were available at the time, the MWC model explained the observations made in allosteric systems.

The model put out shortly thereafter by Koshland, Nemethy, and Filmer adopted the same general concept, but argued that the case need not be as simple as that proposed in the MWC model in that the molecular symmetry, while favored, need not be strictly maintained (28,29). The real drawback to both of these models is the requirement to assume a two-state system and applying that assumption to the experimental data rather than letting the data dictate the model. The advantages of these models were that they could explain most kinetic data being generated, and they allowed the prediction of the general behavior of the systems being studied. As structural data were generated for the allosteric systems, the finding that allosteric enzymes could exist in different forms depending on whether they were activated or inhibited seemed to confirm the concept of the two-state models (13,19,91).

In the modern era, problems have been found in the two-state models. Work such as that by Di Cera on thrombin has been of particular interest because thrombin is a monomeric protein meaning that by definition the two-state models, which are derived for multimeric enzymes, cannot be applied (92,93,94). The work on thrombin and other monomeric allosteric proteins has led to a reevaluation of how allosteric signals might be

propagated. Ernesto Freire has proposed that the nature of the two-state models is too restrictive and in reality there is an ensemble of structures some competent to bind and others not, and through local perturbations of folding states ligands can alter the ensemble to bring about the allosteric nature of the system (95). Others have looked to protein dynamics as the source of allostery, holding that the change in dynamics brought on by ligand binding is responsible for the alteration of properties (96). Both of these concepts hold the potential that only a small subset of interactions in the protein may be responsible for the communication between sites. The identification of these interactions has become a major effort, and structural studies with thrombin have been successful in elucidating the pathway of communication between the allosteric site and active site (93,94).

Thrombin remains the only allosteric enzyme for which a defined pathway has been identified, but identification efforts in other systems have been helped by new analysis techniques. Protein covariation analysis developed by Ranganathan has proven to be able to pick out apparent pathways connecting sites in various proteins that have been conserved through evolution (97). A modeling approach that maps the secondary and tertiary interactions that change in reported R-and T-states of various allosteric enzymes has been developed by Gray and shown to highlight apparent pathways of communication between sites (98) . Unfortunately, the attempt to model such structural changes in phosphorylase failed to identify such a pathway. Similarly, covariation analysis is not likely to succeed in phosphorylase due to the need for a large number of related sequences to statistically identify residues that are evolutionarily covariant (97).

The mammalian enzymes are thought to have developed their regulation via a fusion at the N-terminus, meaning that the N-terminal region is only conserved among mammalian species, which severely limits the application of covariation analysis (2).

As early as the 70's, Weber called out the warning to the scientific community that attempting to explain allostery simply by a two-state structural model comes at the cost of understanding the kinetic and thermodynamic data available for these systems (99,100). Adopting the two-state models greatly simplified the analysis of allosteric systems for early researchers, but it requires the assumption of a model that may or may not be correct. Weber developed formalisms to deal with allostery on a purely thermodynamic basis without making assumptions to the nature of the system, but the two-state models continued to be widely accepted (99,100).

The approach of Weber was continued and further developed by Reinhart to be applied to a symmetrical dimer including both the theory and experimental approach to test the extent of coupling (101). Similarly, Ackers took a statistical thermodynamics approach to attempt to resolve in finer detail the nature and magnitude of the allosteric communications in his system of interest, hemoglobin (102). Both approaches, referred to as linkage analysis, provide detailed descriptions of the behavior of the allosteric systems, but alone they do not provide insight on how the allostery is structurally transmitted.

De Cera has pointed out in recent years that the data collected via crystallography can be constrained by the crystal lattice itself either obscuring small but important movement or emphasizing irrelevant movements, and structural work itself must be

validated (94). Utilization of thermodynamic linkage allows the testing of hypotheses on how allosteric signals might be transmitted based on the available structural data. Three of the most influential systems considered in the development of the two-state models were phosphorylase, PFK, and hemoglobin (27,28). Ultimately, the linkage analysis approach has been successfully used in combination with protein species containing only single interactions for both PFK and hemoglobin, and the two-state models of allostery were found to be inadequate to explain either of these systems (102,103,104).

Using the theory derived by Reinhart for the symmetrical dimer, which is most applicable to phosphorylase, the magnitude of the coupling between ligands can be established (101,105). This approach allows the determination of the nature and magnitude of the allosteric interactions between different ligands (heterotropic coupling) by the measurement of the dissociation constants for substrate via titration curves in the absence and the saturating presence of the allosteric effector. The coupling constant (Q) is defined as the ratio between the two. For phosphorylase;

$$Q_{AMPPi} = \left[\frac{K_{Pi}^{o}}{K_{Pi}^{\infty}} \right] \tag{1.1}$$

where Q_{AMPPi} is the coupling quotient between AMP and phosphate, K_{Pi}^{o} is the dissociation constant for phosphate in the absence of AMP and K_{Pi}^{∞} is the dissociation constant in the saturating presence of AMP.

Experimentally the value of Q can be determined by taking the ratios of the values of the dissociation constants at the limits of the other ligand (101). This, however, implies that the range of effect for the other ligand, AMP in this case, must be

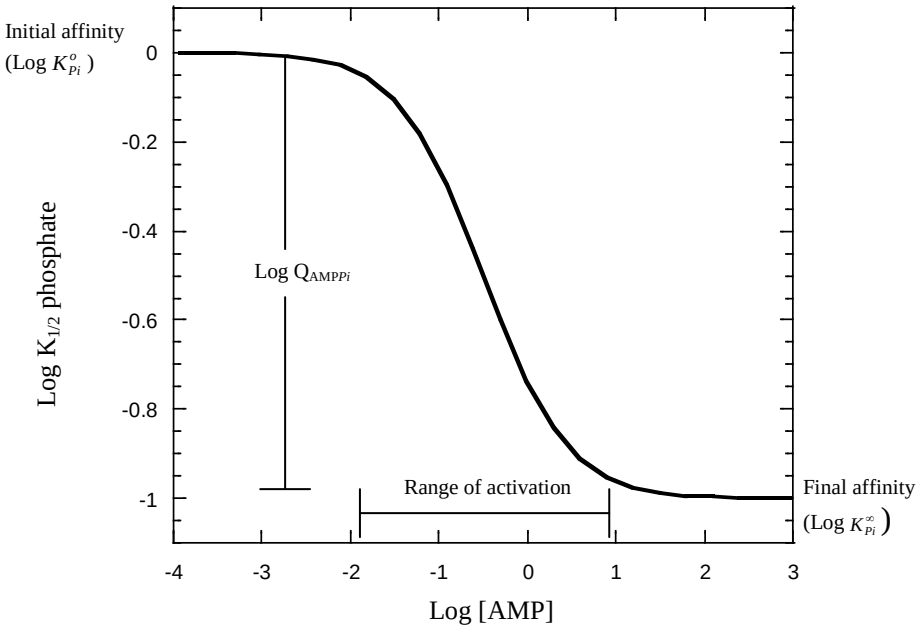

Figure 1.4: Theoretical log-log plot of allosteric activation in phosphorylase *b*. Behavior predicted from equation 1.2. Initial and final affinity for substrate shown as asymptotes at high and low effector. Heterotropic effect is quantified by value of Q_{AMPPi}. Range of activation represents the concentration range over which a change in activator concentration will perturb the apparent affinity for substrate.

determined. Far more information can be gained by examining the relationship between the concentration of effector and the dissociation constant for substrate. As seen in Figure 1.4 the affinity for substrate is dependent on the concentration of effector present with the magnitude of the coupling defining the separation between the plateaus, and the range over which the change in substrate affinity changes is dependent on the affinity for effector and the homotropic cooperativity in its binding. The relationship between these is given for phosphorylase by:

$$K_{1/2} = K_{Pi}^{o}\left[\frac{{K_{AMP}^{o}}^{2} + 2K_{AMP}^{o}[AMP] + Q_{AMP}[AMP]^2}{{K_{AMP}^{o}}^{2} + 2K_{AMP}^{o}Q_{AMPPi}\left[\frac{Q_{AMP}}{Q_{AMP/Pi}}\right]^{1/2}[AMP] + {Q_{AMPPi}}^{2}Q_{AMP}[AMP]^2}\right]^{1/2} \quad (1.2)$$

where $K_{1/2}$ is the measured dissociation constant for phosphate at some concentration of AMP, K_{AMP}^{o} is the dissociation constant for the binding of the first equivalent of AMP in the absence of phosphate, Q_{AMP} is the homotropic coupling quotient for AMP binding in the absence of phosphate, and $Q_{AMP/Pi}$ is the homotropic coupling quotient for AMP binding in the saturating presence of phosphate.

The homotropic coupling quotients describe the degree of homotropic cooperativity observed in binding of a given ligand. Experimentally, these values can be quantified by the relationship to the Hill number determined from titration curves for that ligand. This relationship is given for AMP in the absence of phosphate as,

$$Q_{AMP} = \left[\frac{n_H}{2 - n_H}\right]^2 \quad (1.3)$$

where Q_{AMP} is the coupling quotient for AMP binding and n_H is the Hill number for AMP binding, both in the absence of phosphate. Experimentally, the Hill numbers for AMP binding are determined over a wide range of phosphate concentrations and the average Hill number as phosphate goes to zero is used. Similarly, the coupling quotient for AMP in the saturating presence of phosphate can be determined, as well as the homotropic coupling quotients in phosphate binding.

The treatment of phosphorylase data with such a systematic approach allows for the determination of the magnitude of the couplings between the various sites. Perturbations on the system generated by alterations to the protein sequence can be tested to see explicitly which parameters have been perturbed. The essential assumption that must be made with the two-state system is that only one conformation is active, and resulting data generated can only be interpreted to be stabilizing the active or inactive state (27, 28, 105). The application of linkage analysis to phosphorylase will allow not only the characterization of the effects of AMP on the wild-type system, but also allow perturbations on the system introduced through mutagenesis to be explicitly identified. Rather than simply stating that the enzyme is more or less responsive to effector as has been done in the past (68,70,73,89), linkage analysis offers the chance to determine if the change has come from a perturbation of the binding affinity, disruption of the homotropic cooperativity in binding, or from a disruption of the communication between the AMP and phosphate sites. Each type of perturbation will have a distinct effect on the relationship between the effector and substrate affinity. Considering the theoretical data presented in Figure 1.4, a change in substrate affinity would move the plot up or down. A

change in effector affinity would move the plot left or right. Changing the homotropic cooperativity in effector binding would compress or extend the range over which activation takes place, and altering the heterotropic cooperativity will alter the distance between the plateaus of substrate affinity (101).

This detailed analysis provides a powerful tool to determine the roles of the structural elements in glycogen phosphorylase *b* in the activation by AMP, and provides the opportunity to examine in detail the various models of allostery that have been proposed for phosphorylase *b*. We have set out in this study to determine if the continuous models of allostery in glycogen phosphorylase are correct, and to test the roles of the N-terminus, the acidic patch, the 280's loop, and α-helix 1 in AMP activation of phosphorylase *b*.

CHAPTER II

EXPERIMENTAL TEST OF THE KINETIC MODELS OF PHOSPHORYLASE *b* ALLOSTERY

BACKGROUND

The regulation of phosphorylase has been studied in detail for decades (1,13), however the regulatory mechanism in muscle glycogen phosphorylase is complex and still not well understood. Kinetic data from glycogen phosphorylase have traditionally been analyzed and explained using two-state models of allostery (13,63,70,). Depending on the research group and the type of experiment performed both the MWC and KNF models have been invoked (13,38). Both models can explain the global observations of allosteric systems, and can adequately predict the system's response to a perturbation, but the MWC model has been more extensively utilized due to the reduced number of fitting parameters (13). With hemoglobin and phosphofructokinase, two systems in which the 2-state models have been extensively tested, neither of the 2-state models have adequately described the allosteric properties of these systems (102,103,104). In both cases, the allosteric communications between sites were found to be unique and separable from each other.

Similarly, the 2-state models do not accurately describe the kinetics of glycogen phosphorylase. Even with the wild-type enzyme, major modifications of the 2-state models are required to explain the kinetics of glycogen phosphorylase (106). The

minimal requirement to fit such data has been to allow nonproductive binding of substrate to the inactive state of the enzyme. As a result of these inconsistencies, there has been an effort to derive a model of glycogen phosphorylase that is independent of the 2-state models. Two separate groups have developed continuous models to explain the kinetics of glycogen phosphorylase (74,76,77). One of the models also takes into account the inhibition by high concentrations of AMP (76). What both of these models have in common is the prediction that the enzyme must have AMP bound to both allosteric sites and substrate bound to both active sites before turnover can occur. These predictions are somewhat understandable given the high degree of homotropic cooperativity seen in the binding of substrates and effector (1), but are in contradiction with previous work done with a solid-state hybrid phosphorylase species that only has a single functional active site on a hybrid enzyme covalently linked to a gel matrix (107). The binding of substrate to the inactive site of the gel bound hybrids cannot be completely ruled out because the mode of inactivation used was the substitution of the active site cofactor, meaning that though doubtful the kinetic models could be correct.

Similarly, phosphofructokinase (PFK) hybrids have been studied from two different species, one having a great deal of homotropic cooperativity in effector binding (*Bacillus stearothermophilus* PFK) and the other having a great deal of homotropic cooperativity in substrate binding (*E. coli* PFK) (103,108). Both of these systems retained activity when only a single active site and a single allosteric site were monitored. In light of the previous studies done with phosphorylase and other systems, it is curious that two models developed to explain phosphorylase kinetics would make the

prediction of needing two equivalents of effector to activate the enzyme. It remains possible that the apparent requirement for both allosteric sites to be filled is explained by the high degree of homotropic cooperativity in AMP binding. That is, under normal turnover conditions, phosphorylase *b* would always have two AMP equivalents bound. In the experiments described below this prediction is tested utilizing a hybrid strategy to create a phosphorylase dimer in solution that has only one functional allosteric site. While there are significant experimental difficulties with these hybrids, the data show that activity can be measured in the absence of AMP (albeit only at extreme concentrations of phosphate) and that a very small degree of activation is observed on the binding of a single equivalent of AMP to glycogen phosphorylase *b*. Conversely, glycogen phosphorylase *a* showed full activation upon binding of a single equivalent of AMP.

MATERIALS AND METHODS

Materials: Rabbit liver glycogen, potassium phosphate, β-glycerophosphate, and AMP were purchased from Sigma-Aldrich (St. Louis, MO). Glucose-6-phosphate dehydrogenase was obtained from Roche Applied Sciences (Indianapolis, IN). Phosphoglucomutase was from Sigma-Aldrich or Roche Applied Sciences. NADP was purchased from Research Products International Corporation (Mt. Prospect, IL) Restriction enzymes and T4 DNA ligase were obtained from New England Biolabs (Beverly, MA). Klenow fragment was from Promega (Madison, WI). All other

chemicals were from Sigma-Aldrich. Ion exchange chromatography resins were from G E Healthcare (Piscataway, NJ). Size exclusion resin was from Sigma-Aldrich.

Molecular Biology: Site directed mutagenesis was carried out using a Quik Change Site Directed Mutagenesis Kit from Stratagene (La Jolla, CA). The charge tag mutants of glycogen phosphorylase, K596E and K596E/K792E, were created via site directed mutagenesis using the starting plasmid pTACTAC (65,109) and K596EpTACTAC, respectively. Similarly, the mutant R309E/R310E was created via a single round of site directed mutagenesis with either pTACTAC or K595E/K792EpTACTAC as the starting plasmids.

The plasmid pTACTACΔBglII was created by using site directed mutagenesis to mutate the first of two *Bgl*II sites downstream of the glycogen phosphorylase gene in pTACTAC (109). The sequence was changed from the consensus site AGATCT to AGAACT to prevent cutting by *Bgl*II at this site.

The plasmid pTACTACΔBglIIΔGP was created by removal of the glycogen phosphorylase gene from pTACTACΔBglII. This was accomplished by separate digestion of pTACTACΔBglII and pALTER-Ex2 (Promega) with *Nde*I and *Hind*III. The products were separated by electrophoresis on a 1.5% agarose gel. The large band of the pTACTACΔBglII digest and the small band of the pALTER-Ex2 (100 bp) digest were excised and the DNA purified using a Gel Extraction Kit from Qiagen (Valencia, CA). Approximately 30 ng of the pTACTACΔBglII fragment was combined with a 3-fold molecular excess of the pALTER-Ex2 fragment and ligated together in a 20 μl total volume reaction by overnight incubation at room temperature with T4 DNA ligase and

ATP. The resultant plasmid was transformed into XL1-Blue (*endA*1 *recA*1 *gyrA96 thi*-1 *hsd*R17 *relA1 supE44 lac*[F' *pro*A $^{+}$ B $^{+}$ *lacI*^{q} ZΔM15 *Tn*10(*Tet*^{r})]) competent cells (110). The plasmid isolated from single colonies was verified for size and by comparison to parent plasmids after both were digested with *Nde*I and *Hind*III.

The plasmid pACYC184ΔHindIII was created from pACYC184 (New England Biolabs) by removal of the singular *Hind*III site. Removal of this site was carried out by the digestion of the plasmid with *Hind*III. 17 μl of digested plasmid was mixed with 2 μl of 330 μM dNTPs and 1 μl of Klenow fragment. Reaction was run for 15 min at 25 °C followed by 20 min at 75 °C to kill all enzymes. DNA was purified by ethanol precipitation. Purified plasmid was then religated by overnight reaction with T4 DNA ligase and ATP in a 20 μl total volume reaction. Following ligation, plasmid was incubated with *Hind*III prior to transformation into XL1-Blue competent cells. Plasmid purified from single colonies was verified for correct size and the inability to be cut with *Hind*III.

The plasmid pAB1 was created via cloning from portions of pTACTACΔBglIIΔGP (expression site for glycogen phosphorylase and half of *lacI*^{q}), pACYC184ΔHindIII (p15A origin of replication and chloramphenicol resistance marker), and pJF118EH (one half of *lacI*^{q} gene)(111). Briefly, pTACTACΔBglIIΔGP was digested with *Hpa*I and *Bgl*II. pACYC184ΔHindIII was digested with *Bam*HI and *Ava*I, and pJF118EH was digested with *Ava*I and *Hpa*I. Digestion products were separated by electrophoresis on a 1.5% agarose gel, and the 3.2 kb fragment of

pACYC184ΔHindIII, the 1 kb fragment of pTACTACΔBglIIΔGP and the 0.76 kb fragment of pJF118EH were excised and purified following the protocol from a Gel Extraction Kit from Qiagen. Fragments were mixed in a 1:3:3 molecular ratio of pACYC184ΔHindIII : pTACTACΔBglIIΔGP : pJF118EH using approximately 30 ng of the pACYC184 fragment. Plasmid was then ligated overnight at room temperature by addition of T4 DNA ligase and ATP in a 20 μl total volume reaction. The resulting plasmid was transformed into XL-1Blue competent cells, and plasmid isolated from single colonies was verified by size and digestion with *Nde*1 and *Ava*1.

The plasmid pAB1GP was created by the insertion of wild-type glycogen phosphorylase gene into pAB1 between the *Nde*I and *Hind*III sites. pAB1 and pTACTAC were digested with *Nde*I and *Hind*III separately and the products separated by electrophoresis on a 1.5% agarose gel. The large band from pAB1 and the smaller band of pTACTAC were excised, and the DNA was isolated using a Gel Extraction Kit. Approximately 30 ng of the pAB1 fragment was mixed with a 3-fold molecular excess of the pTACTAC fragment and ligated overnight at room temperature by addition of T4DNA ligase and ATP in a 20 μl total volume reaction.

Protein Expression: The phosphorylase used in this study was from expression of rabbit muscle glycogen phosphorylase in *Escherichia coli* strain DF1020 (*pro-82, glnV44*(AS), *ΔpfkB201, recA56, endA1, Δ(rhaD-pfkA)200, thi-1, hsdR17)* (112,113) as previously described (65). Briefly, homodimeric wild-type or mutant enzymes were expressed from pTACTAC (65,109), and grown to saturation at 37 °C in a 40 mL overnight culture grown. Cells were diluted into 1.5 L LB and further growth was

carried out in the presence of 3 mM $MnCl_2$, 0.5 mM pyridoxine, and 0.25 mM IPTG at 27 °C for 48 hr as previously described (65). Cell pellets were typically frozen at -80 °C prior to use.

Hybrid dimers were formed *in vivo* by the co-expression of wild-type gene on pAB1GP and the gene coding for K596E/K792E/R309E/R310E on pTACTAC in DF1020 cells containing both plasmids. Co-expression required the use of both ampicillin and chloramphenicol in the growth media. Other growth conditions were identical to expression of homodimers.

Protein Purification: Protein purification was carried out with modifications of previously described methods (65). Briefly, for wild-type, cell pellets from 1.5-3 L of culture were thawed and resuspended in 75 mL of resuspension buffer (50 mM β-glycerophosphate (pH 7.0), 30 mM β-mercaptoethanol, 1 mM EDTA, 0.2 mM PMSF, 0.7 μg/mL pepstatin A, 0.5 μg/mL leupeptin, 0.01% benzamidine). Cells were lysed by sonication until the OD_{600} was approximately $1/10^{th}$ of the starting value. Debris was pelleted by centrifugation at 14,000 g for 45 min. The supernatant was brought to 0.5% polyethylenimine by addition of a 10% solution (40 mM β-glycerophosphate, 10% polyethylenimine), and stirred on ice for 30 min. The precipitate was removed by centrifugation at 14,000 g for 45 min. Solid $(NH_4)_2SO_4$ was added to the supernatant to achieve 50% saturation, and stirred on ice for 20 min. The precipitated protein was recovered by centrifugation at 14,000 g for 30 min. The pellet was resuspended in 25 mL of column buffer (25 mM β-glycerophosphate (pH 7.0), 1 mM β-mercaptoethanol, 1 mM EDTA, 0.2 mM PMSF, 0.01% benzamidine), and dialyzed against three changes of

the same buffer. The protein was then applied to DEAE-Sepharose fast flow and SP-Sepharose Fast Flow columns run in tandem. Fractions from the load and wash showing activity were pooled and used for subsequent kinetic experiments.

For mutant enzymes, K596E/K792E and K596E/K792E/R309E/R310E, purification was as for wild-type except for the chromatography. A single DEAE column was used and the protein was eluted with a 0-250 mM KCl gradient in column buffer. Fractions showing activity were pooled for use in kinetic experiments. The purity of homodimeric enzymes was checked by 10% SDS-polyacrylamide gel electrophoresis.

For hybrid dimers, purification was carried out as for the mutant homodimers, except that 2 mM AMP was included in the column buffer. In addition, hybrid dimers were run over a second DEAE column immediately prior to kinetic experiments. The purity of the hybrid was checked using non-denaturing polyacrylamide gel electrophoresis. Protein was quantified using the Pierce (Rockford, IL) BCA Protein Assay.

Kinetic Measurements: Kinetic measurements were carried out in the direction of glycogen degradation utilizing a coupled enzyme assay that linked the formation of the product glucose-1-phosphate to the formation of NADPH (Figure 2.1). Reaction assays were carried out in 600 μl total volume with 50 mM Pipes (pH 6.8), 0.1 mM EDTA, 5 mg/mL glycogen, 0-10 mM AMP, 0.03-1000 mM potassium phosphate with compensating KCl added to match maximal phosphate concentration, 0.36 mM NADP, 4 μM glucose-1,6-bisphosphate, 10 mM MgCl, 6.7 units/mL phosphoglucomutase, and 3 units/mL glucose-6-phosphate dehydrogenase. The formation of NADPH was followed

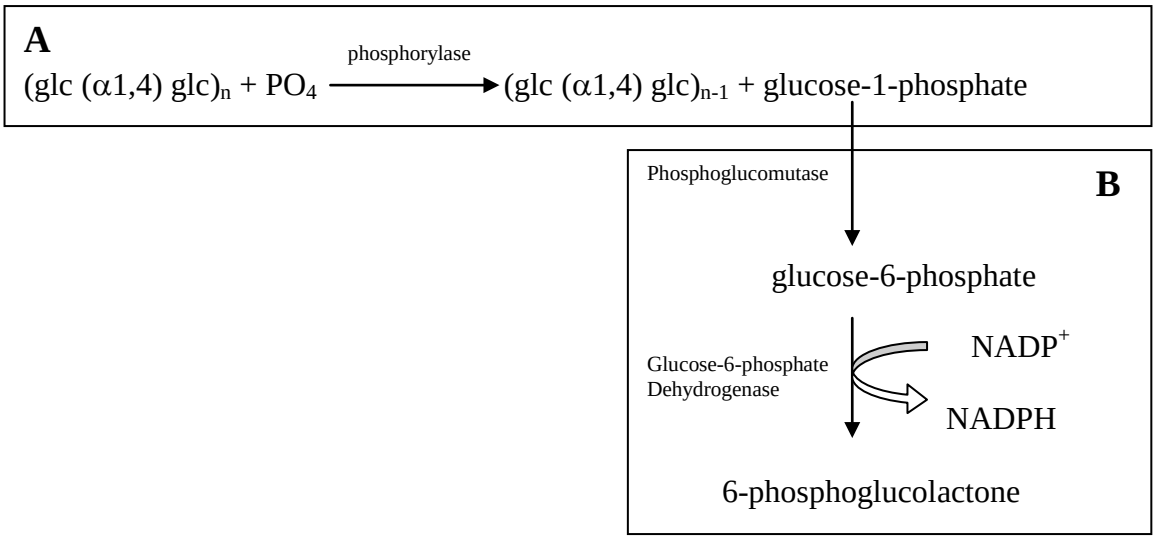

Figure 2.1: Scheme for the coupling of the reaction of glycogen phosphorylase to the production of NADPH. A) Glycogen phosphorylase reaction in the direction of glycogen degradation. B) Enzymes coupling the degradation of glycogen to the production of NADPH which can be followed as and increase in absorbance at 340 nm.

at 340 nm in a Beckman 600 Series UV/Vis spectrophotometer. The temperature was maintained at 25±1 °C by a circulating water bath. Phosphate titrations were carried out at constant AMP concentration, and then repeated at varying AMP concentrations. Forphosphorylase *a* protein was preincubated overnight with 5 mg/mL glycogen prior to kinetic experiments and the phosphate concentration was limited to 0.03-100 mM with KCl added to correspond to the maximal phosphate concentration used. Data are reported as units of activity per milligram of phosphorylase, where 1 unit is equal to 1 μmol glucose-1-phosphate formed per minute.

Native Polyacrylamide Gel Electrophoresis: Polyacrylamide gels (7.5%) were made according to the instructions for the Laemmli SDS-PAGE for Mini Protein Cell from BioRad (Hercules, CA) with the exception that the SDS was left out of the gel and both the loading, and running buffers. Protein samples were mixed with loading buffer and loaded on to the gel without heating. Electrophoresis was performed for 2 hrs at 100 V on ice.

Formation and Purification of Phosphorylase *a*: Phosphorylase *a* was made from purified phosphorylase *b* utilizing commercially available phosphorylase kinase and previously described methods (68). Hybrid phosphorylase *a* was formed by partially purifying phosphorylase via ammonium sulfate precipitation from cells co-expressing wild-type and the K596E/K792E/R309E/R310E mutant and incubating with phosphorylase kinase and ATP. Briefly, following resuspension of the ammonium sulfate pellet, the protein was dialyzed into two changes of column buffer followed by two changes of kinase buffer (50 mM Tris (pH 8), 10 mM MgCl2, and 6 mM NaF).

Phosphorylase kinase (6 mg) and 1 mM final concentration of ATP was added to the protein and allowed to react overnight. The protein was then loaded on a DEAE column at pH 7.3 and eluted with a 0-250 mM KCl gradient. Fractions with peak activity were pooled and concentrated. The protein was then loaded onto a G200 size exclusion column and the purist fractions were loaded onto a second DEAE column equilibrated at pH 7. The cleanest hybrid fractions as accessed by native polyacrylamide gel electrophoresis were selected and incubated overnight with 5 mg/mL glycogen prior to kinetic experiments.

Kinetic Analysis: Initial velocity data in the direction of glycogen degradation were plotted as a function of phosphate concentration. Titration data were fit to a modified version of the Hill equation (114) that takes into account substrate inhibition:

$$v_o = \frac{V_{max}\,[PO_4]^n}{(K_{1/2}{}^n + [PO_4]^n)\,(1 + [PO_4]/K_i)} \tag{2.1}$$

where v_o is the initial velocity measured, V_{max} is the maximal velocity, n is the Hill number, $K_{1/2}$ is the apparent average (geometric mean) dissociation constant for phosphate, and K_i is the inhibition constant for phosphate. The $K_{1/2}$ values were replotted as a function of AMP, and the resulting data were fit to

$$K_{1/2} = K_{pi}\left[\frac{K_{AMP} + [AMP]^2}{K_{AMP} + Q_{AMPPi}[AMP]^2}\right] \tag{2.2}$$

where K_{pi} is the dissociation constant for phosphate in the absence of AMP, K_{AMP} is the dissociation constant for AMP in the absence of phosphate, and Q_{AMPPi} is the heterotropic coupling quotient between AMP and phosphate. Equation 2.2 is a modified

version of the thermodynamic linkage equation derived in the absence of homotropic cooperativity in effector binding (101). The squaring of the effector concentration is an imperfect approximation for dealing with the strong homotropic cooperativity seen in AMP binding to glycogen phosphorylase *b*.

Data from phosphorylase *a*, which does not show homotropic cooperativity in AMP binding were fit to the original thermodynamic linkage equation in the absence of homotropic cooperativity in effector binding(101).

$$K_{1/2} = K_{Pi}\left[\frac{K_{AMP} + [AMP]}{K_{AMP} + Q_{AMPPi}[AMP]}\right] \quad (2.3)$$

Phosphorylase mutants that did not show activation by AMP were fit to the competitive inhibition equation;

$$K_{1/2} = K_{Pi}\left[1 + \frac{[AMP]}{K_{iAMP}}\right] \quad (2.4)$$

where K_{iAMP} is the inhibition constant for AMP (19).

RESULTS

Wild-Type Phosphoryase Kinetics: Studies of glycogen phosphorylase typically follow the reverse reaction to avoid reported non-linear kinetics (68,70). For this study, we have followed the reaction in the physiological direction of glycogen degradation. Due to the high concentrations of phosphate required to measure activity at low AMP concentrations, KCl was added to match the highest concentration of potassium phosphate added. The titration curves showed an apparent substrate inhibition at high

phosphate concentrations, but this can be taken into account by fitting the data to equation 2.1 (Figure 2.2A). Previous studies have described wild-type glycogen phosphorylase *b* as being inactive in the absence of AMP (13). This observation is certainly true under physiological concentrations of phosphate, but at high concentrations of phosphate activity can be measured. The limited data generated at low AMP concentration make determining the V_{max} difficult, but the data can be fit to equation 2.1 with the V_{max} fixed to the value found at higher AMP concentrations. Replots of $K_{1/2}$ as a function of AMP have been prepared to examine the degree of activation by AMP (Figure 2.3). The values of Hill numbers for phosphate binding at low AMP were well beyond the theoretical maximum (i.e. 2) for the dimeric system (data not shown). The finding that glycogen phosphorylase *b* can be active in the absence of AMP indicates that the proposed continuous kinetic models cannot be completely true over all concentrations. However, the modification to the models is minimal, and it is still relevant to ask if the activation by AMP requires two equivalents to be bound.

Unfortunately, the substrate inhibition observed in these experiments was shown to be an experimental artifact cause by an incorrect method of compensating for the salt effects of phosphate. While osmotic affects often dictate the properties of a solution (115), ionic strength, which takes into account the divalency of phosphate, dictates the affects on glycogen phosphorylase. When substrate titrations were carried out under conditions of equal ionic strength no substrate inhibition was observed, and the plots are biphasic indicating that phosphate may activate at high concentrations in a manner

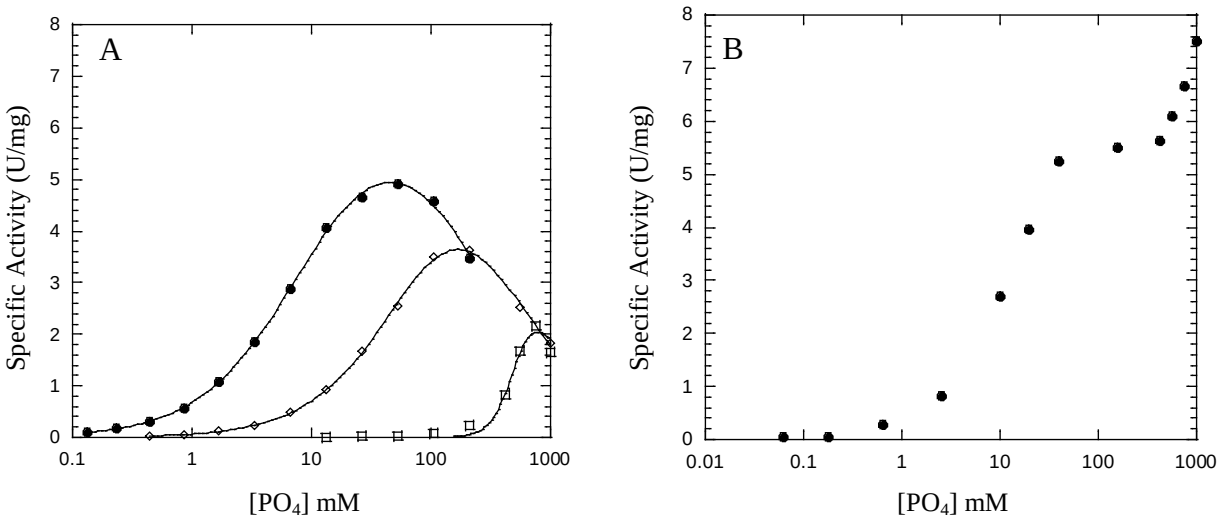

Figure 2.2: Titrations curves of wild-type glycogen phosphorylase *b*. Initial velocity data are reported as units (μmol glc-1-P / min) of activity per milligram of phosphorylase. A) Phosphate diluted with KCl to match osmolarity. AMP was at 2.5 mM (•), 0.02 mM (◊) and $7.6X10^{-5}$ mM (□). Lines represent best fit to equation 2.1. B) Phosphate titration at 0.78 mM AMP under conditions of equal ionic strength. Titrations were performed at 25 °C with 5 mg/mL glycogen.

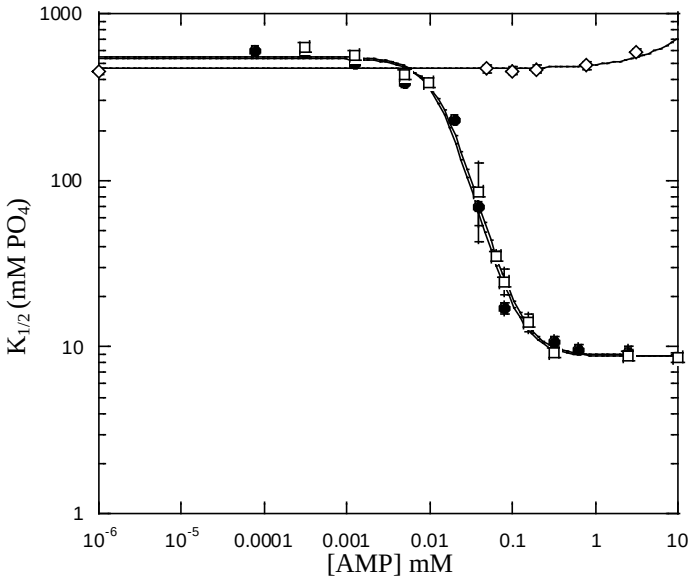

Figure 2.3: $K_{1/2}$ vs. AMP for charge-tag and allosteric site phosphorylase *b* mutants. Replots of $K_{1/2}$ vs. AMP are shown for wild-type (•), K596E/K792E (□), and K596E / K792E / R309E / R310E (◊). $K_{1/2}$ data are determined by fitting substrate titrations of phosphate at constant AMP to equation 2.1. Lines represent the best fit to equation 2.2 for wild-type and K596E/K792E or equation 2.4 for K596E / K792E / R309E / R310E. Experiments were carried out at 25 °C with 5 mg/mL glycogen.

similar to sulfate (Figure 2.2B) (62). This result may explain the high Hill numbers observed in phosphate binding at low AMP. The salt effects on the titration curves make the measured values for the affinities for substrate and effector, as well as the quantification of the heterotropic coupling, meaningless. However, the dramatic changes that have been observed with the mutants and hybrids discussed herein show clearly different trends which are relevant to the question being addressed.

Hybrid Strategy and Mutant Kinetics: Previous studies on hybrid glycogen phosphorylase involved fixing the enzyme to a solid matrix prior to dissociation and hybridization, and the activity of the enzyme was measured while it was still affixed to that matrix (107). For this study, a hybrid system was designed that allowed examination of the hybrid dimer in solution. The first challenge faced in developing our hybrid system was creating a mutant enzyme that does not bind to AMP and that can be separated and distinguished from wild-type phosphorylase. A charge-tag system, similar to what has been used with phosphofructokinase (103), was utilized to alter the chromatographic properties and allow separation via ion exchange chromatography while, at the same time, altering the electrophoretic mobility on a non-denaturing polyacrylamide gel. To this end, two surface residues of glycogen phosphorylase, which according to crystallographic structures do not appear to interact with other residues, were changed from lysine to glutamate. The phosphoryl binding pocket AMP binding site is made partially made up of arginine residues 309 and 310. To diminish the enzyme's ability to bind AMP, residues 309 and 310 were changed to glutamate (13). The resultant mutants were combined to form the final K596E/K792E/R309E/R310E

used to make the hybrid dimers. The mutant K596E/K792E/R309E/R310E could be clearly distinguished from the wild-type homodimer on native-polyacrylamide gel electrophoresis (Figure 2.4, Lanes 1 and 2).

***b* Hybrid Formation:** Despite reports on various methods to reversibly dissociate glycogen phosphorylase *b* (107,116,117), attempts to utilize heat, citrate, KSCN, and mercury benzoate all failed to form hybrid dimers. As such, another strategy had to be employed. Since co-expression of wild-type and mutant *E. coli* PFK was shown to be successful in formation of hybrids in that system (103,104), a similar strategy was applied here. In order to achieve co-expression, the expression strain had to be transformed with two plasmids; one expressing wild-type phosphorylase, and the other expressing a mutant enzyme. In order for two plasmids to be maintained in one cell they had to contain different origins of replication, and different selection markers (118). In addition, glycogen phosphorylase must be under an inducible promoter to avoid cell toxicity (65). The expression strain used here (DF1020) does not contain the *lacI*^{q} gene. The requirements for the second expression plasmid for glycogen phosphorylase were an origin of replication other than colE1, a selection marker other than ampicillin resistance, a lac promoter driving expression of the glycogen phosphorylase gene, and the lacI^{q} gene. No suitable plasmid could be located from commercial sources, so the plasmid pAB1GP was created utilizing the expression cassette from pTACTAC, the p15a origin and chloramphenicol resistance from pACYC184 and the lacIq gene from pJF118EH as described in the Material and Methods section. pAB1GP, being a lower

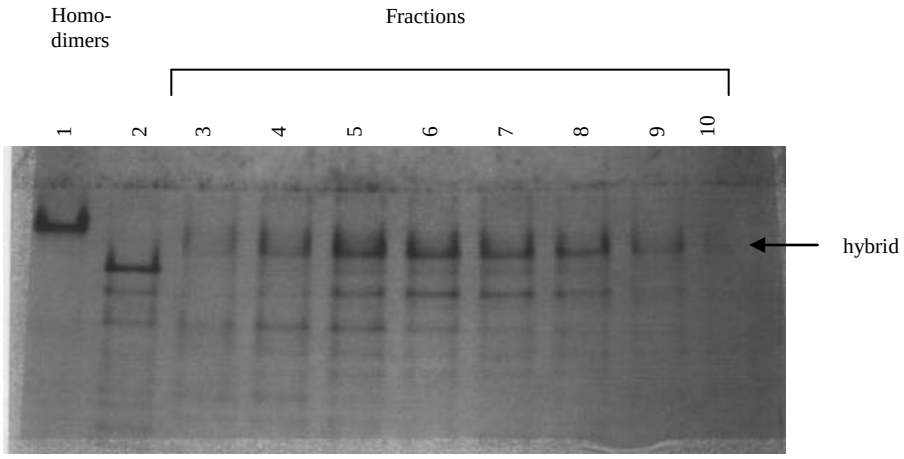

Figure 2.4: Native gel from phosphorylase *b* hybrid purification. Non-denaturing 7.5% polyacrylamide gel showing the positions of the parent homodimers of wild-type (lane 1), K596E/K792E/R309E/R310E (lane 2), and hybrid fractions (lanes 3-10) eluted form DEAE-Fast Flow Sepharose column. Elution was performed by using a 0-250 mM KCl linear gradient. Gel was run on ice for 2 hr at 100 V.

copy number plasmid, was used to express wild-type phosphorylase during hybrid expression.

Cells with both plasmids pTACTAC with the gene for the K596E / K792E / R309E / R310E mutant and pAB1GP were grown in media containing both ampicillin and chloramphenicol, and glycogen phosphorylase was purified normally until resuspension of the ammonium sulfate pellet. 2 mM AMP had to be included in the column buffer in order to stabilize the hybrid dimers. Three peaks of activity eluted from a DEAE-Fast Flow Sepharose column. The first peak eluted in the wash and was shown to be wild-type. On application of a 0-250 mM KCl gradient to the column, two additional peaks were eluted. The first proved to contain hybrid dimer and the second was the mutant parent (Figure 2.4). The hybrids could not be entirely separated from the mutant homo-dimer. Special care was taken to ensure that no wild-type dimer was present in protein used for kinetics. The hybrids proved to be stable for no more than 24 hrs, and after 48 hr wild-type homodimers could be detected in native gels. As such, kinetic experiments were completed within 24 hrs of purifying hybrid dimers.

***a* Hybrid Formation:** Hybrids of phosphorylase *a* were formed via co-expression as with phosphorylase *b*. Conversion to phosphorylase *a* was carried out by phosphorylation during the course of the purification. Isolation of the *a* hybrid dimer proved to be far more challenging than that of phosphorylase *b*. Ultimately, the combination of a size exclusion chromatography column followed by two DEAE chromatography columns (run at slightly different pH values) provided good separation and relatively pure hybrid dimers. (Figure 2.5)

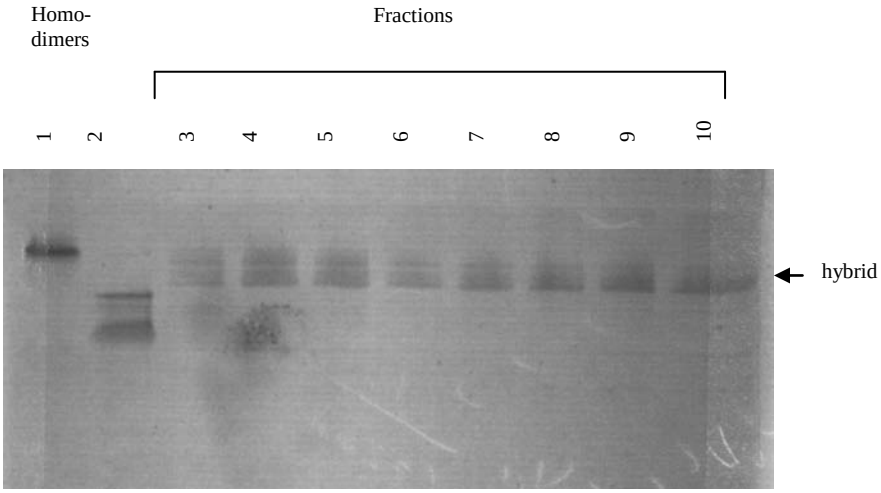

Figure 2.5: Native gel from phosphorylase *a* hybrid purification. Non-denaturing 7.5% polyacrylamide gel showing the positions of the parent homodimers of wild-type (lane 1), K596E/K792E/R309E/R310E (lane 2), and hybrid fractions (lanes 3-10) eluted form DEAE-Fast Flow Sepharose column. Elution was performed by using 0-250 mM KCl linear gradient. Gel was run on ice for 2 hr at 100 V.

Kinetics: The charge-tag mutant K596E/K792E was tested to verify that the introduction of these mutations had not significantly altered the kinetics of the enzyme. As can be seen in Figure 2.3, the affinities for phosphate and the response to AMP is nearly identical to wild-type. This was repeated for the phosphorylase *a* form of both wild-type and the K596E/K792E mutant. As can be seen in Figure 2.6 there is no significant effect of the modifications on the observed kinetic values.

The mutations R309E and R310E were added to selectively knock out binding of AMP to the allosteric site. Inhibition at high AMP is still expected as binding to the purine inhibition site should not be affected. This mutant was tested in both the *a* and *b* forms. The *b* form binds phosphate with slightly higher affinity than wild-type at low AMP, but there is no evidence of activation AMP. (Figure 2.3) As expected at high AMP concentrations the curve trends up presumably due to binding at the purine inhibition site. The *a* form of the mutant binds phosphate with lower affinity than wild-type, but there is no observable activation by AMP (Figure 2.6).

The phosphorylase *b* hybrid dimer bound phosphate at low concentrations of AMP somewhat more weakly than either wild-type or the parent mutant. (Figure 2.7) Unlike the parent mutant the hybrid dimer shows some activation by AMP. This activation is much weaker than that of wild-type, but it is evident from the replot of $K_{1/2}$ that some activation is realized.

Contrary to what was observed with the phosphorylase *b* hybrid, the phosphorylase *a* hybrid bound phosphate more tightly than either wild-type or the parent

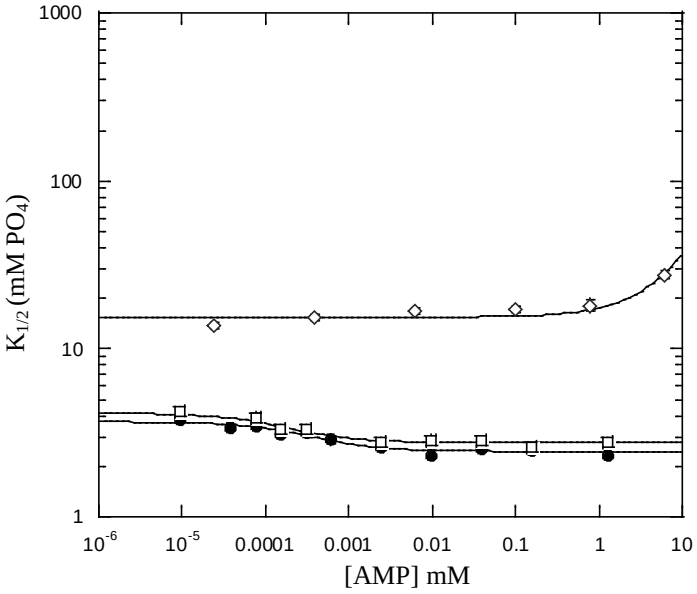

Figure 2.6: $K_{1/2}$ vs. AMP for charge tag and allosteric site phosphorylase *a* mutants. Replots of $K_{1/2}$ vs. AMP are shown for wild-type (•), K596E/K792E (□), and K596E / K792E / R309E / R310E (◊). $K_{1/2}$ data were determined from fitting of individual phosphate titration curves at constant AMP to the Michaelis-Menton equation. Lines are represent the best fit to equation 2.3 for wild-type and K596E/K792E or equation 2.4 for K596E / K792E / R309E / R310E. Experiments were carried out at 25 °C with 5 mg/mL glycogen.

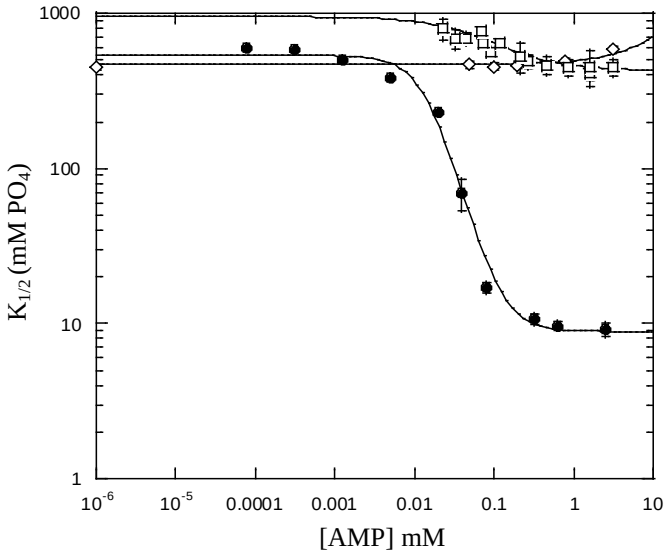

Figure 2.7: Hybrid phosphorylase *b* $K_{1/2}$ vs. AMP. Replot of $K_{1/2}$ for phosphate as a function of AMP are shown for wild-type (•), K596E/K792E/R309E/R310E (◊), and the hybrid dimer (□). $K_{1/2}$ data were determined by fitting individual phosphate titration at constant AMP to equation 2.1. Lines are best fit to equation 2.2 for wild-type and hybrid or equation 2.4 for K596E/K792E/R309E/R310E. Experiments carried out at 25 °C with 5 mg/mL glycogen.

mutant. (Figure 2.8) The degree of activation by AMP is very similar to that found with wild-type.

The maximal activity of the *b* hybrid dimer falls between that of wild-type and the K596E/K792E/R309E/R310E mutant, but it falls short of the mean between them (Table 2.1). The maximal activity of the *a* form of the hybrid falls well below that of either parent mutant for unknown reasons. The difference between the maximal activities between *a* form and *b* form is due to two factors. First, phosphorylation increases the maximal activity of glycogen phosphorylase (Chapter IV). Second, the maximal salt concentration utilized in measuring kinetics of *b* form was nearly 10-fold higher than that used with the *a* form, and there were significant salt effects observed.

DISCUSSION

Most phosphorylase data have been understood with the generally accepted premise that there is an absolute requirement for AMP for the activity of phosphorylase *b* (13,68). Physiologically, where phosphate concentrations are less than 10 mM (19), this is certainly true, but the results with wild-type phosphorylase *b* shown here demonstrate that turnover does occur in the absence of AMP (Figure 2.1 and 2.2). Little data have been generated with phosphorylase at high substrate concentrations, probably due to a general assumption that V_{max} is increased by AMP as well as the effect on $K_{1/2}$ for substrate (1). In this study, there is no evidence of an affect of AMP on V_{max} (Chapter III). There are, however, dramatic effects on the affinity for phosphate. Technically, neither of the proposed continuous kinetic models of AMP activation can

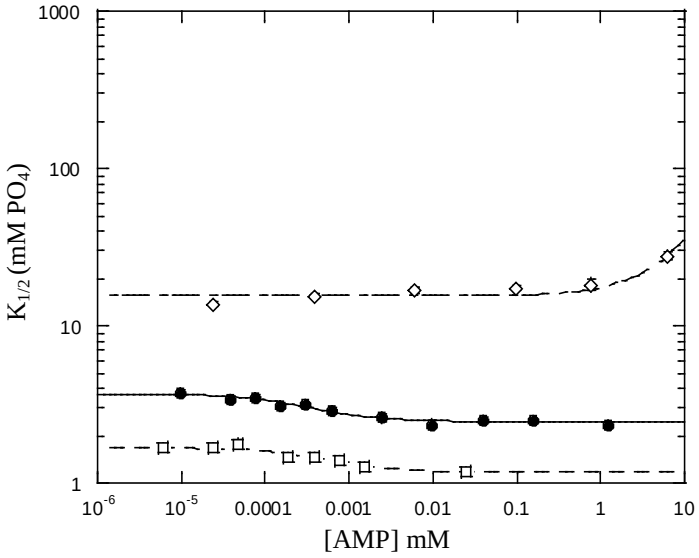

Figure 2.8: Hybrid phosphorylase *a* $K_{1/2}$ vs. AMP. Replot of $K_{1/2}$ for phosphate as a function of AMP are shown for wild-type (•), K596E/K792E/R309E/R310E (◊), and the hybrid (□). $K_{1/2}$ data were determined from fitting of individual phosphate titration curves at constant AMP to the Michaelis-Menton equation. Lines represent the best fit to equation 2.3 for wild-type and hybrid or equation 2.4 for K596E/K792E/R309E/R310E. Experiments carried out at 25 °C with 5 mg/mL glycogen.

Table 2.1: V_{max} for phosphorylase *a* and *b* variants used for hybrids.

	b Form[a]	a Form[b]
Enzyme	**V_{max}** (U/mg)	**V_{max}** (U/mg)
Wild-type	7.1±0.2	29.8±0.3
K596E/K792E/ R309E/R310E	1.47±0.04	28±1
Hybrid dimer	2.8±0.1	11.8±0.24

[a] Determined with salt concentration equal to 1 M potassium phosphate.
[b] Determined with salt concentration equal to 100 mM potassium phosphate

be correct because they both require the binding of AMP prior to any activity (74,76,77). However, given the relevant concentrations under which phosphorylase is active, the addition of turnover in the absence of AMP is a rather minimal alteration. The data collected and used to establish the continuous kinetic models of phosphorylase activation would not be significantly affected by this additional branch (76). Likewise, the finding that a *b* hybrid dimer is activated to a slight degree by AMP must technically mean that the model is not correct with respect to activation by AMP (Figure 2.6). However, the activation is so slight that it would be indistinguishable in the wild-type data used to develop the models (76). The observations made here provide rather dramatic evidence that with respect to wild-type phosphorylase *b* the continuous kinetic models proposed are essentially correct. Only under extreme conditions would phosphorylase be induced to deviate from the models of activation as proposed. It must also be noted that both the models being investigated and the data presented here rule out both of the 2-state models as an accurate description of the kinetics of glycogen phosphorylase *b*.

It is interesting to note that the activation by AMP in the *b* hybrid is similar in extent to that observed with phosphorylase *a* (approximately a 25% decrease in $K_{1/2}$ for phosphate). It may be that the mechanism preserved in the *b* hybrid dimer is the same mechanism by which phosphorylase *a* is activated by AMP.

Given that phosphorylase is a dimeric enzyme and that the mutant forms used in this study have altered maximal activity from wild-type, the maximal activity of a hybrid would be expected to be the mean of the activities of the two parent enzymes as long as both the active sites maintain full function in the hybrid. It must be acknowledged that

the maximal activity of the hybrid dimers do not match the theoretically predicted values. The *b* form of the hybrid has an activity that falls between that of the parent homodimers, but it falls short of the mean. (Table 2.1) This may be in part due to the difficulty in accurately measuring the maximal activity in the face of the apparent substrate inhibition. Of far greater concern is the activity of the *a* hybrid form. The activity of this hybrid falls below that of either parent. (Table 2.1) The Michaelis-Menten type kinetics of phosphorylase *a* allow for a better determination of maximal activity, and the activity observed falls to less than half that of the parent mutants. The low activity suggests a problem with the structure of the hybrid or indicates that only a single active site was functional. The cause of this anomaly is unknown. The activation of phosphorylase *a* being completely preserved in the hybrid is perhaps an indication that it is an intrasubunit effect rather than an intersubunit effect.

CHAPTER III

THE N-TERMINUS OF GLYCOGEN PHOSPHORYLASE *b* IS NOT REQUIRED FOR ACTIVATION BY AMP

BACKGROUND

Glycogen phosphorylase was the first enzymes recognized as being allosterically regulated, as well as the first case of regulation by phosphorylation (8,52,63). The allosteric regulation of glycogen phosphorylase was one of the early examples used in deriving the traditional 2-state models of allostery (27), despite the later realization that the 2-state models do not truly explain the kinetics of glycogen phosphorylase as discussed in Chapter II. The activating phosphorylation of phosphorylase *b* takes place at serine 14 and converts the enzyme to the more active phosphorylase *a*.

Recognition that muscle phosphorylase was activated by phosphorylation at serine 14, led to much early interest in the role of the N-terminus in the activation of phosphorylase (31, 43). The work done to establish the role of the N-terminus was published in 1968 and utilized phosphorylase *b'*, a form of the enzyme that had the first 16 residues removed via proteolysis (31). The reported results stated that all of the allostery in phosphorylase was lost in the absence of the N-terminus. Specifically, it was found that AMP did not affect the affinity for phosphate and phosphate did not affect the affinity for AMP. In addition, there was no homotropic cooperativity in the binding of substrate or effectors observed with phosphorylase *b'*. These findings led to the conclusion that the N-terminus was responsible for transmitting the allosteric signal in

phosphorylase *b*. As the age of structural biology was born, the conclusions drawn from phosphorylase *b'* were and have remained the basis for interpreting the crystallographic structures of glycogen phosphorylase (63,68,83). It must be noted, however, that phosphorylase *b'* was derived by limited proteolysis of enzyme purified from rabbit muscle, and that there were additional effects of proteolysis on the primary structure of the enzyme. Given that modern experimental techniques, particularly in molecular biology and data analysis, have advanced the ability to specifically address the role of the N-terminus of glycogen phosphorylase, we have undertaken this study to evaluate the significance of the N-terminus of glycogen phosphorylase *b* in activation by AMP. We report here, for the first time, the full magnitude of the effect of AMP on glycogen phosphorylase *b*. We also show that the N-terminal truncate lacking the first 17 residues, Δ2-17, of rabbit muscle glycogen phosphorylase retains all of the heterotropic and homotropic cooperativity observed in wild-type phosphorylase, but Δ2-17 has a reduced affinity for both AMP and phosphate. In addition, we were able to apply the same experimental design to the proteolytically derived phosphorylase *b'*. These data and experimental techniques are compared to the original findings with phosphorylase *b'*.

The use of constant ionic strength in these experiments allows the quantification of the kinetic constants for glycogen phosphorylase without ambiguity. Unlike the data reported in Chapter II, the data reported here are not obscured by salt effects from the addition of phosphate, and reflect the properties of the enzyme under the experimental conditions.

MATERIALS AND METHODS

The phosphorylase used in this study was obtained from bacterial expression of the recombinant rabbit muscle glycogen phosphorylase gene in the plasmid pTACTAC obtained from Robert J. Fletterick as previously described (65). Purified phosphorylase was stored at 4 ºC and generally used within one week. β-glycerophosphate was from Sigma-Aldrich (St. Louis, MO) or USB (Cleveland, OH). Restriction enzymes were from New England Biolabs (Beverly, MA). Ion exchange chromatography resins were from Amersham Biosciences (Piscataway, NJ). Size exclusion resin, glycogen phosphorylase kinase, trypsin, and soybean trypsin inhibitor were from Sigma-Aldrich. Glucose-6-phosphate dehydrogenase was from Roche Applied Sciences (Indianapolis, IN). Phosphoglucomutase was from Roche Applied Sciences or Sigma-Aldrich. Other chemicals were from Sigma-Aldrich.

Mutagenesis/Molecular Biology: The plasmid pTACTAC with the gene for wild-type glycogen phosphorylase gene from rabbit muscle inserted between *Nde*I and *Hind*III sites as previously described was used as the starting template for mutagenesis (65). The truncate Δ2-17 was created by using Quik Change Site Directed Mutagenesis Kit (Stratagene, La Jolla, CA) to introduce a second *Nde*I cut site positioning the starting ATG at codon 17. The resulting plasmid was digested to completion with *Nde*I and gel purified to remove the DNA sequence between codons 1 and 17. The plasmid was then re-ligated to obtain the plasmid with a phosphorylase gene missing the DNA residues coding for amino acids 2 through 17.

Protein Expression and Purification: Wild-type and mutant phosphorylase were expressed from plasmid pTACTAC as previously described (65) with the exception that the growth was carried out in *E. coli* strain DF1020 (*pro-82, glnV44*(AS), *ΔpfkB201, recA56, endA1, Δ(rhaD-pfkA)200, thi-1, hsdR17*) (112, 113) for 48 hr at 27 ºC in 1.5 L cultures that were inoculated with 40 mL of culture grown to saturation at 37 ºC in the absence of inducer. Cell pellets from expression were stored at -80 ºC prior to protein purification. Protein purification was carried out with modifications of previously described methods (65). Briefly, wild-type cell pellets from 1.5-3 L of culture were thawed and resuspended in 75 mL of resuspension buffer (50 mM β-glycerophosphate (pH 7.0), 30 mM β-mercaptoethanol, 1 mM EDTA, 0.2 mM PMSF, 0.7 μg/mL Pepstatin A, 0.5μg/mL Leupeptin, 0.01% Benzamidine). Cells were lysed by sonication until the OD_{600} was approximately $1/10^{th}$ of the starting value. Debris were pelleted by centrifugation at 14,000 g for 45 min. The supernatant was brought to 0.5% polyethylenimine by addition of a 10% solution (40 mM β-glycerophosphate, 10% polyethylenimine) and stirred on ice for 30 min. The precipitate was removed by centrifugation at 14,000 g for 45 min. Solid $(NH_4)_2SO_4$ was added to the supernatant to 50% saturation, and stirred on ice for 20 min. The precipitated protein was recovered by centrifugation at 14,000 g for 30 min. The pellet was resuspended in 25 mL of column buffer (25 mM β-glycerophosphate (pH 7.0), 1 mM β-mercaptoethanol, 1 mM EDTA, 0.2 mM PMSF, 0.01% Benzamidine), and dialyzed against three changes of the same buffer. Protein was then run over DEAE-Sepharose Fast Flow and SP-Sepharose Fast

Flow columns run in tandem. Fractions from load and wash showing activity were pooled and used for subsequent kinetic and fluorescence experiments.

For Δ2-17, purification was the same as above until the chromatography. Δ2-17 was loaded on a Q-Sepharose Fast Flow column and eluted with a 0-300 mM KCl gradient in column buffer. The cleanest fractions (as assessed by 10% SDS-polyacrylamide gel electrophoresis) with activity were pooled, dialyzed to remove salt, and loaded on a DEAE-Sepharose Fast Flow column. Elution was done with a 0-300mM KCl gradient in column buffer. The cleanest fractions with activity were pooled and dialyzed to remove salt prior to use in kinetic and fluorescence studies. Protein was quantified using Pierce (Rockford, IL) BCA protein assay.

Phosphorylase *a* and Phosphorylase *b'*: Phosphorylase *a* was synthesized and isolated utilizing purified phosphorylase *b* and commercially available phosphorylase kinase as previously described (70). Phosphorylase *b'* was made using phosphorylase *a* following the protocol of Graves (31).

Kinetic Measurements: Glycogen phosphorylase activity was followed in the direction of glycogen degradation at 25 ºC utilizing phosphoglucomutase and glucose-6-phosphate dehydrogenase in a coupled enzyme assay system to link the degradation of glycogen to the production of reduced NADPH, which was followed at 340 nm on a Beckman 600 series UV/VIS spectrophotometer. Assays were carried out in a 600 µL reaction volume containing 50 mM PIPES (pH6.8), 100 µM EDTA, 5 mg/mL rabbit liver glycogen, 0-5 mM AMP, 0-300 mM potassium phosphate, 360 µM NADP, 4 µM glucose-1,6-bisphosphate, 10 mM $MgCl_2$, 6.7 U/mL phosphoglucomutase, 3 U/mL glucose-6-

phosphate dehydrogenase. Changes in ionic strength due to varying phosphate concentrations were compensated for by the addition of appropriate amounts of KCl. Temperature was maintained within 1 ºC by a circulating water bath. The assay mixes were preincubated at 25 ºC, and the reaction was initiated by addition of appropriately diluted glycogen phosphorylase.

Steady State Fluorescence: Spectral measurements were collected on an SLM-4800 instrument with a Phoenix upgrade package from ISS (Champaign, IL). Spectra were collected with a 295 nm excitation wavelength at 25 ºC in a 1 cm by 1 cm cuvette. Excitation slits were set to 2 nm, and emission slits were set to 8 nm. All measurements were collected with protein in column buffer. The same buffer without protein was used as a blank to correct spectra. For experiments with AMP, 2 mM AMP was added to the blank as well as the sample.

Data Analysis: Initial velocity data were plotted as titrations for both phosphate and AMP and individual titration curves fit to the Hill equation to determine $K_{1/2}$ and Hill number (114). Replots of Hill number for AMP vs. phosphate were used to establish the homotropic coupling between AMP sites at low phosphate concentration per equation 3.1 (101).

$$Q_{AMP} = \left[\frac{n_H}{2 - n_H} \right]^2 \tag{3.1}$$

where Q_{AMP} is the homotropic coupling quotient in AMP binding in the absence of phosphate. n_H is the Hill number for AMP binding in the absence of phosphate. Analogous approaches were used to quantify the homotropic coupling quotient for AMP

binding in the saturating presence of phosphate, as well as the homotropic coupling quotient for phosphate binding in the absence and saturating presence of AMP.

Quantification of the heterotropic coupling between AMP and phosphate was carried out with replots of $K_{1/2}$ for phosphate as a function of AMP utilizing the thermodynamic linkage approach of Reinhart (equation 3.2) with the values for homotropic coupling quotients for AMP binding fixed to the values established by the replots of Hill number (101).

$$K_{1/2} = K_{Pi}^{o}\left[\frac{K_{AMP}^{o\ 2} + 2K_{AMP}^{o}[AMP] + Q_{AMP}[AMP]^2}{K_{AMP}^{o\ 2} + 2K_{AMP}^{o}Q_{AMPPi}\left[\frac{Q_{AMP}}{Q_{AMP\,/\,Pi}}\right]^{1/2}[AMP] + Q_{AMPPi}{}^2 Q_{AMP}[AMP]^2}\right]^{1/2} \quad (3.2)$$

where K_{Pi}^{o} is the dissociation constant for phosphate in the absence of AMP. K_{AMP}^{o} is the dissociation constant for the first equivalent AMP in the absence of phosphate. Q_{AMP} is the homotropic coupling for AMP binding in the absence of phosphate. $Q_{AMP\,/\,Pi}$ is the homotropic coupling for AMP binding in the saturating presence of phosphate. Q_{AMPPi} is the heterotropic coupling quotient between AMP and phosphate.

The measured coupling quotients were converted to the free energy of coupling by the relationship between free energy and the coupling quotient given in equation 3.3.

$$\Delta G_{coupling} = -RT\ln Q \quad (3.3)$$

where $\Delta G_{coupling}$ is the free energy of coupling, R is the gas constant, T is the temperature, and Q is the coupling quotient of interest.

Activity Gels: Equal units of activity for WT and Δ2-17 glycogen phosphorylase *b* were applied to 7.5% non-denaturing polyacrylamide gel, and electrophoresis was carried out at 100 V for 2 hr on ice. As previously described, gels were in incubated with 1% glycogen, 20 mM glucose-1-phosphate, 10 mM AMP in 50 mM PIPES buffer (pH 6.8) for AMP activation, or 1% glycogen 30 mM glucose-1-phosphate, 0.6M$(NH_4)_2$ SO_4 in 50 mM PIPES (pH 6.8) for sulfate activation (3). Incubation was carried out for 4 hr at room temperature. Following incubation gels were stained with a saturated solution of I_2 and photographed.

RESULTS

Wild-type Phosphorylase *b* Expression and Kinetics: Glycogen phosphorylase when expressed in *E. coli* is isolated as pure *b* form due to the lack of phosphorylase kinase. Wild-type phosphorylase *b* was successfully expressed in *E. coli* DF1020 and gave similar yields to those previously reported (65). Titrations were carried out from 0 to 330 mM phosphate and 0-5 mM AMP under constant ionic strength. There is little to no effect on V_{max} for the enzyme upon addition of AMP while there is a dramatic effect on the affinity for phosphate. The replots of Hill number vs. phosphate or AMP allow the quantification of the homotropic cooperativity (Figure 3.1 and Table 3.1). Once the values for homotropic effects in AMP binding are established the replot of $K_{1/2}$ for phosphate vs. AMP can be fit to equation 3.2 and the coupling between AMP and phosphate can be quantified (Figure 3.2 and Table 3.1). This experimental approach

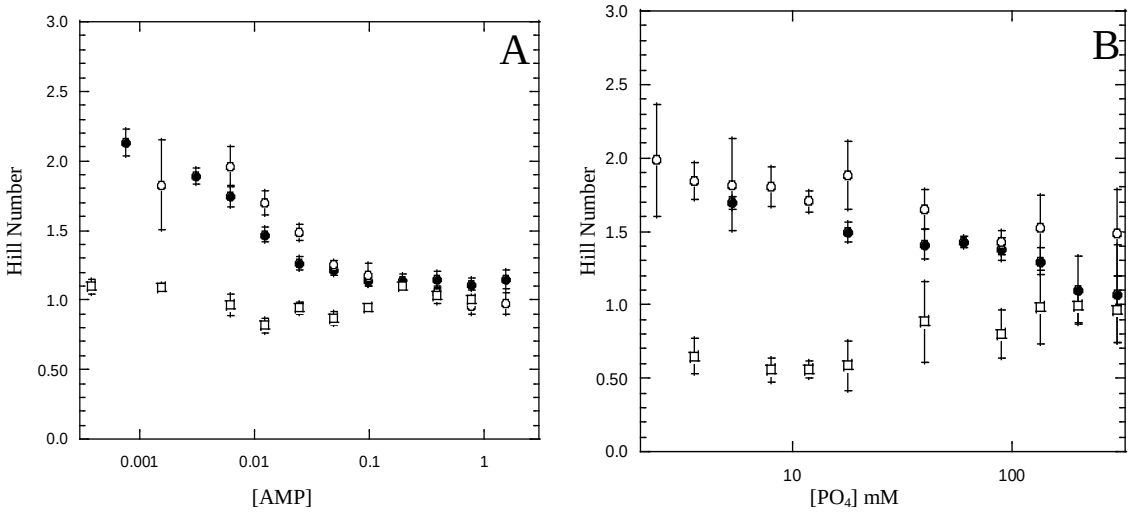

Figure 3.1: Replots of Hill number vs. the other ligand for wild-type and N-terminal truncates. (A) Replot of Hill number for phosphate vs. AMP. (B) Replot of Hill number for AMP vs. phosphate. Wild-type is shown as filled circles (•). Δ2-17 is shown as open circles (o). Phosphorylase *b'* is shown as open squares (□).

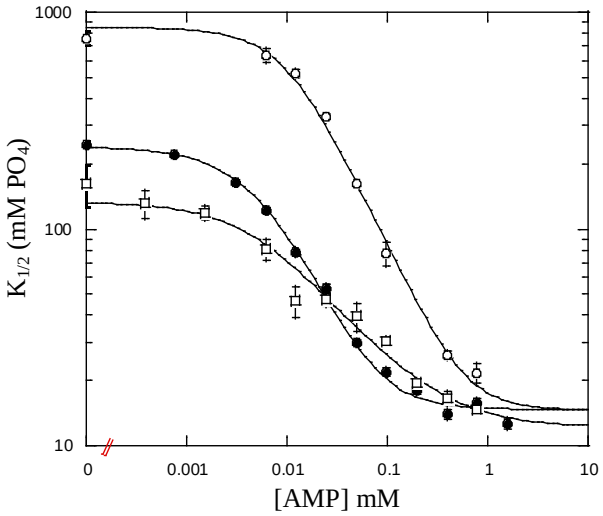

Figure 3.2: Replot of $K_{1/2}$ for phosphate as a function of AMP for wild-type and N-terminal truncates. Wild-type (•), Δ2-17 (o), and Phosphorylase *b'* (□) are shown with standard errors. $K_{1/2}$ data were determined from phosphate titrations fit with the Hill equation. Lines represent the best fit to equation 3.2 with values for homotropic coupling quotients for AMP fixed to the values determined from the Hill numbers observed in AMP titrations at high and low phosphate. All experiments were carried out with constant ionic strength at 25° C and with 5 mg/mL glycogen present.

Table 3.1: Kinetic constants and coupling free energies for wild-type (WT *b*), Δ2-17, and phosphorylase *b'* (*b'*).

	WT *b*	Δ2-17	*b'*
K_{Pi}^{o} (mM)[a]	259±3	848±29	129±10
K_{AMP}^{o} (mM)[a]	0.43±0.01	5.8±0.4	0.033±0.005
$\Delta G_{Pi\text{-}AMP}$ (kJ/mol)[b]	-7.5±0.4	-10±2	-6±1
ΔG_{Pi} (kJ/mol)[c]	-15± 4	-11±2	0.0
$\Delta G_{Pi/AMP}$ (kJ/mol)[c]	-1.4± 0.2	-0.2±0.1	0.0
ΔG_{AMP} (kJ/mol)[d]	-5.9± 4	-11.5±0.6	4.6±0.8
$\Delta G_{AMP/Pi}$ (kJ/mol)[d]	-0.9± 0.4	-7±2	-0.39±0.07

[a]Dissociation constants and heterotropic coupling free energy determined from replots of $K_{1/2}$ for phosphate as a function of AMP. [b]$\Delta G_{Pi\text{-}AMP}$ is coupling free energy between AMP and phosphate, which is calculated from the heterotropic coupling quotient. [c]ΔG_{Pi} and $\Delta G_{Pi/AMP}$ are homotropic couplings in absence and saturating presence of AMP respectively. [d]ΔG_{AMP} and $\Delta G_{AMP/Pi}$ are homotropic coupling free energy for AMP in absence and saturating presence of phosphate respectively. Homotropic free energies calculated from Hill numbers in absence and saturating presence of other ligand.

allows the measurement of activity in the absence of AMP allowing the complete quantification of the coupling between AMP and phosphate.

Δ2-17 Expression and Kinetics: DNA manipulation of the gene for rabbit muscle glycogen phosphorylase allows for the creation of a mutant protein that lacks the N-terminus (Δ2-17). The mutant protein was successfully created, expressed, and purified. When the kinetics of the Δ2-17 mutant are measured, it displays a reduced affinity for AMP and phosphate as can be observed by the curve being shifted up and to the right in Figure 3.2 (also Table 3.1). A clear dependence of the affinity for phosphate on the presence of AMP is observed, and conversely there is a clear dependence of the affinity for AMP on the presence of phosphate (Figures 3.2 and 3.3). Comparing the free energies of coupling in Table 3.1, it can be seen that there is slightly more cooperativity observed between AMP and phosphate binding with the Δ2-17 mutant compared to wild-type. The absence of the N-terminus clearly did not alleviate the heterotropic cooperativity in phosphorylase. The Δ2-17 enzyme also retains homotropic cooperativity with respect to both AMP and phosphate as reported in Table 3.1. To rule out the possibility of significantly altered secondary or tertiary structure in the Δ2-17 mutant, the intrinsic tryptophan fluorescence emission spectrum was recorded with excitation at 295 nm. The spectrum of Δ2-17 matched the spectra of wild-type for both apo and with 2 mM AMP (data not shown). To test the ability of sulfate to activate Δ2-17, electrophoresis was carried out with wild type and Δ2-17 on 7.5% non-denaturing polyacrylamide gels. After reaction in the direction of glycogen synthesis by incubation

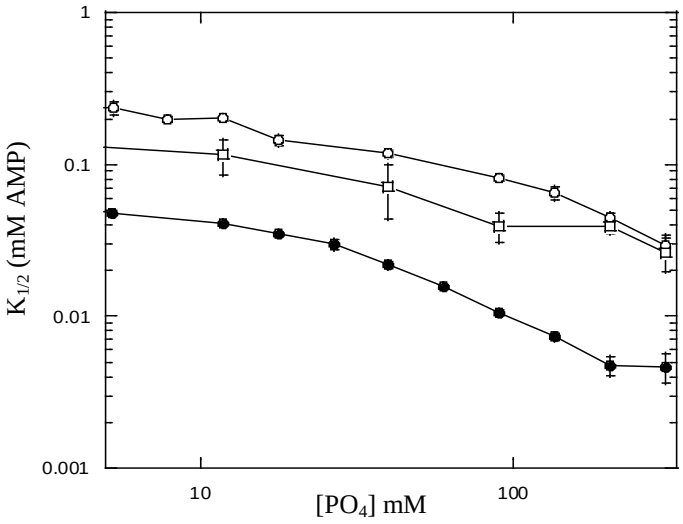

Figure 3.3: Line plot of $K_{1/2}$ for AMP as a function of phosphate for wild-type and N-terminal truncates. Wild-type (•), Δ2-17 (o), and Phosphorylase *b'* (□) are shown with standard errors. Data generated with constant ionic strength at 25°C with 5 mg/mL glycogen.

with glycogen and glucose-1-phosphate the gels were stained with iodine. Although AMP activates both wild-type and Δ2-17, Δ2-17 is not activated by sulfate (Figure 3.4).

Phosphorylase *b'*: To assess the differences between our findings with Δ2-17 and the originally published results in the absence of the N-terminus, we created phosphorylase *b'* from wild-type phosphorylase *a* according to the original protocols (31). As previously reported, phosphorylase *b'* had a higher affinity for phosphate and AMP (Figure 3.2 and Table 3.1). However, there is still a great dependence of the affinity for phosphate on the presence of AMP. Interestingly, the slope of the transition region is much reduced with respect to both wild-type and Δ2-17. In agreement with the previous work (31), there is no evidence for cooperativity in binding of phosphate at any concentration of AMP. At low phosphate concentrations, the Hill number for AMP is approximately 0.56±0.03 indicating significant negative homotropic cooperativity in AMP binding. (Figure 3.1B) The Hill number returns to unity at higher concentrations of phosphate, indicating that this is a real case of negative homotropic cooperativity.

DISCUSSION

Wild-Type Phosphorylase: Previously, phosphorylase *b* has been held to be inactive without AMP present (13,52,63), but under the experimental conditions used in this study, activity can be measured and affinity for phosphate can be determined even in the absence of AMP. These data, when analyzed with linkage analysis rather than simply using a model that assumes an equilibrium between active and inactive forms of the

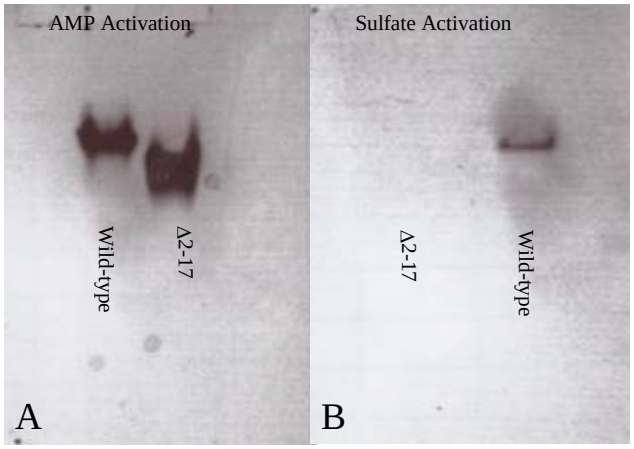

Figure 3.4: Activity gels with wild-type and Δ2-17 glycogen phosphorylase *b*. Activity shown by 4hr incubation of equal units of wild-type and Δ2-17 in (A) 1% glycogen, 20 mM glc-1-phosphate, 10 mM AMP or (B) 1% glycogen, 20 mM glc-1-phosphate, and 1 M $(NH_4)_2SO_4$. Stain developed by incubation with iodine.

enzyme, allow the complete quantification of the allostery in glycogen phosphorylase *b* with respect to AMP and phosphate. Many previous reports have shown the activation by AMP, but none have quantified the extent of coupling (13,31,67). This report provides a complete analysis of the extent of heterotropic coupling between phosphate and AMP in glycogen phosphorylase *b*.

Δ2-17 and Phosphorylase *b'*: The results with the truncate Δ2-17 are in clear disagreement with the previously reported loss of cooperativity in phosphorylase *b'* (31). Loss of affinity for both substrate and effector is evident, but there is no loss in heterotropic coupling. (Figure 3.2) In contrast, it is clear that substantial homotropic cooperativity with both AMP and phosphate has been retained in the absence of the N-terminus. In light of these findings, the current proposal that the N-terminus transmits the allosteric signal across the subunit interface becomes highly improbable. The possibility that these differences are due to the trivial cause of different experimental conditions has been ruled out by examination of phosphorylase *b'*. When phosphorylase *b'* was tested under the same conditions as Δ2-17, results similar to those originally reported were found, confirming that there are different heterotropic and homotropic cooperativities in Δ2-17 and phosphorylase *b'*. The likely source of these differences is the use of proteolysis to generate phosphorylase *b'*. It has been reported previously (31) that phosphorylase is cleaved multiple times under the conditions used to remove the N-terminus. These additional cleavages were assumed to be inconsequential. However, the findings that Δ2-17, which is of known primary structure, retains both homotropic and heterotropic cooperativity indicate that the additional cleavage sites in phosphorylase *b'*

have dramatic effects. Irrespective of these differences, examining phosphorylase *b'* over a much larger concentration range of AMP shows that there is a great deal of heterotropic activation retained. The two variants lacking the N-terminus both show that allosteric activation by AMP is present in the absence of the N-terminus, though it is much reduced with phosphorylase *b'* (Figure 3.2), leading to the conclusion that the N-terminus is not required for the activation by AMP.

The N-terminus being located at the subunit interface may be an artifact of the crystallization method rather than the mechanism by which the allosteric signal is transmitted. It appears that the N-terminus probably does have a role in establishing the binding characteristics of phosphorylase, since the affinities for phosphate and AMP are greatly altered in its absence. However that role is independent of any role in the allosteric coupling in the enzyme, which is not greatly disturbed. Also of interest, the N-terminus is clearly implicated in activation by phosphorylation and by high concentrations of sulfate (61,62). It has been a long standing theory that the activation of phosphorylase proceeds via the same mechanism irregardless of what the activation input is (13,52). Of course, phosphorylase cannot be activated by phosphorylation in the absence of the N-terminus, but activation by sulfate is also dependent on the N-terminus (Figure 3.4) (62). Previous structural studies have shown that the activation by sulfate proceeds via an interaction with both the N-terminus and the phosphoserine recognition site (62). The lack of activation by sulfate in the absence of the N-terminus (Figure 3.4) provides a strong indication that the mechanism of activation with phosphorylation may in fact be distinct from the activation by AMP.

Conclusions: Our understanding of the activation of glycogen phosphorylase has all been based on research looking at very narrow concentration ranges of substrates and AMP, and with a proteolytically derived enzyme of unknown primary structure (31). The new findings reported here indicate that the proteolysis dramatically altered the properties of phosphorylase in ways unrelated to the N-terminus and the broader concentration ranges used here have unmasked the effects of AMP in the absence of the N-terminus. The structural interpretations of the activation of glycogen phosphorylase should be reevaluated in the light of these new findings.

CHAPTER IV

THE ROLE OF THE ACIDIC PATCH OF GLYCOGEN PHOSPHORYLASE *b* BY AMP

BACKGROUND

Glycogen phosphorylase was the first enzyme to be characterized as an allosteric enzyme as well as the first enzyme to be shown to be regulated by phosphorylation (8). Physiologically, phosphorylase is activated by either phosphorylation of serine 14 or the noncovalent binding of AMP (8). *In vitro*, phosphorylase can also be activated by sulfate and polyamines (30,61). There are numerous crystallographic structures of glycogen phosphorylase in both the more active phosphorylated form (phosphorylase *a*) and the less active unphosphorylated form (phosphorylase *b*) as well as in numerous ligation states with both activators and inhibitors bound (for reviews see ref 8 and 13).

Much of our understanding of phosphorylase regulation hinges on the interpretations of crystallographic data. The N-terminus (residues 1-22) is located at the acidic patch (residues 96, 105, 109, 110, 120, 501, 493, 505, 509) on its own subunit in some, but not all, reported inactive conformations, and the N-terminus is found at the subunit interface in some reported active structures (71). It has long been thought that this movement is a key mechanism of activation that brought about the tertiary and quaternary changes that lead to activation (13). The location of the phosphoserine recognition site at the subunit interface, being partially made up of arginines 43 and 69 of the opposite subunit, has been well established structurally as well as confirmed

kinetically (13,89). The issue is far more complicated with respect to activation by AMP. The current proposal is that the activation of phosphorylase utilizes the same global mechanism of activation whether activated by AMP or phosphorylation, though some small local differences have been recognized (8,13). The first key piece of evidence that supports the proposal of a single activation mechanism was the failure of phosphorylase *b'* (a proteolytically derived variant) to be activated by AMP suggesting that the N-terminus was required for activation by AMP (31). Second, crystallographic structures of reported R-state phosphorylase *b* showed the N-terminus bound at the subunit interface with a sulfate replacing the phosphoryl group of phosphorylase *a* (13). New evidence from our lab has shown that the N-terminus is not required for activation by AMP (Chapter III), but that the lack of the N-terminus greatly diminishes the affinity for AMP and phosphate.

It is clear that the N-terminus plays a role in establishing the kinetic properties of both phosphorylase *a* and *b*. However, the finding that the N-terminus is required for activation by sulfate but not by AMP has raised the question of whether or not activation by AMP is mechanistically equivalent to activation by phosphorylation. In order to address this question, we have made mutations to alter the interactions of the N-terminus with the acidic patch to either favor the binding of the N-terminus (K544E) or diminish the binding (E105A) as well as altering arginine 16 on the N-terminus that is poised to interact with these residues (66). In addition, we have examined the fluorescence emission from the active site cofactor in the apo and AMP bound forms of both phosphorylase *a* and *b*. Contrary to previous proposals, our results show that activation

of phosphorylase *b* by AMP results in an active site different from that of phosphorylase *a*. We also show modification of residues expected to support the interaction of the N-terminus with the acidic patch enhance activity while modifications expected to destabilizing binding of the N-terminus to the acidic patch leads to a less active enzyme. These data support the hypothesis that the active form of glycogen phosphorylase *b* has the N-terminus bound at the acidic patch rather than at the subunit interface, and that the activations by AMP and phosphorylation are not equivalent.

MATERIALS AND METHODS

The phosphorylase used in this study was obtained from bacterial expression of the recombinant rabbit muscle glycogen phosphorylase gene obtained from Robert Fletterick as previously described (65). Purified protein was stored at 4 ºC and generally used within one week. β-glycerophosphate was from Sigma-Aldrich (St. Louis, MO) or USB (Cleveland, OH). Restriction enzymes were from NEB (Beverly, MA). Ion exchange chromatography resins were from Amersham Biosciences (Piscataway, NJ). Size exclusion resin and glycogen phosphorylase kinase were from Sigma-Aldrich. Glucose-6-phosphate dehydrogenase was from Roche Applied Sciences (Indianapolis, IN). Phosphoglucomutase was from Roche Applied Sciences or Sigma-Aldrich. Other chemicals were from Sigma-Aldrich.

Mutagenesis/Molecular Biology: The plasmid pTACTAC with the gene for wild-type glycogen phosphorylase gene from rabbit muscle inserted between *Nde*I and *Hind*III sites as previously described was used as the starting template for mutagenesis (65). The

mutants K544E, E105A, R16A and R16E were created by using Quik Change Site Directed Mutagenesis Kit (Stratagene, La Jolla, CA). K544E/Δ2-17 used the previously described Δ2-17 phosphorylase gene in pTACTAC as the starting plasmid for mutagenesis (Chapter III). Resulting plasmids were sequenced to verify the mutations.

Protein Expression and Purification: Wild-type and mutant phosphorylase were expressed from plasmid pTACTAC as previously described (65) with the exception that the growth was carried out in *Escherichia coli* strain DF1020 (*pro-82, glnV44*(AS), *ΔpfkB201, recA56, endA1, Δ(rhaD-pfkA)200, thi-1, hsdR17*) (112,113) for 48 hr at 27 ºC in 1.5 L cultures that were inoculated with 40 ml of culture grown to saturation at 37 ºC in the absence of inducer. Cell pellets from expression were stored at -80 ºC prior to protein purification. Protein purification was carried out with modifications of previously described methods (65). For wild-type, cell pellets from 1.5-3 L of culture were thawed and resuspended in 75 mL of resuspension buffer (50 mM β-glycerophosphate (pH 7.0), 30 mM β-mercaptoethanol, 1 mM EDTA, 0.2 mM PMSF, 0.7 μg/mL Pepstatin A, 0.5μg/mL Leupeptin, 0.01% Benzamidine). Cells were lysed by sonication until the OD_{600} was approximately $1/10^{th}$ of the starting value. Debris was pelleted by centrifugation at 14,000g for 45 min. The supernatant was brought to 0.5% polyethylenimine by addition of a 10% solution (40 mM β-glycerophosphate, 10% polyethylenimine), and stirred on ice for 30 min. The precipitate was removed by centrifugation at 14,000g for 45 min. Solid $(NH_4)_2SO_4$ was added to the supernatant to 50% saturation, and stirred on ice for 20 min. The precipitated protein was recovered by centrifugation at 14,000g for 30 min. The pellet was resuspended in 25 mL of column

buffer (25 mM β-glycerophosphate (pH 7.0), 1 mM β-mercaptoethanol, 1 mM EDTA, 0.2 mM PMSF, 0.01% Benzamidine), and dialyzed against three changes of the same buffer. Protein was then run over DEAE-Sepharose fast flow and SP-Sepharose Fast Flow columns run in tandem. For K544E the columns were washed with 50 mM KCl in Column Buffer. Fractions from load and wash showing activity were pooled and used for subsequent kinetic and fluorescence experiments.

The purification of K544E/Δ2-17was the same as above until the chromatography step. K544E/Δ2-17 was loaded on a Q-Sepharose Fast Flow column and eluted with a 0-300 mM KCl gradient in column buffer. The cleanest fractions (as assessed by 10% SDS-polyacrylamide gel electrophoreses) with activity were pooled, dialyzed to remove salt and loaded on a DEAE-Sepharose Fast Flow column and eluted with a 0-300 mM KCl gradient in Column buffer. The cleanest fractions with activity were pooled and dialyzed to remove salt prior to use in kinetic and fluorescence studies. Protein was quantified using Pierce (Rockford, IL) BCA protein assay.

Phosphorylase *a*: Phosphorylase *a* was synthesized and isolated utilizing purified phosphorylase *b* and commercially available phosphorylase kinase as previously described (70).

Kinetic Measurements: Glycogen phosphorylase activity was followed in the direction of glycogen degradation at 25 ºC utilizing phosphoglucomutase and glucose-6-phosphate dehydrogenase in a coupled enzyme assay system to link the degradation of glycogen to the production of reduced NADPH, which was followed at 340 nm on a Beckman 600 series UV/VIS spectrophotometer. Assays were carried out in a 600 µL reaction volume

containing 50 mM PIPES (pH6.8), 100 µM EDTA, 5 mg/mL rabbit liver glycogen, 0-5 mM AMP, 0-300 mM potassium phosphate, 360 µM NADP, 4 µM glucose-1,6-bisphosphate, 10 mM $MgCl_2$, 6.7 U/mL phosphoglucomutase, 3 U/mL glucose-6-phosphate dehydrogenase. Changes in ionic strength due to varying phosphate concentrations were compensated for by the addition of appropriate amounts of KCl. Temperature was maintained within 1ºC by a circulating water bath. The assay mixtures were preincubated at 25ºC, and the reaction was initiated by addition of appropriately diluted glycogen phosphorylase.

Steady State Fluorescence: Spectral measurements were collected on an SLM-4800 instrument with a Phoenix upgrade package from ISS (Champaign, IL). Spectra were collected with a 330 nm excitation wavelength at 25 ºC in a 1cm by 1cm cuvette. Excitation slits were set to 2 nm, and emission slits were set to 8 nm. All measurements were collected with protein in column buffer. The same buffer without protein was used as a blank to correct spectra. For experiments with AMP, 2 mM AMP was added to the blank as well as the sample.

Data Analysis: Initial velocity data were plotted as titrations for both phosphate and AMP and individual titration curves fit to the Hill equation to determine $K_{1/2}$ and Hill number (114). Replots of Hill number for AMP vs. phosphate were used to establish the homotropic coupling between AMP sites at low phosphate concentration per equation 4.1 (101).

$$Q_{AMP} = \left[\frac{n_H}{2 - n_H} \right]^2 \qquad (4.1)$$

where Q_{AMP} is the homotropic coupling quotient in AMP binding in the absence of phosphate. n_H is the Hill number for AMP binding in the absence of phosphate. Analogous approaches were used to establish the homotropic coupling quotient for AMP under saturating concentrations of phosphate.

Quantification of the heterotropic coupling between AMP and phosphate was carried out with replots of $K_{1/2}$ for phosphate as a function of AMP utilizing the thermodynamic linkage formalism of Reinhart (eq. 4.2) with the values for homotropic coupling in AMP binding fixed to the values established by the replots of Hill number as described above (101).

$$K_{1/2} = K_{Pi}^{o}\left[\frac{{K_{AMP}^{o}}^{2} + 2K_{AMP}^{o}[AMP] + Q_{AMP}[AMP]^2}{{K_{AMP}^{o}}^{2} + 2K_{AMP}^{o}Q_{AMPPi}\left[\frac{Q_{AMP}}{Q_{AMP\,/\,Pi}}\right]^{1/2}[AMP] + {Q_{AMPPi}}^{2}Q_{AMP}[AMP]^2}\right]^{1/2} \quad (4.2)$$

where K_{Pi}^{o} is the dissociation constant for phosphate in the absence of AMP. K_{AMP}^{o} is the dissociation constant for AMP in the absence of phosphate. Q_{AMP} is the homotropic coupling for AMP binding in the absence of phosphate. $Q_{AMP\,/\,P}$ is the homotropic coupling for AMP binding in the saturating presence of phosphate. Q_{AMPPi} is the heterotropic coupling between AMP and phosphate. Alternatively, the coupling quotient Q_{AMPPi} can be determined directly as the ratios of $K_{1/2}$ for phosphate in the absence and saturating presence of AMP. Free energies of coupling were calculated using the following relationship between Q and ΔG.

$$\Delta G = -RT\ln Q \quad (4.3)$$

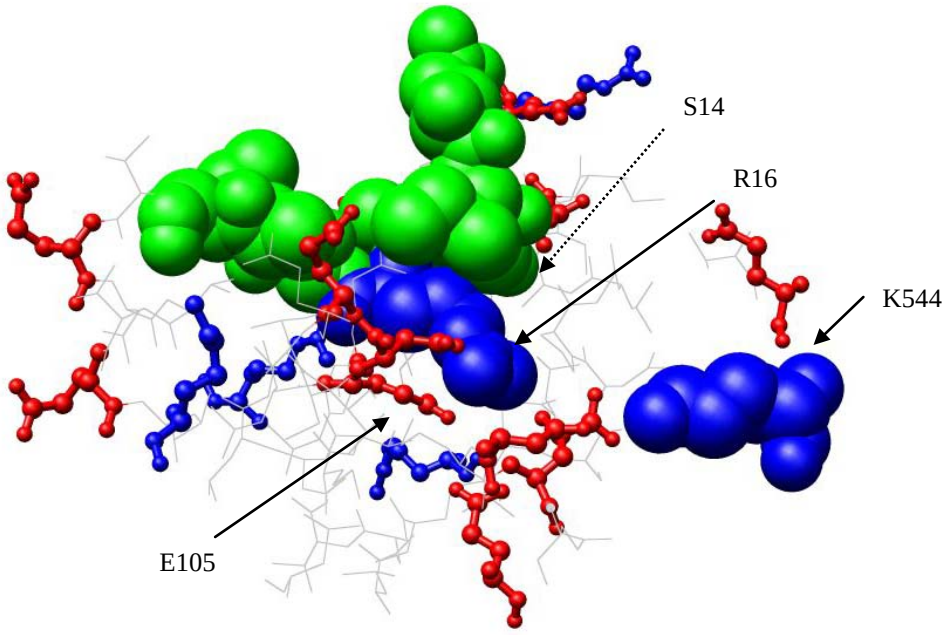

Figure 4.1: The acidic patch of glycogen phosphorylase. K544, R16, and the remainder of the N-terminus (from residue 12) are shown in space-filling. Uncharged residues of the N-terminus are shown in green. Positively charged residues are shown in blue, and negatively charged residues are shown in red. S14 extends behind N-terminus (shown with dashed arrow).

Molecular Modeling: Graphic of acidic patch of glycogen phosphorylase was generated from crystal structure solved by Martin, Johnson, and Withers (Protein Data Bank 2gpb) using the UCSF Chimera package from the Resource for Biocomputing, Visualization, and Informatics at the University of California, San Francisco (supported by NIH P41 RR-01081) (119,120).

RESULTS

The Acidic Patch: In an effort to establish the roles of the N-terminus and the acidic patch, mutations were made in the acidic patch to strengthen or weaken interactions with the N-terminus. In a reported T-state conformation, the positive charge on lysine 544 is shown to line up with the positive charge of arginine 16 (Figure 4.1) (66). The mutation K544E was made to enhance the affinity of the N-terminus at the acidic patch by replacing this unfavorable ionic interaction with a favorable one. The K544E mutant binds phosphate and AMP more tightly as can be seen as a shift down and left in the replot of $K_{1/2}$ for phosphate as a function of AMP in Figure 4.2. The heterotropic coupling between AMP and phosphate was reduced slightly, though the free energy of coupling remains within error (Figure 4.3 and Table 4.1). Fitting of the curve shown in Figure 4.4A shows that the binding affinity for the first equivalent of AMP is reduced somewhat, however there is also an enhancement in homotropic cooperativity in AMP binding (Figure 4.5). The net result is that there is a significant reduction in $K_{1/2}$ for AMP with the K544E mutation (Figure 4.4B). The mutation K544E is predicted to

Table 4.1: Kinetic constants for wild-type and acidic patch mutants of glycogen phosphorylase *b*.

	K^{o}_{Pi} [a,e] (mM)	K^{o}_{AMP} [c,e] (mM)	Q_{AMPPi} [d,e]	k_{cat} (s^{-1})	n_{HPi} [g] -AMP / +AMP	n_{HAMP} [h] - Pi / +Pi
Wild-type b[b]	940±40	0.44±0.02	92±5	40±2	1.90±0.05 / 1.14±0.01	1.52±0.05 / 1.11±0.03
Wild-type a	21±1	ND	1.7[f]	51±1	1[i] / 1[i]	1[i] / 1[i]
K544E	430±30	1.82±0.08	53±4	8.9±0.2	1.88±0.02 / 1.07±0.02	1.90±0.05 / 1.46±0.03
E105A	1160±80	3.39±0.08	86±6	46±5	1.98±0.06 / 1.05±0.04	1.95±0.06 / 1.63±0.03
R16A	118±1	0.093±0.004	10.40±0.02	16.7±0.3	1.63±0.05 / 1.15±0.01	1.42±0.05 / 1.02±0.02
R16E	77±4	0.024±0.002	6.3±0.3	24.4±0.5	1.31±0.03 / 1.07±0.03	1.23±0.02 / 1.06±0.06

[a] Dissociation constant for phosphate in absence of AMP. [b] Initial affinity for phosphate value differ from values reported in Chapter III (and consequently the coupling quotient value) due to a change in glycogen lot used. Values are constant with a given lot of glycogen, but vary from lot to lot. [c] Dissociation constant for the first equivalent of AMP in the absence of phosphate. [d] Coupling quotient between phosphate and AMP. [e] Determined from fitting replots of $K_{1/2}$ for phosphate vs. AMP to equation 4.2. [f] Determined directly from ratio of affinity for phosphate in the absence and saturating presence of AMP rather than by curve fitting. [g] Hill number in phosphate binding in the absence and saturating presence of AMP. [h] Hill number in AMP binding in the absence and saturating presence of phosphate. [i] No homotropic cooperativity is obsereved with phosphorylase *a*.

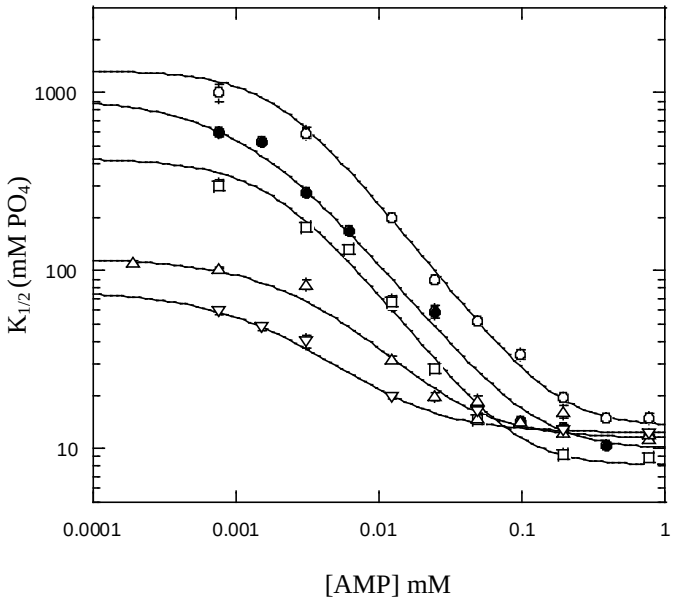

Figure 4.2: Replot of $K_{1/2}$ for phosphate as a function of AMP for wild-type and acidic patch mutants. $K_{1/2}$ data were determined from fitting phosphate titrations at constant AMP to the Hill equation. Data are shown for wild-type (•), K544E (□), E105A (o), R16A (Δ), R16E (∇). Lines represent best fit to equation 4.2 with the homotropic coupling quotients for AMP fixed to the values calculated from the Hill numbers observed in AMP binding. Experiments carried out at 25°C under constant ionic strength. Glycogen was at 5 mg/ml.

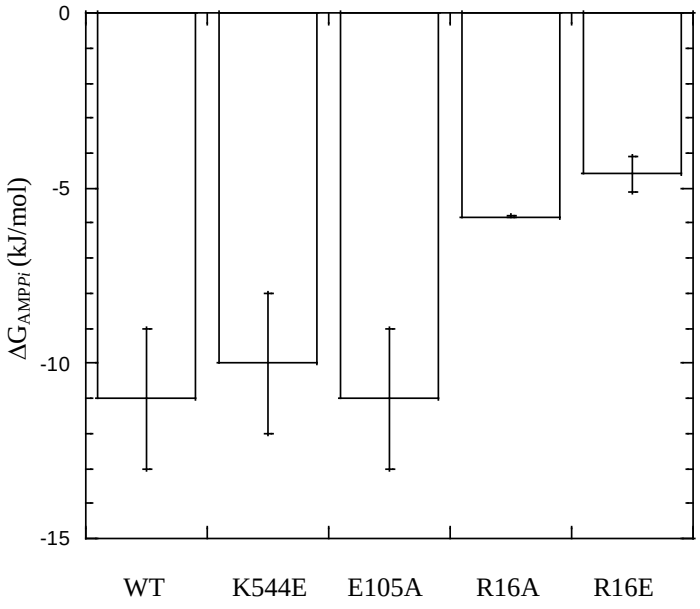

Figure 4.3: Heterotropic free energy of coupling between AMP and phosphate for wild-type and acidic patch mutants of glycogen phosphorylase. ΔG_{AMPPi} are calculated from Q_{AMPPi} determined from fitting of replots of $K_{1/2}$ for phosphate as a function of AMP to equation 4.2.

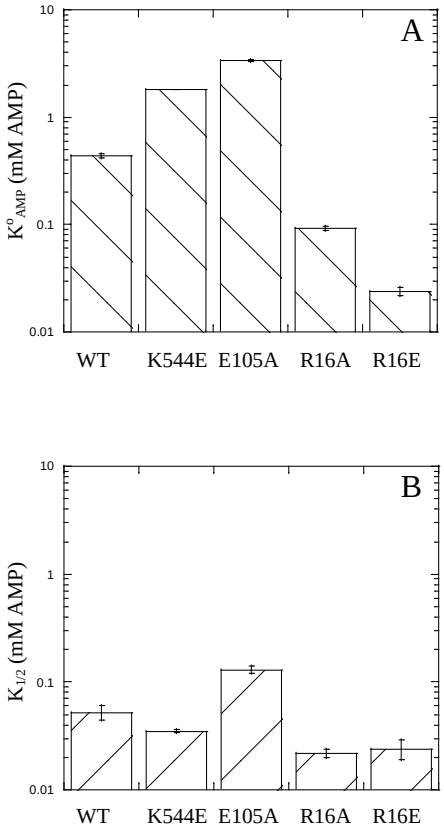

Figure 4.4: Affinity for AMP at low concentrations of phosphate for wild type and acidic patch mutants. A) The binding affinity of first equivalent of AMP as found from fits of the replot of $K_{1/2}$ for phosphate as a function of AMP is shown for wild-type and each mutant. B) The binding affinity for AMP determined from titrations of AMP at low concentrations of phosphate is shown for wild-type and each mutant. The tighter binding shown in B is the result of homotropic cooperativity in AMP binding.

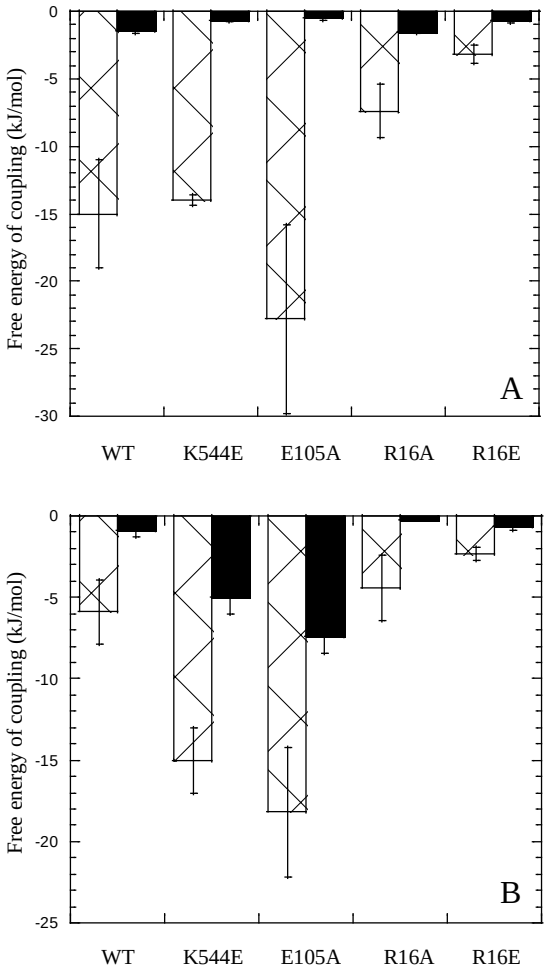

Figure 4.5: Free energies of homotropic coupling for wild-type and acidic patch mutants. A) The homotropic coupling in phosphate binding. B) The homotropic coupling in AMP binding. Cross hatched columns are in absence of other ligand. Filled columns are in the saturating presence of other ligand. Values come from averaging the Hill numbers at the limits of replots of Hill number as a function of the other ligand. Conversion to free energy was done using relationships in equations 4.1 and 4.3. Error bars are standard error of averages.

support binding of the N-terminus to the acidic patch. To rule out the possibility that the effect of K544E was simply an effect on overall protein structure, the K544E mutant was combined with a truncate lacking the N-terminus. It was found that in the absence of the N-terminus the kinetics closely resembled the truncate alone (data not shown).

Glutamate 105 makes favorable contacts with arginine 16 at the acidic patch. To test the effect of weakening the binding of the N-terminus at the acidic patch the mutant E105A was constructed. Contrary to what was seen with the K544E mutant, the replots of $K_{1/2}$ for phosphate as a function of AMP for the E105A mutant show a curve that is shifted up and over to the right indicating a weakening of binding for both AMP and phosphate (Figure 4.2). Indeed, the kinetic constants determined for E105A show this mutant does bind to AMP and phosphate with less affinity than wild-type (Table 4.1 and Figure 4.4). The heterotropic coupling between AMP and phosphate remain similar to wild-type, while there is an enhancement in homotropic cooperativity for the binding of both AMP and phosphate.

Arginine 16: The effects of both K544E and E105A are expected to be mediated through an interaction with arginine 16. For purposes of comparison position 16 was mutated to both alanine and glutamate. As can be seen in Figure 4.2 both mutants enhance the binding of phosphate in the absence of AMP with the effect of R16E being stronger than that of R16A. Likewise both position 16 mutants show an enhanced binding to AMP (Table 4.1 and Figure 4.4). There is a reduction in the heterotropic coupling seen between AMP and phosphate as well as reduced homotropic cooperativity in both AMP and phosphate binding with both mutants which is all consistent with the

apo state of these mutants more closely resembling the fully saturated form (Figures 4.3 and 4.5).

Inspection of Figure 4.2, demonstrates that while the mutants tested have a wide range of effect on the affinity for phosphate in the absence of AMP, the curves all converge to similar values in the saturating presence of AMP. This observation is consistent with the N-terminus affecting the initial affinity for phosphate but not the activation by AMP. This idea is further lent support by comparison of the results of homotropic cooperativities particularly in the absence of the other ligand. In all cases, mutants that enhanced affinity diminished the homotropic cooperativity, while mutants that diminished affinity also enhanced homotropic cooperativity for that mutant. The results with K544E and E105A would seem to indicate that stabilizing the N-terminus at the acidic patch stabilizes the active state of the enzyme. This is contrary to the notion that activation by phosphorylation and AMP result in similar conformations with the N-terminus bound at the subunit interface.

Fluorescence of Phosphorylase *a* and *b*: To further investigate the differences by AMP and phosphorylation, fluorescence spectroscopy was utilized to examine the cofactor at the active site for each (Figure 4.6). High concentrations of phosphorylase *a* were unobtainable due to the propensity to crystallize at higher concentrations (89), and the lower concentration of protein resulted in the emission spectra for phosphorylase *a* being far more noisy. It is clear, however, that the emission spectra differ between phosphorylase *a* and *b* in the absence and presence of AMP as well as in the observed response to AMP binding. The two peaks observed are due to the two conformations of

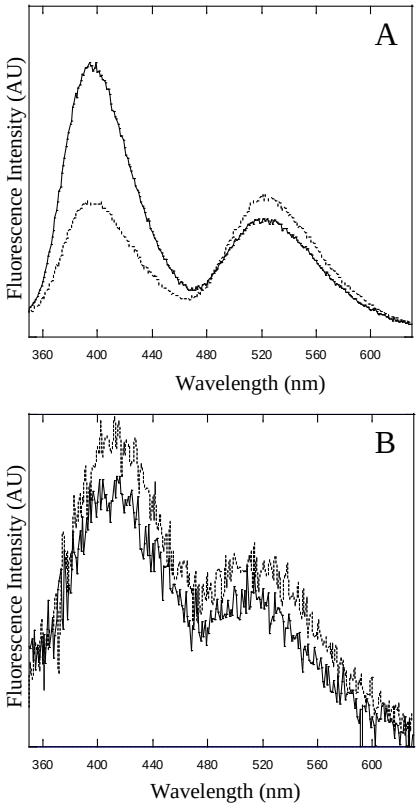

Figure 4.6: Steady-state fluorescence emission spectra of wild-type glycogen phosphorylase cofactor excited at 330 nm. A) The emission of phosphorylase *b*. B) The emission from phosphorylase *a*. Solid line is apo emission. Dotted line is with 2 mM AMP. Change seen in A is by far the most dramatic observed.

cofactor (121). The lower wavelength peak is due to the enol form of the cofactor, while the higher wavelength peak is due to the keto form, and the ratio between forms is sensitive their environments. The relative emission from the enol and keto peaks of phosphorylase *a* and *b* have been shown to vary significantly between protein preparations. However, it has been found that the relative positions of the peaks are consistent between purifications and independent of AMP. It can be seen that phosphorylation shifts the peaks closer together (approximately 400 nm and 520 nm for *b* form and 410 nm and 510 nm for *a* form). The addition of AMP to phosphorylase *b* does not induce such a shift. Addition of AMP does however induce a reduction in enol form emission and an increase in keto form emission from phosphorylase *b*. This diminishing of the enol emission with addition of AMP to phosphorylase *b* occurred with different preparations of phosphorylase *b*, however the magnitude of the change is clearly dependent on the relative amount enol form in the apo enzyme. Figure 4.6A shows the most dramatic difference observed. This effect on the ratio between peaks is not seen on addition of AMP to phosphorylase *a*, however an overall increase in intensity was noted.

DISCUSSION

The accepted structural mechanism of glycogen phosphorylase activation involves the movement of the N-terminus from the acidic patch to the subunit interface (13). Our previous results have shown that this could not be completely true due to the full activation seen in the absence of the N-terminus (Chapter III). It is clear, however,

that the N-terminus has a profound effect on the initial affinities for both phosphate and AMP. The findings with K544E and E105A are inconsistent with the idea that the N-terminus occupies the acidic patch only in the inactive state of the enzyme. K544E was expected to stabilize the binding of the N-terminus at the acidic patch. K544E has a less dramatic effect than mutations at position 16, however it similarly brought about a more active enzyme without a loss of homotropic cooperativity. E105A, which was expected to weaken the interaction between the N-terminus and the acidic patch, produces an enzyme that has a reduced affinity for both effector and substrate. It is interesting to note that position 105 in the liver isozyme, which is less sensitive to AMP regulation, has a neutral glutamine residue and is the only position in the acidic patch not conserved between the liver and muscle isozymes(2).

Data for the R16E mutation has been previously reported as single AMP activation curves in the direction of glycogen synthesis (89). We show here that the kinetic values measured, specifically total activity, affinity for substrate and effector, and Hill numbers, are functions of both effector and substrate making comparison to the previous work difficult. Overall, both the previous work and this report show that mutation of position 16 results in a more active phosphorylase *b*. Similar results were found with mutations that placed a negative charge at position 14 (70). However, both of these previous works speculated that the observed results were due to an enhanced interaction of the N-terminus at the subunit interface therefore bringing about a more phosphorylase *a* like structure.

The results reported here indicate that the binding of the N-terminus to the acidic patch may in fact enhance the affinities for both AMP and phosphate in the absence of the other while not affecting the final activated state. Examination of the crystal structure reveals that removal of the positive charge at position 16 could in fact have a favorable effect on binding at the acidic patch due to the relief of ionic clash with K544. It could not have been predicted whether or not the alanine mutation at position 16 would have enhanced the binding of the N-terminus to the acidic patch due to the loss of both favorable and unfavorable ionic interactions. The acidic patch has a negative overall charge, but there are potential interactions with positive residues for a negative charge at position 16 which could explain the effects seen with R16E. Detailed structural considerations indicate that the results seen with mutants at position 16 may not come from an enhanced interaction of the N-terminus at the subunit interface as previously proposed, but rather from an enhanced interaction at the acidic patch.

It is important to note that an enhanced interaction at the subunit interface, specifically at the phosphoserine recognition site, would be expected to activate phosphorylase *b*. This has been demonstrated through sulfate activation (61). However, sulfate activation is dependent on the N-terminus and gives a concomitant loss of homotropic cooperativity and increases the observed activity in the absence of AMP (61,62). The results with the acidic patch mutants are intriguing due to their seeming inverse nature with respect to the proposed role of the acidic patch (13). These results would indicate that the binding of the N-terminus at the acidic patch enhances the affinities for phosphate and AMP which could help explain how polyamines activate

phosphorylase *b*. None of these mutations seem to have a significant effect on the AMP saturated state of the enzyme which is in agreement with the finding that phosphorylase can be fully activated by AMP in the absence of the N-terminus. The affinity for phosphate under saturating AMP concentration for all of the mutants tested is nearly equal to the affinity for substrate seen with phosphorylase *a* under similar conditions. The effect of the N-terminus seems to be in determining the affinity for phosphate and AMP in the absence of the other, and there is a strong implication that the N-terminus interacting with the acidic patch enhances those affinities.

If activation by AMP does indeed involve binding of the N-terminus to the acidic patch, that would be a strong indication that activation by AMP is not structurally equivalent to activation by phosphorylation. Supporting this idea are the data presented here showing that the fluorescence from the active site cofactor is affected differently by phosphorylation and AMP. In addition, glycogen phosphorylase *b* is a K-type system. Both with wild-type and all mutants tested here there is no dependence of V_{max} on the concentration of AMP present. However, it is well recorded in the literature and has been observed in our studies that phosphorylase *a* has a significantly higher V_{max} (61,68). Only E105A did not show a decrease in V_{max} for the mutant enzyme when compared to wild-type. None of the mutations that were proposed to bring about a phosphorylase *a*-like structure have the hallmarks of phosphorylase *a* that include a lose of homotropic cooperativity and an increase in V_{max} (63). To date all the data observed can be explained by the notion that the active form of phosphorylase *b* has the N-terminus occupying the acidic patch. It is important to realize, however, that if this suggestion is correct then

activation could be realized by either enhanced binding at the acidic patch or at the subunit interface, and the AMP activated form of phosphorylase *b* does not require either, but the initial affinity for substrate and effector is enhanced by the N-terminus interacting with the acidic patch.

CHAPTER V

THE FUNCTION OF THE 280's LOOP AND α-HELIX 1 IN THE ACTIVATION OF GLYCOGEN PHOSPHORYLASE *b*: CONFIRMATION OF THEIR ROLES IN ALLOSTERY

BACKGROUND

Glycogen phosphorylase catalyzes the breakdown of glycogen stores (2). In the mammalian system, there are three isozymes that vary in their regulation with the most extensively studied being the muscle enzyme from rabbit. The structure of glycogen phosphorylase is well known from crystallographic studies. The catalytically active form of the enzyme is a dimer with a molecular mass of 97.5 kDa per subunit (8,63). The subunit itself can be divided into 2 domains, the N-terminal regulatory domain and the C-terminal catalytic domain. The active site lies in a cleft between the two domains of the subunit and contains the required cofactor pyridoxial-5-phosphate. It has been proposed that access to the active site is controlled in part by the positioning of residues 280-286 (the 280's loop) along this cleft, and in the closed conformation the active site is cut off from solvent (13).

Physiologically, glycogen phosphorylase must be activated to carry out its function. Activation can come via the phosphorylation of serine 14 yielding the more active species phosphorylase *a* (the unphosphorylated form is known as phosphorylase *b*)(63). Phosphorylation results in the N-terminus (residues 1-22) moving to the subunit

interface where the phosphoserine recognition site is located (13). Activation can also be achieved via the binding of AMP to the allosteric sites, though AMP activation only induces the enhanced affinity for substrate, not the increase in V_{max} observed upon conversion to phosphorylase *a* (Chapter IV). The addition of AMP to phosphorylase *a* has also been shown to enhance substrate affinity though it is a much smaller effect compared to the effect of AMP has on phosphorylase *b* (63). Glycogen phosphorylase can be inhibited by purines which occurs via binding at the apex of the active site cleft (2,8). Various inhibitors, including ATP, caffeine and at high concentrations AMP, bind with concomitant aromatic stacking between F285 and Y613 (8).

The extensive structural work that has been done with glycogen phosphorylase has led to proposals on the roles of the subunit interface, the N-terminus, and the 280's loop. The subunit interface is made up of two sets of interactions (13). First, the tower helices (α-helix 7) interact with their counterparts across the interface (Figure 5.1A). On the opposing side of the interface, α-helix 1 (residues 23-35) and α-helix 2 (residues 48-78) act as a group to make up the remainder of the interface (Figure 5.1B). Between α-helix 1 and 2 is the cap loop (residues 36-47) which is seen lying across the top of the allosteric site in the AMP activated enzyme (13). It has been proposed that this interaction between the cap loop and AMP causes a shift in α-helix 2 which rearranges the interface and causes a rotation between subunits that activates the enzyme. This shift has focused attention on the role of α-helix 2 in the allosteric activation by AMP while the roles of α-helix 1 and the tower helices have been thought to be somewhat consequential to the movement of α-helix 2.

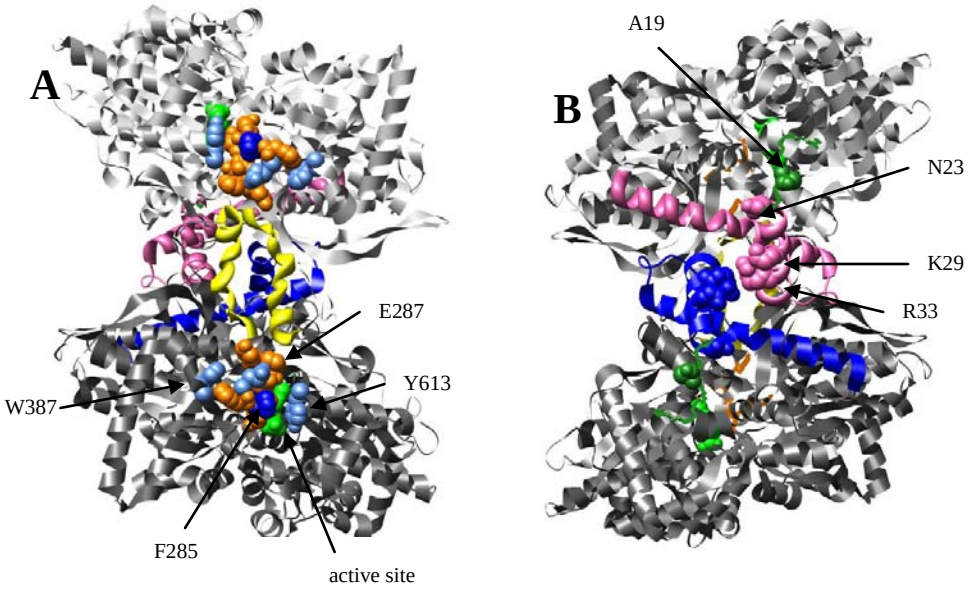

Figure 5.1: Dimeric structure of glycogen phosphorylase *b* inhibited by glucose. Subunit 1 is colored light grey. Subunit 2 is colored dark grey. α-helices 1 and 2 are shown in blue for subunit 2 and pink for subunit 1. Tower helices are shown in yellow. Active site cofactor is shown in green. N-terminus is shown in forest green. The 280's loop is shown in orange. A) View of active site face of dimer showing the 280's loop at the active site cleft. Residues interacting with the 280's loop that were mutated are shown in light blue. F285 on the 280's loop is shown in dark blue. B) View of the dimer from the back of the enzyme. Residues mutated are shown in space-filling. A19 in green is on the N-terminus. N23, K29, and R33 are shown in pink on α-helix 1 of one monomer and blue on the other. Only one subunit is labeled for clarity.

The reported T-state of phosphorylase *b* shows the 280's loop bound across the opening to the active site with a direct interaction between F285 and Y613 (13). In addition, the side chain of D284 was seen to point into the active site and occupies the site where phosphate binds during catalysis. The positioning of a negative residue at this site is proposed to prevent the binding of substrate in the inactive state. In the R-state structures, the 280's loop is displaced allowing solvent access to the active site, and R569 occupies the site previously held by D284 (13). This exchange has been hypothesized as one of the key mechanisms to the activation of the enzyme, along with the opening of the active site. However, a similar mechanism to allostery was ruled out in phosphofructokinase (6). The role of the 280's loop has been examined previously by site directed mutagenesis of the residues in the loop itself (73). Unfortunately, such mutations had severe consequences on the activity of the enzyme and ultimately the authors acknowledged that the mutants behaved differently, but the differences could not be ascribed to a change in allostery.

In this study, we have focused on the roles of α-helix 1 and the 280's loop in activation of glycogen phosphorylase *b* by AMP. Residues of α-helix 1 that differ between the isozymes of phosphorylase have been modified. To overcome the compromised activity seen on modification of the 280's loop, this study has focused on the residues making contact with the 280's loop when it is bound across the entry to the active site. In addition, residue A19, which is on the N-terminus, and residue F285, which is in the 280's loop and part of the purine inhibition site, were examined. Mutants of α-helix 1 predominately exhibited effects on homotropic cooperativity rather than

heterotropic activation by AMP. Some of the 280's loop mutants have dramatic effects on the activity of the enzyme, but others have far less dramatic effects. The allostery of these mutants is significantly altered from wild-type revealing that indeed the 280's loop has a major role in the activation by AMP.

MATERIALS AND METHODS

The phosphorylase for this study was obtained from bacterial expression of the recombinant rabbit muscle glycogen phosphorylase gene as previously described (65). Purified proteins were stored at 4 ºC and generally used within one week. β-glycerophosphate was from Sigma-Aldrich (St. Louis, MO) or USB (Cleveland, OH). Restriction enzymes were from New England Biolabs (Beverly, MA). Ion exchange chromatography resins were from Amersham Biosciences (Piscataway, NJ). Size exclusion resin and glycogen phosphorylase kinase were from Sigma-Aldrich. Glucose-6-phosphate dehydrogenase was from Roche Applied Sciences (Indianapolis, IN). Phosphoglucomutase was from Roche Applied Sciences or Sigma-Aldrich. Rabbit liver glycogen from Sigma-Aldrich was used in the kinetic experiments. Other chemicals were from Sigma-Aldrich.

Mutagenesis/Molecular Biology: The plasmid pTACTAC with the gene for wild-type glycogen phosphorylase gene from rabbit muscle inserted between *Nde*I and *Hind*III sites as previously described was used as the starting template for mutagenesis (65). The phosphorylase mutants A19V, N23D, E26A, K29A, R33A, F285A, E287A, W387A, R569A, H571A, Y613A, and Y613H were created using a Quik Change Site Directed

Mutagenesis Kit (Stratagene, La Jolla, CA). Resulting plasmids were sequenced to verify the mutations.

Protein Expression and Purification: Wild-type and mutant phosphorylase were expressed from plasmid pTACTAC as previously described (65) with the exception that the growth was carried out in *E. coli* strain DF1020 (*pro-82, glnV44*(AS), *ΔpfkB201, recA56, endA1, Δ(rhaD-pfkA)200, thi-1, hsdR17*)(9,10) for 48 hr at 27 ºC in 1.5 L cultures that were inoculated with 40 ml of culture grown to saturation at 37 ºC in the absence of inducer. Cell pellets from expression were stored at -80 ºC prior to protein purification. Protein purification was carried out with modifications of previously described methods (8). Briefly, cell pellets from 1.5-3 L of culture were thawed and resuspended in 75 mL of resuspension buffer (50 mM β-glycerophosphate (pH 7.0), 30 mM β-mercaptoethanol, 1 mM EDTA, 0.2 mM PMSF, 0.7 μg/mL pepstatin A, 0.5 μg/mL leupeptin, 0.01% benzamidine). Cells were lysed by sonication until the OD_{600} was approximately $1/10^{th}$ of the starting value. Debris was pelleted by centrifugation at 14,000 g for 45 min. The supernatant was brought to 0.5% polyethylenimine by addition of a 10% solution (40 mM β-glycerophosphate, 10% polyethylenimine), and stirred on ice for 30 min. The precipitate was removed by centrifugation at 14,000 g for 45 min. Solid $(NH_4)_2SO_4$ was added to the supernatant to 50% saturation, and stirred on ice for 20 min. The precipitated protein was recovered by centrifugation at 14,000 g for 30 min. The pellet was resuspended in 25 mL of column buffer (25 mM β-glycerophosphate (pH 7.0), 1 mM β-mercaptoethanol, 1 mM EDTA, 0.2 mM PMSF, 0.01% benzamidine), and dialyzed against three changes of the same buffer. The protein was then applied to

DEAE-Sepharose Fast Flow and SP-Sepharose Fast Flow columns run in tandem. Fractions from the load and wash showing activity were pooled and used for subsequent kinetic and fluorescence experiments. Protein was quantified using Pierce (Rockford, IL) BCA protein assay.

Kinetic Measurements: Glycogen phosphorylase activity was followed in the direction of glycogen degradation at 25 ºC utilizing phosphoglucomutase and glucose-6-phosphate dehydrogenase in a coupled enzyme assay system to link the degradation of glycogen to the production of reduced NADPH, which was followed at 340 nm on a Beckman 600 series UV/VIS spectrophotometer. Assays were carried out in a 600 µL reaction volume containing 50 mM PIPES (pH6.8), 100 µM EDTA, 5 mg/ml rabbit liver glycogen, 0-5 mM AMP, 0-300 mM potassium phosphate, 360 µM NADP, 4 µM glucose-1,6-bisphosphate, 10 mM $MgCl_2$, 6.7 U/mL phosphoglucomutase, 3 U/mL glucose-6-phosphate dehydrogenase. Changes in ionic strength due to varying phosphate concentrations were compensated for by the addition of appropriate amounts of KCl. Temperature was maintained within 1 ºC by circulating water bath. The assay mixes were preincubated at 25 ºC, and the reaction was initiated by addition of appropriately diluted glycogen phosphorylase.

Data Analysis: In order to quantify homotropic and heterotropic couplings, initial velocity data were plotted as titrations of both phosphate and AMP and individual titration curves fit to the Hill equation to determine the K1/2 and Hill number in binding (114). The homotropic coupling quotient for AMP binding in the absence of phosphate

was determined from the limit value of the Hill number at low phosphate observed in replots of Hill number for AMP vs. phosphate according to equation 5.1 (101).

$$Q_{AMP} = \left[\frac{n_H}{2 - n_H} \right]^2 \tag{5.1}$$

where Q_{AMP} is the homotropic coupling quotient for AMP binding in the absence of phosphate. n_H is the Hill number for AMP binding in the absence of phosphate. Analogous approaches were used to determine the homotropic coupling quotient for AMP in the saturating presence of phosphate and the homotropic coupling quotient for phosphate binding in the absence and presence of AMP.

Quantification of the heterotropic coupling between AMP and phosphate was carried out with replots of $K_{1/2}$ for phosphate as a function of AMP utilizing the thermodynamic linkage approach described by Reinhart (101) (equation 5.2) with the values for homotropic coupling in AMP binding fixed to the values established by the replots of Hill number.

$$K_{1/2} = K_{Pi}^{o} \left[\frac{{K_{AMP}^{o}}^2 + 2K_{AMP}^{o}[AMP] + Q_{AMP}[AMP]^2}{{K_{AMP}^{o}}^2 + 2K_{AMP}^{o} Q_{AMPPi} \left[\frac{Q_{AMP}}{Q_{AMP/Pi}} \right]^{1/2} [AMP] + {Q_{AMPPi}}^2 Q_{AMP}[AMP]^2} \right]^{1/2} \tag{5.2}$$

where K_{Pi}^{o} is the dissociation constant for phosphate in the absence of AMP. K_{AMP}^{o} is the dissociation constant for AMP in the absence of phosphate. Q_{AMP} is the homotropic coupling quotient for AMP binding in the absence of phosphate. $Q_{AMP/P}$ is the homotropic coupling quotient for AMP binding in the saturating presence of phosphate. Q_{AMPPi} is the

observed heterotropic coupling quotient between AMP and phosphate and can alternately be defined as;

$$Q_{AMPPi} = Q^2_{(AMPPi)}\left[\frac{Q_{AMP/p}}{Q_{AMP}}\right]\left[\frac{Q_{Pi/AMP}}{Q_{Pi}}\right]^{1/2} \quad (5.3)$$

where $Q_{(AMPPi)}$ is the true heterotropic coupling between AMP and phosphate. $Q_{AMP/p}$ is the homotropic coupling quotient in AMP binding with only one equivalent of phosphate bound. Alternatively, the coupling quotient Q_{AMPPi} can be determined directly as the ratios of $K_{1/2}$ for phosphate in the absence and saturating presence of AMP. Free energies of coupling were calculated using the relationship between Q and ΔG.

$$\Delta G = -RT\ln Q \quad (5.4)$$

Molecular Modeling: Graphics of glycogen phosphorylase were generated from crystal structure solved by Martin, Johnson, and Withers (Protein Data Bank 2gpb) using the UCSF Chimera package from the Resource for Biocomputing, Visualization, and Informatics at the University of California, San Francisco (supported by NIH P41 RR-01081) (119,120).

RESULTS

All mutants were successfully created and expressed. However the variants E26A, R569A and Y613A gave no measurable activity. H571A gave detectible activity but it was reduced more than 200-fold with respect to wild-type and as a result kinetic parameters could not be verifiably established. For the remaining variants the effects on V_{max}, with the exception of Y613H, were less than 4-fold (Table 5.1).

Table 5.1: Kinetic constants for wild-type, α-helix 1, and 280's loop mutants of glycogen phosphorylase *b*.

	K^{o}_{Pi} [a,d] (mM)	K^{o}_{AMP} [b,d] (mM)	Q_{AMPPi} [c,d]	k_{cat} (s^{-1})	n_{HPi} [e] -AMP / +AMP	n_{HAMP} [f] -Pi / +Pi
Wild-type b	940±40	0.44±0.02	92±5	41±2	1.9±0.05 / 1.14±0.01	1.52±0.05 / 1.11±0.03
A19V	244±1	.85±0.03	25.5±0.7	42±2	1.84±0.16 / 1.04±0.02	1.74±0.05 / 1.31±0.06
N23D	7000±1000	1.47±0.06	500±100	24.7±0.5	1.13±0.01 / 1.01±0.01	1.86±0.02 / 1.66±0.06
K29A	1700±100	1.05±0.03	160±10	32.7±0.3	1.70±0.01 / 1.15±0.01	1.61±0.07 / 1.54±0.02
R33A	4700±600	4.6±0.2	470±60	32±0.5	1.48±0.03 / 1.16±0.02	1.74±0.03 / 1.53±0.04
F285A	1300±100	2.8±0.1	19±2	10.9±0.3	1.88±0.01 / 1.20±0.03	1.93±0.06 / 1.56±0.04
E287A	86±1	0.018±0.001	10.4±0.3	22.9±0.2	1.37±0.04 / 1.08±0.02	1.07±0.04 / 1.10±0.02
W387A	260±10	0.0091±.0007	7.6±0.3	9.4±0.2	1.35±0.03 / 1.02±0.02	1.07±0.04 / 1.07±0.04
Y613H	4000±2000	0.17±.02	70±40	0.93±0.07	1.81±0.05 / 1.15±0.22	1.18±0.02 / 1.63±0.03

[a] The dissociation constant for phosphate in the absence of AMP. [b] The dissociation constant for the binding of the first equivalent of AMP in the absence of phosphate. [c] The ratio of the dissociation constant for phosphate in the absence and saturating presence of AMP. [d] Determined form fitting of replots of $K_{1/2}$ for phosphate vs. AMP to equation 5.2. [e] Determined form fitting phosphate titrations at high and low concentrations of AMP to the Hill equation. f Determined by fitting AMP titrations at high and low concentrtions of phosphate to the Hill equation.

α-Helix 1 Mutants: The variants N23D, K29A and R33A (collectively referred to as the α-helix 1 mutants) have varying effects on the kinetics of the enzyme. They all show a weaker affinity for phosphate in the absence of AMP as well as a weaker affinity for AMP (Figures 5.2 and 5.3A and Table 5.1). A19V, which is on the N-terminus, is a more complex case. The affinity for phosphate is improved in the absence of AMP. The binding affinity for the first equivalent of AMP is reduced but that is offset by an increase in homotropic cooperativity in AMP binding meaning that the overall affinity for AMP is greater than that of wild-type (Figure 5.4C). Homotropic coupling in AMP binding for the α-helix 1 mutants in absence of phosphate is greater than or similar to that of wild-type. The cooperativity in AMP binding in the presence of phosphate was greatly enhanced compared to wild-type (Figure 5.4C). For all of the α-helix 1 mutants, the homotropic cooperativity in phosphate binding is diminished compared to wild-type with and without AMP, but the larger change is observed in the absence of AMP. All of the α-helix 1 mutants are activated to a similar functional state as wild-type by AMP, as can be seen by the convergence of curves to a similar point at the right side of Figure 5.1.

280's Loop Mutants: Mutagenesis of the 280's loop binding partners, E287A, W387A, and Y613H, as well as F285A was done with the expectation of reducing the binding of the 280's loop at the active site cleft. The effects on the activation by AMP were then assessed. Replots of $K_{1/2}$ for phosphate as a function AMP for the 280's loop mutants show a much different pattern than that observed with the α-helix 1 mutants. The disruption of the 280's loop caused significant changes in affinity for phosphate in both

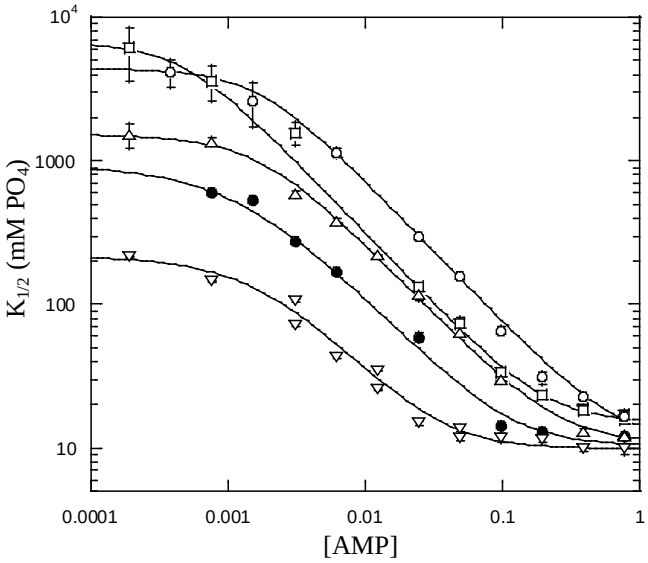

Figure 5.2: Replot of $K_{1/2}$ for phosphate as a function of AMP for wild-type, A19V and α-helix 1 mutants. Data is shown for wild-type (•), A19V (∇), N23D (□), K29A (Δ), and R33A (o). $K_{1/2}$ data were determined from fitting individual phosphate titrations at constant AMP to the Hill equation. Lines represent best fit to Equation 5.2 with homotropic coupling quotients for AMP fixed to the values calculated from the Hill number for AMP binding in the absence and presence of phosphate. Experiments carried out with 5 mg/ml glycogen at 25°C.

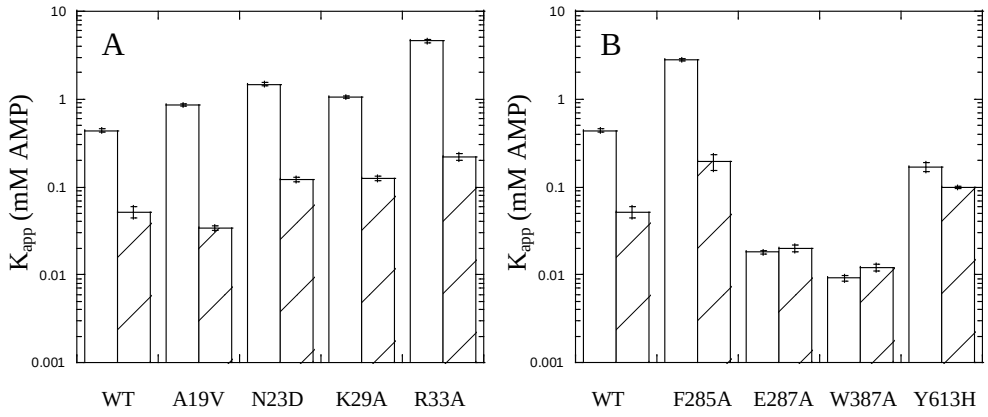

Figure 5.3: AMP binding affinity in the absence of phosphate for α-helix 1 and 280's loop mutants. Open bars are affinity for the first equivalent of AMP determined from fitting replots of $K_{1/2}$ for phosphate vs. AMP to equation 5.2 (K^{o}_{AMP}). Hatched bars are $K_{1/2}$ for AMP at low phosphate determined from fitting AMP titration at fixed phosphate to the Hill equation. A) AMP affinities for α-helix one mutants and A19V. B) AMP affinities for 280's loop mutants.

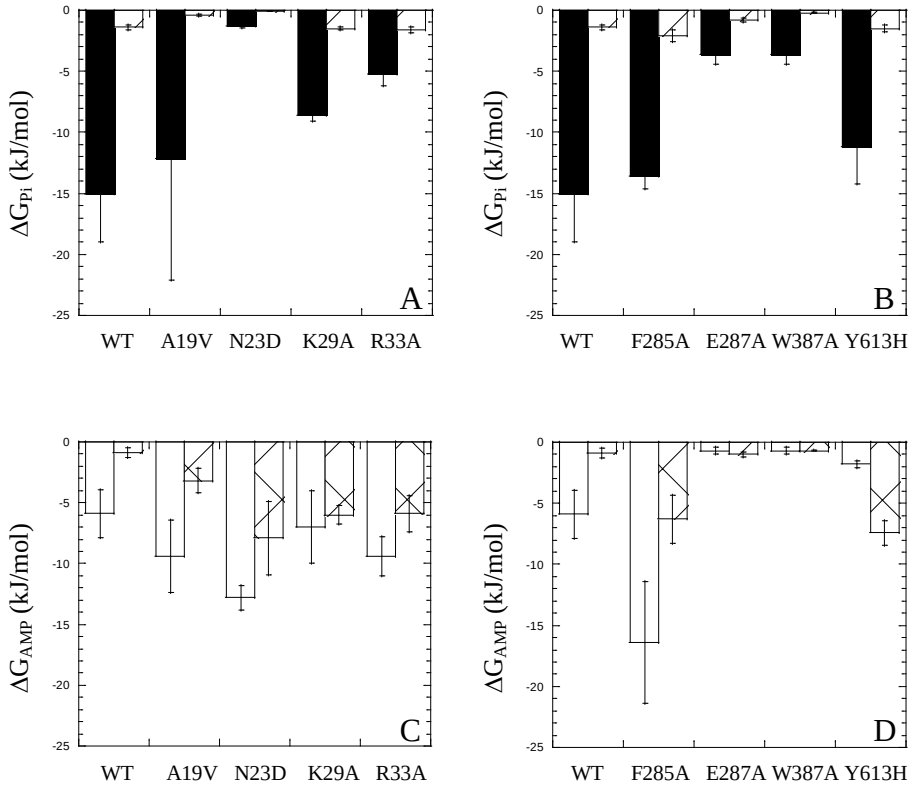

Figure 5.4: Homotropic free energy of coupling for wild-type, α-helix 1, and 280's loop mutants of glycogen phosphorylase *b*. Free energies of homotropic coupling are calculated from the Hill number in ligand binding determined by fitting titration curves to the Hill equation. A) Free energy of coupling in phosphate binding for α-helix 1 mutants and A19V. B) Free energy of coupling in phosphate binding for 280's loop mutants. A & B) Free energy of coupling in absence of AMP is shown as filled bar. Free energy of coupling in the saturating presence of AMP is shown as bars with diagonal lines. C) Free energy of coupling in AMP binding for α-helix 1 mutants and A19V. D) Free energy of coupling in AMP binding for 280's loop mutants. C & D) Open bars are free energy of coupling in absence of phosphate. Cross hatched bars are free energy of coupling

the apo and the AMP saturated states of the enzyme (Figure 5.5). E287A and W387A improved the affinity for phosphate in the absence of AMP, while F285A and Y613H diminished the affinity for phosphate (Table 5.1). All, except F285A, improved the binding of AMP to the enzyme (Figure 5.2B). The affinity for the first equivalent of AMP and the observed $K_{1/2}$ for AMP nearly agree for three of the mutants (Figure 5.2). Examination of the homotropic cooperativity in AMP binding for the E287A, W387, and Y13A variants reveals that there is little to no cooperativity in these mutants meaning that the affinity for the first equivalent should match the measured $K_{1/2,}$ as is observed (Figure 5.3). The F285A variant has greater homotropic cooperativity in AMP binding. All of the 280's loop mutants diminished homotropic cooperativity in phosphate binding to some degree, but it is observed that the variants that improve the binding of phosphate (E287A and W387A) diminished the homotropic cooperativity in phosphate binding to a greater extent than the variants that decreased the affinity for phosphate (F285A and Y613H). The maximal activity of these mutants is affected to varying degrees. Y613H shows a 40-fold decrease whereas the E287A shows less than a two-fold change. All of the 280's loop mutants show a decrease in heterotropic coupling between phosphate and AMP. It was also found in this study that Y613H yielded the smallest change in heterotropic coupling between AMP and phosphate, while E287A showed a much greater alteration in heterotropic coupling without a dramatic loss of activity. (Table 5.1).

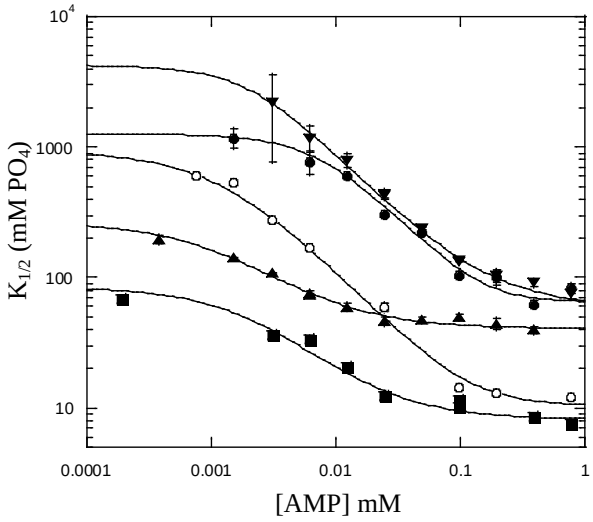

Figure 5.5: Replot of $K_{1/2}$ for phosphate as a function of AMP for wild-type and 280's loop mutants. Data are shown for wild-type (o), F285A (•), E287A (■), W387A (▲), Y613H (▼).$K_{1/2}$ data were determined from fitting individual phosphate titrations at constant AMP to the Hill equation. Lines represent best fit to Equation 5.2 with homotropic coupling quotients for AMP fixed to the values calculated from the Hill number for AMP binding in the absence and presence of phosphate. Experiments carried out with 5 mg/ml glycogen at 25°C.

DISCUSSION

The 280's loop has long been thought to be important for activation of glycogen phosphorylase (13,73). The potential to act as a cap to the active site thereby sealing it off from substrates, and the finding that purine inhibitors bind and stabilize the 280's loop in the active site cleft, makes the 280's loop a prime candidate for the regulation of substrate binding. The previous study that attempted to address this hypothesis focused on alterations of the 280's loop residues and found that the apparent regulation was significantly different from wild-type (73). Unfortunately, the observed changes in properties could not be attributed to a change in allostery because the maximal activity of the enzymes was greatly compromised. The alternate approach taken here has identified mutants that are expected to alter the ability of the 280's loop to bind in the active site cleft without compromising the activity of the enzyme dramatically. This search discovered numerous mutations that completely inactivated the enzyme, as well as some that retained extremely low activities, which again highlights the importance of this region for the activity of phosphorylase. Other mutations identified did not have such dramatic effects on the specific activity, but did significantly alter the response to AMP. E287A and W387A in particular nearly eliminate both heterotropic and homotropic communication between sites while maintaining significant activity. This finding implicates the 280's loop in the allosteric regulation of glycogen phosphorylase *b*. The dramatic effect on homotropic communication shows that communication across the subunit interface has been compromised. While it was not specifically addressed by

this study, it is tempting to speculate that the communication being disrupted is via the tower helices that directly connect the 280's loop to the subunit interface (13).

Comparison of Figures 5.1 and 5.4 shows that the 280's loop and the α-helix 1 mutants have dramatically different effects on phosphorylase *b*. Mutations of the 280's loop affected the affinity for phosphate in both the apo and AMP saturated states of the enzyme whereas the α-helix 1 mutations only appear to affect the affinity in the apo enzyme.

Mutations of α-helix 1 primarily have effects on the homotropic cooperativity. All of the α-helix 1 mutations dramatically diminish homotropic cooperativity in phosphate binding indicating that the communication between active sties is lost. Also, phosphate is no longer able to relieve the homotropic cooperativity in AMP binding, indicating that communication between active site and allosteric site has been lost. It has been shown structurally that α-helix 1 and 2 shift on AMP binding. The same shift would be expected to be brought on by the binding of phosphate to the apo enzyme due to the ability of phosphate to enhance the affinity for AMP in the wild-type enzyme and relieve the homotropic cooperativity in AMP binding. It may be that this shift of α-helices 1 and 2 is no longer possible upon phosphate binding with the modified α-helix 1 residues, resulting in homotropic cooperativity in AMP binding even in the presence of high phosphate. Similarly, it is understandable that in the absence of such a shift, binding of a single phosphate could no longer activate the other subunit due to a lack of the reinforcing effect of the shift of α-helix 1 and 2 at the subunit interface.

Similarly, a study that mutated P48 in α-helix 2 found a loss of homotropic communication in AMP binding (68). Despite this, variants at position 48 maintained activation by AMP. Some of the mutants actually showed tighter binding for AMP even without homotropic cooperativity. These results may indicate that the shift of α-helix 1 and 2 at the interface had already occurred in the apo enzyme.

AMP still seems to fully activate the α-helix 1 mutants, despite the apparent loss of communication caused by modification of the α-helix 1 residues. The heterotropic coupling between AMP and phosphate is in fact greater for these mutants. However, the reduction in homotropic cooperativity in phosphate binding is expected to cause an apparent increase in the dissociation constant for phosphate in the absence of AMP. The expected behavior is observed in Figure 5.1 as the elevated $K_{1/2}$ for phosphate in the absence of AMP and the convergence of the curves to a similar point under saturating AMP concentrations. Wild-type phosphorylase *b* has a great deal of homotropic cooperativity in phosphate binding in the absence of AMP, but very little homotropic cooperativity in the presence of AMP. As given in equation 5.3, the ratio between these homotropic couplings in substrate binding affects the measured heterotropic coupling. In the case of the α-helix 1 mutants, the ratio is closer to unity due to the loss of homotropic cooperativity in the absence of AMP. Examination of the square root of the ratios of the homotropic coupling quotient in the presence and the absence of AMP for these mutants shows that they follow the same pattern as the differences in measured heterotropic cooperativity (Figure 5.6). It is then likely that the apparent changes in coupling between AMP and phosphate are actually a manifestation of the altered

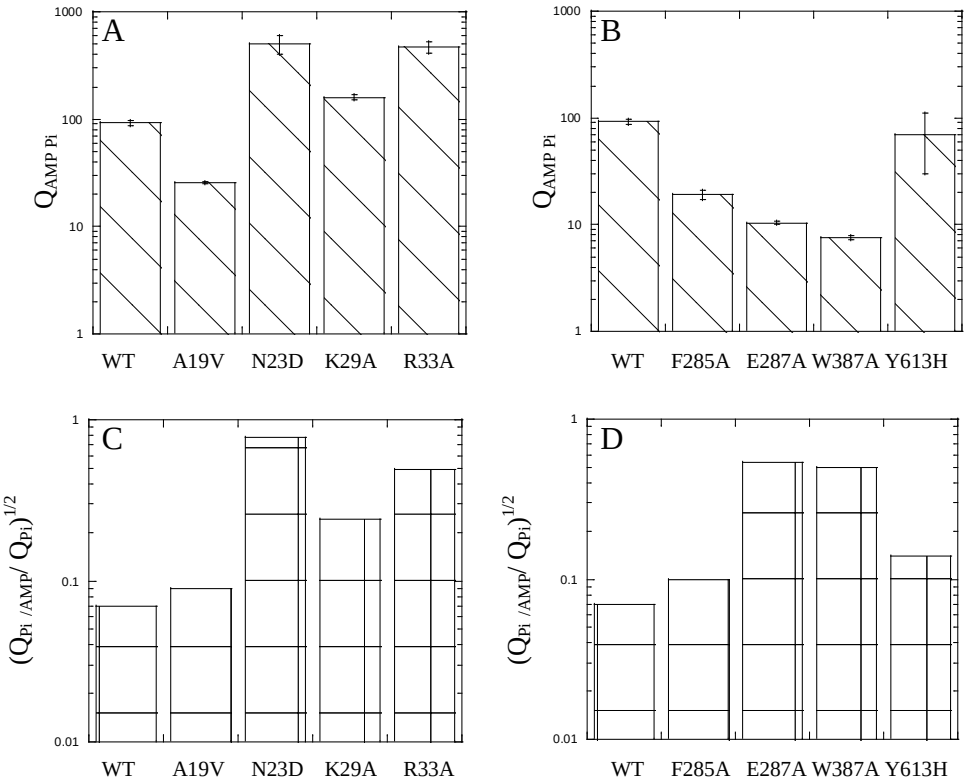

Figure 5.6: Apparent heterotropic cooperativity and ratios of homotropic cooperativity in glycogen phosphorylase *b* wild-type, α-helix 1 and 280's loop mutants. A) Heterotropic cooperativity between AMP and phosphate for α-helix 1 mutants and A19V. B) Heterotropic cooperativity between AMP and phosphate for 280's loop mutants. C) Square root of the ratio of homotropic cooperativity for phosphate in the saturating presence of AMP and the homotropic cooperativity for phosphate in the absence of AMP for the α-helix 1 mutants and A19V. D) Square root of the ratio of homotropic cooperativity for phosphate in the saturating presence of AMP and the homotropic cooperativity for phosphate in the absence of AMP for the 280's mutants. Ratios are a term that contributes to the apparent heterotropic cooperativity.

homotropic coupling, and the true heterotropic coupling may not be perturbed to any great extent. The ability to disconnect homotropic cooperativity from heterotropic coupling, particularly when that disconnection can come with either retention or loss of the homotropic cooperativity in AMP binding, indicates that AMP may have two distinct effects on phosphorylase *b*. One would bring about the homotropic cooperativity in AMP binding, and the other would activate the enzyme for catalysis. In wild-type phosphorylase *b*, these events are connected, but the fact that they can be disconnected shows that they are distinct from each other. If the changes in the packing of α-helix 1 and 2 observed in crystallographic studies are, as has been proposed, the mechanism by which AMP affinity increases, then the repacking of α-helix 1 and 2 would be responsible for the homotropic cooperativity in phosphorylase *b*, but not the events that lead to activation. The finding here that activity can be measured without homotropic cooperativity in the absence of AMP indicates that the repacking of the interface need not take place for catalysis, and the observation that AMP can bind noncooperatively, but is still required for activation, indicates that even when the enzyme is predisposed to the shift of α-helix 1 and 2, it need not be active. This observation may help to explain why phosphorylase *a*, which is active in the absence of AMP, still shows a slight activation upon AMP binding. The phosphorylation event could have opened the active site, but AMP binding could still cause a slight rearrangement the active site causing further activation of the enzyme.

A19V does not follow the pattern seen with the α-helix 1 mutants, probably due to A19 being on the N-terminus rather than in α-helix 1. The results observed with the

A19V mutant bears some resemblance to other mutants constructed to assess the functionality of the N-terminus (Chapter IV). The AMP saturated state of the enzyme is not perturbed, and the apo state of the enzyme is more like the activated species in its kinetic parameters. The reduced heterotropic coupling can simply be understood as the active form being more favored by the apo enzyme. This argument is supported by the finding that the homotropic effects track with changes in affinity. In other words, the initial decrease in AMP affinity is coupled to an increase in homotropic coupling in binding, and the enhanced affinity for phosphate is linked to a decrease in its cooperative binding. Similar results were observed with the mutations at position 16 in another study (Chapter IV,89). The distinct types of effects that mutations of the N-terminus and α-helix 1 have indicate that these structural elements have distinct roles in the activation by AMP.

This study has verified that the 280's loop is involved in the allosteric activation of phosphorylase *b* by AMP. While it was beyond the scope of this study, the linking of the 280's loop to the interface by the tower helix is probably critical for this activation. The other interface, namely the packing of α-helices 1 and 2, is important in the transmission of homotropic signals between the active sites and the allosteric sites, but that role is independent of the effect of AMP on the active sites. In wild-type, these effects are coupled to one another, but alterations of these helices can uncouple the homotropic and heterotropic effects.

CHAPTER VI

CONCLUSIONS: A NEW PICTURE OF GLYCOGEN PHOSPHORYLASE

Much work has been done to unravel the complex regulation of glycogen phosphorylase with the major focus being on structural studies (1,8,13,71). Difficulties have been acknowledged in these studies, but a generally accepted structural model has emerged based on the two-state models of allostery (2,13). Accordingly, it has been proposed and generally accepted that the activated form of glycogen phosphorylase is the same whether that activation comes via phosphorylation or from the binding of AMP.

Glycogen phosphorylase served as part of the motivation in the development of the two-state models of allostery (27,28,29), but glycogen phosphorylase *b* kinetics cannot be described purely by the two-state systems (38,68,106). Alternate continuous models of allostery have been derived to explain the observed kinetics of wild-type phosphorylase *b*, but those models had never been tested despite the rather unexpected requirements predicted for activation (74,76,77). The application of linkage analysis to the phosphorylase system along with the perturbation of protein structure reported here has provided a wealth of new understanding of the allosteric communication. Using linkage analysis in combination with site-directed mutagenesis we have experimentally tested the continuous models of allostery in phosphorylase *b*, and we have examined the roles of the N-terminus, the 280's loop, and α-helix 1 in allosteric activation by AMP.

MAJOR ADVANCES FROM THIS STUDY

It is now shown that the continuous models of allostery for phosphorylase provide a fairly accurate representation of wild-type glycogen phosphorylase *b* activity, but are inadequate to describe the kinetics of phosphorylase *b* under all conditions (74,76,77). Glycogen phosphorylase *b* is active in the absence of AMP, though only at extremely high concentrations of phosphate. The bulk of activation by AMP binding takes place on the binding of the second equivalent of AMP to the dimer. The continuous models for phosphorylase were generated from wild-type data in the direction of glycogen synthesis rather than the physiological direction of glycogen breakdown (74, 76,77). Both models call for a requirement that substrate be bound to both active sites prior to catalysis. In this study, the phosphorylase reaction has been studied in the direction of glycogen degradation utilizing phosphate rather than glucose-1-phosphate as the variable substrate. It is possible that two equivalents of AMP must be bound for the reaction in the direction of glycogen synthesis to take place, but in light of the findings presented here that becomes doubtful.

AMP activation of phosphorylase *b* does not require the presence of the N-terminus. The N-terminus plays a role in establishing the affinity for phosphate and AMP in apo phosphorylase *b*. In the absence of the N-terminus the affinity for both is significantly diminished. Surprisingly, the binding of the N-terminus at the acidic patch on its own subunit appears to be the mechanism by which the N-terminus establishes the affinity for phosphate and AMP. Mutations that are expected to stabilize binding to the acidic patch enhance the affinity for AMP and phosphate in the apo enzyme, while

mutations that are expected to diminish the binding of the N-terminus to the acidic patch diminish the affinity for both AMP and phosphate.

It has been demonstrated here that the activation of phosphorylase by phosphorylation and AMP binding are not equivalent. Activation by phosphorylation is probably unique in that it directly involves three of the four structural units that make up the subunit interface (13). Phosphorylation occurs on the N-terminus which then relocates to the phosphoserine recognition site at the subunit interface thereby restructuring the interface. The binding of the phosphoserine at the subunit interface remodels α-helix 1, and directly interacts with residues of α-helix 2 as well as residues of the cap-loop. Along with an increase in affinity for phosphate and the loss of homotropic cooperativity in phosphate binding, the activation by phosphorylation includes an increase in V_{max} (61,68). Activation by AMP does not result in an equivalent increase in V_{max} indicating that there are differences at the active site between phosphorylase *a* and AMP activated phosphorylase *b*, a finding reinforced by differences in cofactor fluorescence between the two.

The 280's loop has been proposed to have a role in the allosteric activation by AMP due to the finding that it blocks the active site from solvent in inhibitor bound structures (13,50). Unfortunately, structural work on phosphorylase has not provided any insight as to the role of the 280's loop in the active enzyme. Modification of residues of the 280's loop has demonstrated that the loop is important for catalysis, but the nature of that role remains undetermined (73). The apparent role in catalysis has prevented the definitive determination of any role in allostery.

In this study, the 280's loop is confirmed to have a major role in the allostery of glycogen phosphorylase. Mutations expected to disrupt the binding of the 280's loop at the active site cleft disrupt the heterotropic communication between the AMP and actives sites. Of the structural units that have been modified in this study only the mutations affecting the 280's loop demonstrated definitively that the heterotropic coupling had been disrupted. Unlike previous attempts to alter the 280's loop, the alteration in heterotropic communication can be demonstrated without great loss of catalytic activity by altering the interacting partners of the 280's loop (73).

The restructuring of subunit interface has been proposed to be important in the allosteric activation by AMP. Much attention has been given to the altered interactions of α-helix 2 and the cap-loop in the activated versus inhibited structures of phosphorylase, but little attention has been given to α-helix 1 (13,52,68). α-helix 1 has also been shown to have altered interactions between reported structural states, and sequence alignments have shown that residues are not conserved between the isozymes of phosphorylase (2,13).

In this study, α-helix 1 is shown to have a role in homotropic communication in phosphorylase *b*, but it does not appear to have a significant role in the heterotropic activation by AMP. The mutations in α-helix 1 disrupt the effect of phosphate binding on the homotropic cooperativity in AMP binding resulting in an enzyme species that shows homotropic cooperativity in AMP binding under all concentrations of phosphate. These mutants uncoupled the homotropic effects but do not alter the heterotropic effect. This result is similar to previous work done on the subunit interface by Robert Fletterick

that modified residue 48 on α-helix 2. AMP was shown to bind with high affinity and activated the enzyme but without homotropic cooperativity in AMP binding (68).

Implications for the Structural Model of Activation: Based on the findings presented herein modifications must be made to the current structural understanding of phosphorylase activation. First, there is an implication that activation by phosphorylation and AMP binding are not equivalent. Structural work has seemed to support the notion that the active form of phosphorylase is the same regardless of the route of activation. However, it must be considered that the crystal structure of "active" phosphorylase *b* was solved with sulfate mimicking the phosphoryl group at position 14, and the resultant structure was very similar to the phosphorylated enzyme (51). The alternate structure solved without sulfate was intentionally solved under conditions that caused the protein to form a tetramer similar to that of phosphorylase *a* prior to crystallization (122). The enzymatically active form of phosphorylase is well established as a dimer, but the structure generally accepted as the active form of phosphorylase *a* and *b* were solved as a tetramer (11,13). The propensity of phosphorylase *a* to form a tetramer may indicate that it is physiologically relevant for the phosphorylated enzyme, but the hypothesis that the tetramer structure of phosphorylase *b* is the true active structure does not appear correct.

The work described here indicates at the very least that the active form of phosphorylase *b* need not be the same as that of phosphorylase *a*. The mechanism for activation of phosphorylase by phosphorylation has held up fairly well to testing (89).

The phosphoserine recognition site has been confirmed via mutagenesis, and the enzyme structure was solved as the form that persisted in solution indicating that for phosphorylase *a* it may indeed be a relevant structure (23). Inhibition of phosphorylase *a* typically comes about by binding inhibitors to the active site which occlude substrate, and stabilize the binding of the 280's loop across the active site cleft (9,66,108). While typically referred to as stabilizing the T-state, such inhibitors do not cause the rearrangement of the α-helix 1 and 2 bundle to what is seen in apo phosphorylase *b*.

The data presented here are consistent with the hypothesis that the active form of phosphorylase *b* has the N-terminus located at the acidic patch. The implication is that the activation of phosphorylase *b* does not involve the movement of the N-terminus to the subunit interface. The rearrangement of the α-helix 1 and 2 bundle at the interface appears to be important for the transmission of the homotropic signal across the interface, but that is distinct from the transmission of the heterotropic activation to the active site. The alternate conformations are well established and are in part brought about by direct binding to AMP, indicating that the two conformations are relevant to the properties of phosphorylase (1,13). The combined finding that homotropic cooperativity in AMP binding can be retained or lost at all concentrations of phosphate indicates that the α-helix 1 and 2 bundle can be in either conformation for heterotropic activation to take place (68).

The 280's loop plays an important role in activation by AMP. Whether that role comes from a simple occlusion of substrates from the active site, or if the binding of the 280's loop alters the structure of the active site itself cannot be resolved at this time. A

major question that remains is what role the 280's loop plays in the active enzyme. Mutations to the 280's loop have severe consequences on the activity of the enzyme indicating that the 280's loop does have a role in the functional enzyme (73). It is speculated by the laboratory of Louise Johnson that the 280's loop has a role in binding the polysaccharide substrate based on work done with MalP from *E. coli* (123), but beyond this the role of the 280's loop is unknown for the active enzyme.

AN ALTERNATE MODEL FOR PHOSPHORYLASE *b*

Since repacking of the subunit interface alone is not enough to cause the activation of phosphorylase *b,* some other connection between the active site and the allosteric site must be critical in the activation by AMP. α-helix 8 (residues 289-312) potentially provides such a connection (Figure 6.1). α-helix 8 contains at its C-terminus the phosphoryl binding residues of the allosteric site. The N-terminus of α-helix 8 lies at the active site cleft and is poised to interact with both the 280's loop and the base of the tower helix. This location provides a direct connection between the allosteric site, elements of the subunit interface, and the 280's loop.

Therefore it is proposed that the binding of AMP to the allosteric site leads to changes in the packing of α-helix 8 which diminishes its interaction with the 280's loop and the tower helix residues. The loss of a stabilizing interaction allows the 280's loop to

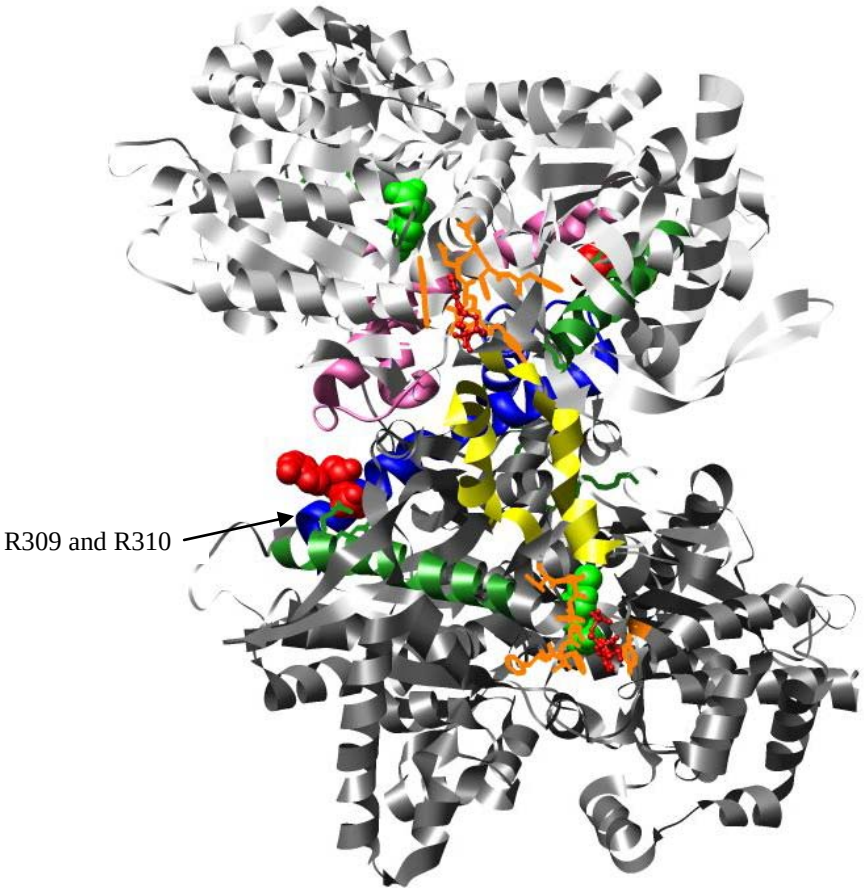

Figure 6.1: α-helix 8 of glycogen phosphorylase. Subunit 1 is shown in light grey. Subunit 2 is shown in dark grey. AMP is shown in red. α-helix 8 which links to AMP site to the 280's loop and tower helix is shown in forest green. AMP interacting residues side chains 309 and 310 highlighted. Tower helices are shown in yellow. Tyrosine 613 (purine inhibition site) and 280's loop are shown in orange. Active site cofactor is shown in green. α-helices 1 and 2 on opposite face of enzyme are shown in pink (subunit 1) and blue (subunit 2). Structure from Protein Data Bank 7gpb. Figure prepared using Chimera software.

dissociate from the active site cleft. The mutation of residue 287, which falls between α-helix 8 and the 280's loop, is one of the mutations that diminished the heterotropic interaction between AMP and phosphate, thereby supporting this hypothesis.

The dissociation of the 280's loop from each subunit would allow for the movement of the tower helices. The tower helices sliding past each other on the release of the 280's loop would account for the loss of homotropic cooperativity in phosphate binding upon AMP binding. The concerted movement of the tower helices would also explain why there is little heterotropic activation on the binding of a single equivalent of AMP. The tower helices must both move relative to each other to open the active site. Binding a single equivalent of AMP would release only a single 280's loop, but that loop would be held in place by the tower helix until the second equivalent could bind allowing the tower helices to slide past each other.

In addition to its effect on the 280's loop, the movements of α-helix 8 probably have a small effect directly on to the active site, explaining why the binding of a single equivalent of AMP to phosphorylase *b* caused a slight activation. Similarly, an effect transmitted by α-helix to the active site would provide an explanation of why phosphorylase *a* is activated by AMP to a similar extent as that seen on the binding of a single equivalent of AMP to phosphorylase *b*.

Binding of AMP involves residues of the cap loop and α-helix 2. In wild-type phosphorylase *b* these interactions would bring about the restructuring of the interface. These changes in conformation would be reinforced by the movement of the tower helices explaining how the homotropic cooperativity of both substrate and effector is

relieved in the presence of the other. These reinforcing effects can be lost by mutation as has been shown with mutations to α-helix 1. In the modified enzymes, the repacking of the interface is not expected to be as favorable. The binding of phosphate to the active site is no longer enough to bring about the repacking of the interface resulting in the loss of homotropic cooperativity in phosphate binding and the retention of AMP homotropic cooperativity at all concentrations of phosphate. It is important to note that the restructuring of the α-helix 1 and 2 side of the interface is only a reinforcing effect. Mutation of P48 showed the high affinity for AMP without homotropic cooperativity indicating that the interface was already in its high affinity conformation. AMP still showed its activating effect in this modified enzyme indicating that the altered conformation of the interface alone is not enough to activate the enzyme.

The essential argument of the structural model put forth here is that the binding of AMP differs from phosphorylation in how the signal is transmitted to the active site. In the case of phosphorylation the N-terminus is relocated to the subunit interface. This action carries with it the unique ability to simultaneously rearrange the entire interface. The conformation of the N-terminus is altered by its phosphorylation which also prevents its interaction with the acidic patch. The movement of the N-terminus alters the conformation of α-helix 1. The cap loop and α-helix 2 both provide residues to the phosphoserine recognition site. This complete restructuring of the interface presumably provides enough energetic input to slide the tower helices past each other and pull the 280’s loop out of the active site cleft thereby activating the enzyme.

By contrast, it is proposed here that the activation by AMP is the result of releasing the 280's loop from the active site cleft by altering its interaction with α-helix 8. Because the structural basis for activation is different, it is no surprise that the final state of the enzyme differs as is seen in the different V_{max} for phosphorylase *a*. While it remains to be definitively proven that the allosteric signal is transmitted from the AMP binding site to the active site by α-helix 8, the model proposed herein provides a reasonable explanation of all the observations made to date.

A FINAL NOTE ON THERMODYNAMIC LINKAGE

Thermodynamic linkage provides a unique ability to quantify the interactions in an allosteric system (92, 93, 100, 101). There is no need to assume a model prior to analysis of the experimental data, and it provides a means to separate the various effects, that is homotropic and heterotropic, from one another. While thermodynamic linkage provides no structural information, it provides a means by which a structural hypothesis can be tested. As seen in this report, altering various structural units can have unique affects on the system as a whole. It would be impossible to interpret the results reported here by two-state models, but the utilization of thermodynamic linkage has allowed the resolution of the kinetic data to provide a clearer picture of allostery in phosphorylase *b*. This approach has been able to identify the roles of various structural units in the phosphorylase system and provided unique insights into how this system carries out its functions.

REFERENCES

1. Johnson, L. N., Barford D., Acharya R., Oikonomakos N. G., and Martin, J. L. (1992) Allosteric regulation of glycogen phosphorylase. *The Robert A. Welch Foundation Conference on Chemical Research XXXVI Regulation of Proteins by Ligands*, 17-35
2. Hudson, J. W., Golding, G. B., and Crerar, M. M. (1993) Evolution of allosteric control in glycogen phosphorylase. *J. Mol. Biol. 234*, 700-721
3. Proux, D. and Dryfus, J.-C. (1973) Phosphorylase isozymes in tissue: Prevalence of the liver type in man. *Clin. Chim. Acta 48*, 167-172
4. Hudson, J. W., Hefferon, K. L., and Crerar, M. M. (1993) Comparative analysis of species-independent, isozyme-specific amino-acid substitutions in mammalian muscle, brain and liver glycogen phosphorylases. *Biochim. Biophys. Acta 1164*, 197-208
5. Green, A. A. and Cori, G. T. (1943) Crystalline muscle phosphorylase: I. Preparation, properties, and molecular weight. *J. Biol. Chem.151*, 21-29
6. Helmreich, E., and Cori, C. F. (1964) The role of adenylic acid in the activation of phosphorylase. *Proc. Natl. Acad. Sci. 51*, 131-138
7. Morgan, H. E., and Parmeggiani, A. (1964) Regulation of glycogenolysis in muscle: III. Control of muscle glycogen phosphorylase activity. *J. Biol. Chem. 239*, 2440-2445
8. Johnson, L. N. (1992) Glycogen phosphorylase: Control by phosphorylation and allosteric effectors. *FASEB J. 6*, 2274-2282

9. Withers, S. G., Sykes, B. D., Madsen, N. B., and Kasvinsky, P. (1979) Identical structural changes induced in glycogen phosphorylase by two nonexclusive allosteric inhibitors. *Biochemistry 18*, 5342-5348
10. Kasvinsky, P. J., Shechosky, S., and Fletterick, R. J. (1978) Synergistic regulation of phosphorylase *a* by glucose and caffeine. *J. Biol. Chem. 253*, 9102-9106
11. Wang, J H., Shonka, M. L., and Graves, D. J. (1965) Influence of carbohydrates on phosphorylase structure and activity: I. Activation by preincubation with glycogen. *Biochemistry 4*, 2296-2301
12. Cori, C. F., and Illingworth, B. (1957) Prosthetic group of phosphorylase. *Proc. Natl. Acad. Sci. U.S.A. 43*, 547-552
13. Barford, D., Hu, S.-H., and Johnson, L. N. (1991) Structural mechanism for glycogen phosphorylase control by phosphorylation and AMP. *J. Mol. Biol. 218*, 233-260
14. Withers, S. G., Madsen, N. B., Sprang, S. R., and Fletterick, R. J. (1982) Catalytic site of glycogen phosphorylase: Structural changes during activation and mechanistic implications. *Biochemistry 21*, 5372-5382
15. Kasvinsky, P. J., Madsen, N. B., Fletterick, R. J., and Sygusch, J. (1978) X-ray crystallographic and kinetic studies of oligosaccharide binding to phosphorylase. *J. Biol. Chem. 253*, 1290-1296
16. Cori, G. T., Colowick, S. P., and Cori, C. F. (1938) The formation of glucose-1-phosphoric acid in extracts of mammalian tissues and of yeast. *J. Biol. Chem. 123*, 375-380

17. Cori, G. T., Colowick, S. P., and Cori, C. F. (1938) The action of nucleotides in the disruptive phosphorylation of glycogen. *J. Biol. Chem. 123*, 381-389

18. Cori, G. T., Colowick, S. P., and Cori, C. F. (1939) The activity of the phosphorylating enzyme in muscle extracts. *J. Biol. Chem. 127*, 771-782

19. Vote, D., Vote, J. G., and Prat, C. W. (2006) in *Fundamentals of Biochemistry: Life at the Molecular Level* 2nd ed., John Wiley & Sons, Inc., Hoboken

20. Cori, G. T. and Cori, C. F. (1945) The enzymatic conversion of phosphorylase *a* to *b*. *J. Biol. Chem. 158*, 321-332

21. Keller, P. J. (1955) The action of trypsin on phosphorylase *a*. *J. Biol. Chem. 214*, 135-141

22. Krebs, E. G., and Fischer, E. H. (1956) The phosphorylase *b* to *a* converting enzyme of rabbit skeletal muscle. *Biochim. Biophys. Acta 20*, 150-157

23. Madsen, N. B. and Cori, C. F. (1956) The interaction of muscle phosphorylase with p-chloromercuribenzoate: I. Inhibition of activity and effect on the molecular weight. *J. Biol. Chem. 223*, 1055-1065

24. Fischer, E. H., Kent, A. B., Snyder, E. R., and Krebs, E. G. (1958) The reaction of sodium borohydride with muscle phosphorylase. *J. Am. Chem. Soc. 80*, 2906-2907

25. Fischer, E. H. and Krebs, E. G. (1958) The isolation and crystallization of rabbit skeletal muscle phosphorylase *b*. *J. Biol. Chem. 231*, 65-71

26. Fischer, E. H., Graves, D. J., Snyder Crittenden, E. R., and Krebs, E. G. (1959) Structure of the site phosphorylated in the phosphorylase *b* to *a* reaction. *J. Biol. Chem. 234*, 1698-1704

27. Monod, J., Wyman, J., and Changeux, J. P. (1965) On the nature of allosteric transitions: A plausible model. *J. Mol. Biol. 12*, 88-118

28. Koshland, D. E. Jr., Nemethy, G., and Filmer, D. (1966) Comparison of experimental binding data and theoretical models in proteins containing subunits. *Biochemistry 5*, 365-385

29. Kirtley, M. E. and Koshland, D. E., Jr. (1967) Models for cooperative effects in proteins containing subunits: Effects of two interacting ligands. *J. Biol. Chem. 242*, 4192-4205

30. Wang, J. H., Humniski, P. M., and Black, W. J. (1968) Effects of polyamines on glycogen phosphorylase: Differential electrostatic interactions and enzymatic properties. *Biochemistry 7*, 2037-2044

31. Graves, D. J., Mann, S. A. S., Philip, G., and Oliveira, R. J. (1968) A probe into catalytic activity and subunit assembly of glycogen phosphorylase: Desensitization of allosteric control by limited tryptic digestion. *J. Biol. Chem. 243*, 6090-6098

32. Puchwein, G., Kratky, O., Golker, C. F., and Helmreich, E. (1970) Small-angle X-ray scattering measurements on rabbit muscle glycogen phosphorylase dimer *b* and tetramer *b*. *Biochemistry 9*, 4691-4698

33. Wanson, J.-C. and Drochmans, P. (1968) Rabbit skeletal muscle glycogen: A morphological and biochemical study of glycogen β-particles isolated by the precipitation-centrifugation method. *J. Cell Biol. 38*, 130-150

34. Myer, F., Heilmeyer, L. M. G., Haschke, R. H., and Fischer, E. H. (1970) Control of phosphorylase activity in a muscle glycogen particle: I. Isolation and characterization of the protein-glycogen complex. *J. Biol. Chem. 245*, 6642-6648

35. Hers, H. G., De Wulf, H., and Stalmans, W. (1970) The control of glycogen metabolism in the liver. *FEBS Lett. 12*, 73-82

36. Wang, J. H., Tu, J.-I., and Lo, F. M. (1970) Effects of glucose 6-phosphate on the nucleotide site of glycogen phosphorylase *b*: A general approach for negative heterotropic interactions. *J. Biol. Chem. 254*, 3115-3121

37. Anderson, R. A. and Graves, D. J. (1973) Chemistry of the adenosine monophosphate site of rabbit muscle phosphorylase: I. Hydrophobic nature and affinity labeling of the allosteric site. *Biochemistry 12*, 1895-1900

38. Wang, J. H. and Tu, J.-I. (1970) Allosteric properties of glutaraldehyde-modified glycogen phosphorylase *b*: Selective desensitization of homotropic cooperativity. *J. Biol. Chem. 245*, 176-182

39. Fletterick, R. J., Sygusch, J., and Madsen, N. B. (1976) Structure of glycogen phosphorylase *a* at 3.0 Å resolution and its ligand binding sites at 6Å. *J. Biol. Chem. 251*, 6142-6146

40. Kasvinsky, P. J. and Madsen, N. B. (1976) Activity of glycogen phosphorylase in the crystalline state. *J. Biol. Chem. 251*, 6852-6859

41. Koide, A., Titani, K., Ericsson, L. H., Kumar, S., Neurath, H., and Walsh, K. A. (1978) Sequence of the amino-terminal 349 resides of rabbit muscle glycogen

phosphorylase including the sites of covalent and allosteric control. *Biochemistry 17*, 5657-5672

42. Hermann, J., Titani, K., Ericsson, L. H., Wade, R. D., Neurath, H., and Walsh, K. A. (1978) Amino acid sequence of two cyanogen bromide fragments of glycogen phosphorylase. *Biochemistry 17*, 5672-56
43. Carty, T. J., Tu, J.-I., and Graves, D. J. (1975) Regulation of glycogen phosphorylase: Role of the peptide region surrounding the phosphoserine residue in determining enzyme properties. *J. Biol. Chem. 250*, 4980-4985
44. Johnson, L. N., Stura, E. A., Wilson, K. S., Sansom, M. S. P., and Weber, I. T. (1979) Nucleotide binding to glycogen phosphorylase *b* in the crystal. *J. Mol. Biol. 134*, 639-653
45. Weber, I. T., Johnson, L. N., Wilson, K. S., Yeates, D. G. R., Wild, D. L., and Jenkins, J. A. (1978) Crystallographic studies on the activity of glycogen phosphorylase *b*. *Nature 274*, 433-437
46. Sprang, S. R., Goldsmith, E. J., Flettrick, R. J., Withers, S. G., and Madsen, N. B. (1982) Catalytic site of glycogen phosphorylase: Structure of the T-state and specificity for α-D-glucose. *Biochemistry 21*, 5364-5371
47. Sprang, S. R., Goldsmith, E. J., and Fletterick, R. J. (1987) Structure of the nucleotide activation switch in glycogen phosphorylase *a*. *Science 237*, 1012-1019
48. Madsen, N. B., Shechosky, S., Fletterick, R. J. (1983) Site-site interactions in glycogen phosphorylase *b* probed by ligands specific for each site. *Biochemistry 22*, 4460-4465

49. Lorek, A., Wilson, K. S., Sansom, M. S. P., Stuart, D. I., Stura, E. A., Jenkins, J. A., Zanotti, G., Hajdu, J., and Johnson, L. N. (1984) Allosteric interactions of glycogen phosphorylase *b*: A crystallographic study of glucose-6-phosphate and inorganic phosphate binding to di-imidate-cross-linked phosphorylase *b*. *Biochem. J. 218*, 45-60

50. Sprang, S. R., Acharya, K.R. Goldsmith, E. J., Stuart, D. I., Varill, K., Fletterick, R. J., Madsen, N. B., and Johnson, L. N. (1988) Structural changes in glycogen phosphorylase induced by phosphorylation. *Nature 336*, 215-221

51. Barford, D. and Johnson, L. N. (1989) The allosteric transition of glycogen phosphorylase. *Nature 340*, 609-616

52. Newgard, C. B., Hwang, P. K., and Fletterick, R. J. (1989) The family of glycogen phosphorylases: Structure and function. *Crit. Rev. Biochem. Mol. 24*, 69-99

53. Hwang, P. K., and Fletterick, R. J. (1986) Convergent and divergent evolution of regulatory sites in eukaryotic phosphorylases. *Nature 324*, 80-84

54. Nakano, K., Hwang, P. K., and Fletterick, R. J. (1986) Complete cDNA sequence for rabbit muscle glycogen phosphorylase. *FEBS Lett. 204*, 283-287

55. Gelinas, R. P., Froman, B. E., McElroy, R., Tait, R. C., and Gorin, F. A. (1989) Human brain glycogen phosphorylase: Characterization of fetal cDNA and genomic sequences. *Mol. Brain Res. 6*, 177-185

56. Rath, V. L., Newgard, C. B., Sprang, S. R., Goldsmith, E. J., and Fletterick, R. J. (1987) Modeling the biochemical differences between rabbit muscle and human liver phosphorylase. *Proteins 2*, 225-235

57. Johnson, L. N., Acharya, K. R., Jordan, M. D., and McLaughlin, P. J. (1990) Refined crystal structure of the phosphorylase-heptulose 2-phosphate-oligosaccharide-AMP complex. *J. Mol. Biol. 211,* 645-661

58. Johnson, L. N., Hu, S-H., and Barford, D. (1992) Catalytic mechanism of glycogen phosphorylase. *Faraday Discussions 93,* 131-142

59. Mitchell, E. P., Withers, S. G., Ermert, P., Vasella, A. T., Garman, E. F., Oikonomakos, N. G., and Johnson, L. N. (1996) Ternary complex crystal structures of glycogen phosphorylase with the transition state analogue nojirimycin tetrazole and phosphate in the T- and R-states. *Biochemistry 35,* 7341-7355

60. Zographos, S. E., Oikonomakos, N. G., Dixon, H. B. F., Griffin, W. G., Johnson, L. N., and Leonidas, D. D. (1995) Sulfate-activated phosphorylase *b*: The pH-dependence of catalytic activity. *Biochem. J. 310,* 565-570

61. Leonidas, D. D., Oikonomakos, N. G., Papageorgiou, A. C., Xenakis, A., Cazianis, C. T., and Bem, F. (1990) The ammonium sulfate activation of phosphorylase *b*. *FEBS Lett. 261,* 23-27

62. Leonidas, D. D., Oikonomakos, N. G., and Papageorgiou, A. C. (1991) Sulfate activates phosphorylase *b* by binding to the Ser (P) site. *Biochim. Biophys. Acta 1076,* 305-307

63. Johnson, L. N., and Barford, D. (1990) Glycogen phosphorylase: The structural basis of the allosteric response and comparison with other allosteric proteins. *J. Biol. Chem. 265,* 2409-2412

64. Oikonomakos, N. G., Johnson, L. N., Acharya, K. R., Stuart, D. I., Barford, D., Hajdu, J., Varvill, K. M., Melpidou, A. E., Papageorgiou, T., Graves, D. J., and Palm, D. (1987) Pyridoxal phosphate site in glycogen phosphorylase *b*: Structure in native enzyme and in three derivatives with modified cofactors. *Biochemistry 26*, 8381-8389

65. Browner, M. F., Rasor, P., Tugendreich, S., and Fletterick, R. J. (1991) Temperature-sensitive production of rabbit muscle glycogen phosphorylase in *Escherichia coli. Protein Eng. 4*, 351-357

66. Martin, J. L., Veluraja, K., Ross, K., Johnson, L. N., Fleet, G. W. J., Ramseden, N. G., Bruce, I., Orchard, M. G., Oikonomakos, N. G., Papageorgious, A. C., Leonidas, D. D., and Tsitoura, H. S. (1991) Glucose analogue inhibitors of glycogen phosphorylase: The design of potential drugs for diabetes. *Biochemistry 30*, 10101-10116

67. Browner, M. F., and Fletterick, R. J. (1992) Phosphorylase: A biological transducer. *TIBS J. 17*, 66-71

68. Browner, M. F., Hwang, P. K., and Fletterick, R. J. (1992) Cooperative binding is not required for activation of muscle phosphorylase. *Biochemistry* 31, 11291-11296

69. Coats, W. S., Browner, M. F., Fletterick, R. J., and Newgard, C. B. (1991) An engineered liver glycogen phosphorylase with AMP allosteric activation. *J. Biol. Chem. 266*, 16113-16119

70. Buchbinder, J. L., Luong, C. B. H., Browner, M. F., and Fletterick, R. J. (1997) Partial activation of muscle phosphorylase by replacement of serine 14 with acidic residues at the site of regulatory phosphorylation. *Biochemistry 36*, 8039-8044

71. Johnson, L. N., and Barford, D. (1994) Electrostatic effects in the control of glycogen phosphorylase by phosphorylation. *Protein Sci. 3*, 1726-1730

72. Browner, M. F., Hackos, D., and Fletterick, R. J. (1994) Identification of the molecular trigger for allosteric activation in glycogen phosphorylase. *Structural Biology 1*, 327-333

73. Buchbinder, J. L., and Fletterick, R. J. (1996) Role of the active site gate of glycogen phosphorylase in allosteric inhibition and substrate binding. *J. Biol. Chem. 271*, 22305-22509

74. Sergienko, E. A., and Srivastava, D. K. (1997) Kinetic mechanism of the glycogen-phosphorylase-catalyzed reaction in the direction of glycogen synthesis: Co-operative interactions of AMP and glucose-1-phosphate during catalysis. *Biochem. J. 328*, 83-91

75. Bollen, M., Keppens, S., and Stalmans, W. (1998) Specific features of glycogen metabolism in the liver. *Biochem. J. 336*, 19-31

76. Klinov, S. V., and Kurganov, B. I. (2001) Kinetic mechanism of allosteric regulation of muscle glycogen phosphorlyase *b* by adenosine 5’-monophosphate. *Biochemistry (Moscow) 66*, 1374-1377

77. Klinov, S. V., and Kurganov, B. I. (2001) Combined kinetic mechanism describing activation and inhibition of muscle glycogen phosphorylase by adenosine 5'-monophosphate. *Biophys. Chem. 92*, 89-102

78. Oikonomakos, N. G., Skamnaki, V. T., Tsitsanou, K. E., Gavalas, N. G., and Johnson, L. N. (2000) A new allosteric site in glycogen phosphorylase *b* as a target for drug interactions. *Structure 8*, 575-584

79. Oilonomakos, N. G., Kosmopoulou, M., Zographos, S. E., Leonidas, D. D., Chrysina, E. D., Somsak, L. Nagy, V., Praly, J-P., Docsa, T., Toth, B., and Gergely, P. (2002) Binding of N-acetyl-N'-β-D-glucopyranosyl urea and N-benzoyl-N-β-D-glucopyranosyl urea to glycogen phosphorylase *b*: Kinetic and crystallographic studies. *Eur. J. Biochem. 269*, 1684-1696

80. Lu, Z., Bohn, J., Bergeron, R., Deng, Q., Ellsworth, K. P., Geissler, W. M., Harris, G., McCann, P. E., McKeever, B., Myer, R. W., Saperstein, R., Willoughby, C. A., Yau, J., and Chapman, K. (2003) A new class of glycogen phosphorylase inhibitors. *Bioorg. Med. Chem. Lett. 13*, 4125-4128

81. Kosmopoulou, M. N., Leonidas, D. D., Chrysina, E. D., Bischler, N., Eisenbrand, G., Sakarellos, C. E., Pauptit, R., and Oikonomakos, N. G. (2004) Binding of the potential antitumour agent indirubin-5-sulphonate at the inhibitor site of rabbit muscle glycogen phosphorylase *b*: Comparison with ligand binding to pCDK2-cyclin A complex. *Eur. J. Biochem. 271*, 2280-2290

82. Kristiansen, M., Andersen, B., Iversen, L. F., and Westergaard, N. (2004) Identification, synthesis, and characterization of new glycogen phosphorylase inhibitors binding to the allosteric AMP site. *J. Med. Chem. 47*, 3537-3545

83. Lukacs, C. M., Oikonomakos, N. G., Crowther, R. L., Hong, L-N., Kammlott, R. U., Levin, W., Li, S., Liu, C-M., Lucas-McGrady, D., Pietranico, S., and Reik, L. (2006) The crystal structure of human muscle glycogen phosphorlyase *a* with bound glucose and AMP: An intermediate conformation with T-state and R-state features. *Proteins 63*, 1123-1126

84. Rush, J. W. E., and Spriet, L. L. (2001) Skeletal muscle glycogen phosphorlyase *a* kinetics: Effects of adenine nucleotides and caffeine. *J. Appl. Physiol. 91*, 2071-2078

85. Ercan-Fang, N., Gannon, M. C., Rath, V. L., Treadway, J. L., Taylor, M. R., and Nuttall, F. Q. (2002) Integrated effects of multiple modulators on human liver glycogen phosphorylase *a*. *Am. J. Physiol. Endocrinol. Metab.* 283, E29-E37

86. Baker, D. J., Greenhaff, P. L., MacInnes, A., and Timmons, J. A. (2006) The experimental type 2 diabetes therapy glycogen phosphorylase inhibition can impair aerobic muscle function during prolonged contraction. *Diabetes* 55, 1855-1861

87. Shang, J., and Lehrman, M. A. (2004) Activation of glycogen phosphorylase with 5-aminoimidazole-4-carboxamide riboside (AICAR): Assessment of glycogen as a precursor of mannosyl residues in glycoconjugates. *J. Biol. Chem. 279*, 12076-12080

88. Walcott, S., and Lehman, S. L. (2007) Enzyme kinetics of muscle glycogen phosphorylase *b*. *Biochemistry 46*, 11957-11968

89. Biorn, A. C., and Graves, D. J. (2001) The amino-terminal tail of glycogen phosphorylase is a switch for controlling phosphorylase conformation, activation, and response to ligands. *Biochemistry 40*, 5181-5189

90. Gold, A. M., Johnson, R. M., and Tseng, J. K. (1970) Kinetic mechanism of rabbit muscle glycogen phosphorylase *a*. *J. Biol. Chem. 245*, 2564-2572

91. Kimmel, J. L., and Reinhart, G. D. (2000) Reevaluation of the accepted allosteric mechanism of phosphofructokinase from *Bacillus stearothermophilus*. *Proc. Natl. Acad. Sci. U.S.A. 97*, 3844-3849

92. Page, M. J., MacGillivray, R. T. A., and DiCera, E. (2005) Determinants of specificity in coagulation proteases. *J. Thromb. Haemost. 3*, 2401-2408

93. Gandhi, P. S., Chen, Z., Mathews, F. S., and DiCera, E. (2008) Structural identification of the pathway of long-range communication in an allosteric enzyme. *Proc. Natl. Acad. Sci. U.S.A. 105*, 1832-1837

94. Pineda, A. O., Carrell, C. J., Bush, L. A., Prasad, S., Caccia, S., Chen, Z-W., Mathews, F. S., and DiCera, E. (2004) Molecular dissection of Na+ binding to thrombin. *J. Biol. Chem. 279*, 31842-31853

95. Luque, I., Leavitt, S. A., and Freire, E. (2002) The linkage between protein folding and functional cooperativity: Two sides of the same coin? *Annu. Rev. Biophys. Biomol. Struct. 31*, 235-256

96. Gunasekaran, K., Ma, B., and Nussinov, R. (2004) Is allostery an intrinsic property of all dynamic proteins? *Proteins 57*, 433-443

97. Suel, G. M., Lockless, S. W., Wall, M. A., and Ranganathan, R. (2003) Evolutionarily conserved networks of residues mediate allosteric communication in proteins. *Nature Structural Biology 10*, 59-69

98. Daily, M. D., Upadhyaya, T. J., and Gray, J. J. (2008) Contact rearrangements form coupled networks from local motions in allosteric proteins. *Proteins* 71, 455-466

99. Weber, G. (1972) Ligand binding and internal equilibria in proteins. *Biochemistry 11*, 864-878

100. Weber, G. (1975) Energetics of ligand binding to proteins. *Adv. Pro. Chem. 29*, 1-83

101. Reinhart, G. D. (1988) Linked function origins of cooperativity in a symmetrical dimer. *Biophys. Chem. 30*, 159-172

102. Goldbeck, R. A., Esuqerra, R. M., Hoh, J. M., Ackers, G. K., and Kliger, D. S. (2004) The molecular code for hemoglobin allostery revealed by linking the thermodynamics and kinetics of quaternary structural change: 1. Microstate linear free energy relations. *Biochemistry 43*, 12048-12064

103. Kimmel, J. L., and Reinhart, G. D. (2001) Isolation of an individual allosteric interaction in tetrameric phosphofructokinase from *Bacillus stearothermophilus*. *Biochemistry 40*, 11623-11629

104. Ortigosa, A. D., Kimmel, J. L., and Reinhart, G. D. (2004) Disentangling the web of allosteric communication in a homotetramer: Heterotropic inhibition of phosphofructokinase from *Bacillus stearothermophilus. Biochemistry 43*, 577-586

105. Reinhart, G. D. (1983) The determination of thermodynamic allosteric parameters of an enzyme undergoing steady-state turnover. *Archives of Biochem. and Biophys. 224*, 389-401

106. Cuadri-Tome, C., Baron, C., Jara-Perez, V., Parody-Morreale, A., Martinez, J. C., and Camara-Artigas, A. (2006) Kinetic analysis and modeling of the allosteric behavior of liver and muscle glycogen phosphorylase. *J. Mol. Recognit. 19*, 451-457

107. Feldmann, K., Zeisel, H., and Helmreich, E. (1972) Interactions between native and chemically modified subunits of matrix-bound glycogen phosphorylase. *Proc. Natl. Acad. Sci. U.S.A. 69*, 2278-2282

108. Fenton, A. W., Paricharttanakul, N. M., and Reinhart, G. D. (2004) Disentangling the web of allosteric communication in a homotetramer: Heterotropic activation in phosphofructokinase from *Escherichia coli*. *Biochemistry 43*, 14104-14110

109. Muchmore, D. C., McIntosh, L. P., Russell, C. B., Anderson, D. E., and Dahlquist, F. W. (1989) [3] Expression and nitrogen-15 labeling of proteins for proton and nitrogen-15 nuclear magnetic resonance. *Methods in Enzymology* 177, 44-73

110. Bullock, W. O., Fernandez, J. M., and Short, J. M. (1987) XL1-Blue: A high efficiency plasmid transforming recA *Escherichia coli* strain with beta-galactosidiase selection. *Biotechniques 5*, 376-378

111. Furste, J. P., Pansegrau, W., Frank, R., Blocker, H., Scholz, P., Bagdasarian, M., and Lanka, E. (1986) Molecular cloning of the plasmid RP4 primase region in a multi-host-range *tac*P expression vector. *Gene 48*, 119-131

112. Daldal, F. (1983) Molecular cloning of the gene for phosphofructokinase-2 of *Escherichia coli* and the nature of a mutation, *pfkB1*, causing a high level of the enzyme. *J. Mol. Biol. 168*, 285-305

113. Hellinga, H. W., and Evans, P. R. (1985) Nucleotide sequence and high-level expression of the major *Escherichia coli* phosphofructokinase. *Eur. J. Biochem. 149*, 363-373

114. Hill, A. V. (1910) The possible effects of the aggregation of the molecules of haemoglobin on its dissociation curves. *J. Physiol-London 40*, iv-vii

115. van Holde, K. E., Johnson, W. C., and Ho, P. S. (1998) Molecular thermodynamics in *Principles of Physical Biochemistry*, pp 90-147, Prentice Hall, Upper Saddle River, NJ

116. Graves, D. J., Carlson, G. M., Skuster, J. R., Parrish, R. F., Carty, T. J., and Tessmer, G. W. (1975) Pyridoxal phosphate-dependent conformational studies of glycogen phosphorylase as probed by interconverting enzymes. *J. Biol. Chem. 250*, 2254-2258

117. Kurganov, B. I., Kornilaev, B. A., Chebotareva, N. A., Malikov, V. P., Orlov, V. N., Lyubarev, A. E., and Livanova, N. B. (2000) Dissociative mechanism of thermal denaturation of rabbit skeletal muscle glycogen phosphorylase *b*. *Biochemistry 39*, 13144-13152

118. Datta, N. (1979) Plasmid classification: Incompatibility grouping. In *Plasmids of Medical, Environmental and Commercial Importance* (ed. Timmin, K. N. and Puhler, A.), pp 3-12, Elsevier, Amsterdam

119. Martin, J. L., Johnson, L. N., and Withers, S. G. (1990) Comparison of the binding of glucose and glucose-1-phosphate derivatives to T-state glycogen phosphorylase *b*. *Biochemistry 29*, 10745-10757

120. Petterson, E. F., Goddard, T. D., Huang, C. C., Couch, G. S., Greenblatt, D. M., Meng, E. C., and Ferrin, T. E. (2004) USCF Chimera – A visualization system for exploratory research and analysis. *J. Comput. Chem. 25*, 1605-1612

121. Chattopadhyay, A., Meier, M., Ivaninskii, S., and Burkhard, P. (2007) Structure, mechanism and conformational dynamics of O-acetylserine sulfhydrylase form *Salmonella typhimurium*: Comparison of *a* and *b* isozymes. *Biochemistry 46*, 8315-8330

122. Sprang, S. R., Withers, S. G., Goldsmith, E. J., Fletterick, R. J., and Madsen, N. B. (1991) Structural basis for the activation of glycogen phosphorylase *b* by adenosine monophosphate. *Science 254*, 1367-1371

123. Watson, K. A., McCleverty, C., Geremia, S., Cottaz, S., Driguez, H., and Johnson, L. N. (1999) Phosphorylase recognition and phosphorolysis of its oligosaccharide substrate: Answers to a long outstanding question. *EMBO J. 18*, 4619-4632

VITA

Name:	Andrew Nathan Bigley
Address:	Department of Biochemistry and Biophysics 103 Biochemistry/Biophysics Building Texas A&M University 2128 TAMU College Station, TX 77840-2128
Email Address:	a_bigley@tamu.edu
Education:	B.S. Biological Sciences, University of Houston Clear Lake in Houston Texas, 2003 Ph.D. Biochemistry, Texas A&M University, 2009